8-2021

EFFECT OF LACTOFERRIN TO INCREASE DRUG PERMEABILITY OF PRIMARY PULMONARY MYCOBACTERIAL GRANULOMAS

Thao Nguyen

Thao KT Nguyen

EFFECT OF LACTOFERRIN TO INCREASE DRUG PERMEABILITY OF PRIMARY PULMONARY MYCOBACTERIAL GRANULOMAS

by

Thao Khanh Thanh Nguyen, B.A.

APPROVED:

_____
Jeffrey K. Actor, Ph.D.
Advisory Professor

_____
Marian L. Kruzel, Ph.D.

_____
Robert L. Hunter, M.D. Ph.D.

_____
Pamela L.Wenzel, Ph.D.

_____
Scott E. Evans, M.D.

APPROVED:

_____
Dean, The University of Texas
MD Anderson Cancer Center UTHealth Graduate School of Biomedical Sciences

EFFECT OF LACTOFERRIN TO INCREASE DRUG PERMEABILITY OF PRIMARY PULMONARY MYCOBACTERIAL GRANULOMAS

A

THESIS

Presented to the Faculty of

The University of Texas

MD Anderson Cancer Center UTHealth

Graduate School of Biomedical Sciences

in Partial Fulfilment

of the Requirements

for the Degree of

MASTER OF SCIENCE

by

THAO KHANH THANH NGUYEN, B.A.

August 2021

COPYRIGHT

The American Journal of Pathology and the Biochemistry and Cell Biology Journal permit authors to reuse their articles or parts of their articles in several ways including in support of his/her thesis or dissertation.

The full list of copyrights and permissions granted to authors who publish in these journals can be found at the following web addresses:

https://www.elsevier.com/about/policies/copyright

https://cdnsciencepub.com/authors-and-reviewers/author-rights

Reprinted with permission of Elsevier and Canadian Science Publishing.

DEDICATION

This thesis is dedicated to all the members of my immediate support system who have always been there, even before I had the courage to start this work: my principal investigator Dr. Actor, my husband Matt, my loving parents ba Bình and mẹ Thuỷ, my "sister" Quyên (Quinn), my mentor Shen-An (Anne), my best friends Zachary, Joyce, and Luân (Jack), and my rescued cat Xoài (Mango).

ACKNOWLEDGMENTS

First and foremost, acknowledgment is too small of a word for everything that my principal investigator, Jeffrey K. Actor Ph.D, did for me and my graduate education. His wisdom, passion, encouragement, care, and unconditional support have continuously inspired me to grow. Just like the vegetables and trees in his garden, I blossomed during the years in his laboratory working on groundbreaking science. As we learned everyday through our discoveries, I learned more about myself and the person I want to become: a brilliant and inspiring scientist like Dr. Actor. Thank you for my first Immunology book, for bringing joy to learning, for your patience as I explored scientific techniques outside of my comfort zone, for the opportunities that I could never have dreamed of, for understanding my struggles, and for this once-in-a-lifetime chance to be your student. All of this is possible because of your compassion and mentorship. Similarly, I am incredibly thankful for Dr. Shen-An Hwang, who went the extra mile to help my research. She taught me how to work with advanced experimental models, generated years of high-quality data that set the strong foundation for my work, showed me the art of developing protocols, and became my role model of an outstanding female scientist.

Secondly, I would like to express my gratitude for my advisory committee members – Marian L. Kruzel, Ph.D.; Robert L. Hunter, M.D., Ph.D.; Pamela L. Wenzel, Ph.D; and Scott E. Evans M.D. . This work is the result of me standing on the shoulders of giants: Dr. Kruzel, a distinguished expert of Lactoferrin, and Dr. Hunter, a world leading expert in the area of

disease pathology and Tuberculosis in humans. Thank you for sharing your expertise, your innovative discoveries, and for the phenomenal resources throughout my research. I want to thank Dr. Wenzel and Dr. Evans for your teaching during my years in the Immunology program, for inputs and suggestions that strengthened my findings, and for your incredible support as I applied for the PhD program.

I am indebted to my family members who have always been there for me during my time in graduate school. Thank you to my husband Matthew Pribadi who has always been there for me through the hardest times and the brightest days. I am the luckiest person to have you and Xoài by my side. To my parents, thank you for raising me and for your unconditional love. Growing up in our small house in Vietnam, my dream to pursue biomedical research and graduate education required too much financial commitment to be feasible. However, instead of asking me to follow a different path, you continued to support me from afar and your endless sacrifice allowed me to follow my dream. I am forever grateful for you, ba mẹ. I also want to thank my late grandmother, Uyên Ninh, who profoundly shaped me during my childhood and showed me the meaning of life through helping and serving others.

All research was performed in part to fulfill requirements for the Master of Science degree from The University of Texas MD Anderson Cancer Center UTHealth Graduate School of Biomedical Sciences; located within the University of Texas Medical Center in Houston, Texas 77030. I would like to acknowledge and thank Louise D. McCullough, MD.,

Ph.D., for assistance with flow cytometry and use of her facilities and reagents for cellular analysis (Chapters 2 and 3). A special thank you goes to Marian L. Kruzel, Ph.D. for guidance and technical assistance for work presented in Chapter 4, which was presented in part at the 14th International Conference on Lactoferrin Structure, Function and Applications, held in Lima, Peru (2019) [1]. I would also like to acknowledge Gustavo Ayala, MD., for our use of the Nuance Cri Multispectral Imaging System which was instrumental in examination of responses presented in Chapters 3 and 4. Finally, this project was supported in large part by NIH Grant 1R42-AI117990.

ABSTRACT

Effect of Lactoferrin to increase drug permeability of primary pulmonary mycobacterial granulomas

Thao Khanh Thanh Nguyen, B.A.

Advisory Professor: Jeffrey K. Actor, Ph.D.

Despite extensive research and worldwide eradication efforts, *Mycobacterium tuberculosis* (*Mtb*) remains a major infectious pathogen to the human population with about 10 million cases of infection per year globally. The host-pathogen interaction, pulmonary granuloma formation, and *Mtb* adaptions result in increased complexity of the disease. Granulomas are formed by active immune responses generated during *Mtb* infection, and serve to contain and limit bacterial dissemination. The major mycobacterial surface mycolic acid, trehalose 6,6'-dimycolate (TDM), functions in multiple ways to enhance immune cell recruitment of sites of infection, to induce inflammation and granulomatous responses, and to initiate survival strategies for the organism inside macrophages. *Mtb* also benefits from establishment of a tightly formed granuloma, which both protects it from immune reactivity and serves as a physical boundary to limit penetration of drugs during therapeutic treatment. In order to demystify the complicated relationship between the host and pathogen, many studies have been performed around the primary *Mtb*-induced granuloma to combat the challenges that come with this specific immunopathology. We hypothesized that by altering the immunopathology of granulomas using lactoferrin, an immunomodulating agent, it will allow greater penetration of

therapeutics into the site of focal inflammation. Our lab has reported that oral bovine lactoferrin treatments during the innate immune response leads to significant modulation of the primary *Mtb* granuloma response and lessen *Mtb* burden in mouse lungs. Here, we show that such modulation during granuloma development can also be achieved by using recombinant human lactoferrin oral treatments to increase granuloma permeability and promotes drug penetration in both TDM-induced granulomatous inflammation as well as during active *Mtb*-infection. Findings from this work show lactoferrin's potential as a host-directed therapeutic that can be combined with current TB standard treatment to reduce pathological damage in the lungs post mycobacterial infection.

TABLE OF CONTENT

LIST OF ILLUSTRATIONS

LIST OF TABLES

ABBREVIATIONS

ANOVA	Analysis of variance
APC	Antigen-presenting cell
B cell	B lymphocyte cell
BCG	Bacillus Calmette–Guérin
CARD9	Caspase recruitment domain-containing protein 9
CD	Cluster of differentiation
CFU	Colony-forming unit
CHO	Chinese hamster ovary cells
DAB	3,3’-Diaminobenzidine
DMEM	Dulbecco's modified Eagle's medium
EDTA	Ethylenediaminetetraacetic acid
EGR2	Early growth response protein 2
ELISA	Enzyme-linked immunosorbent assay
FBS	Fetal bovine serum
FITC	Fluorescein isothiocyanate
HEPES	4-(2-hydroxyethyl)-1-piperazineethanesulfonic acid
HIV	Human immunodeficiency viruses
HLF	Human Lactoferrin
HRP	Horseradish peroxidase
IFN-γ	Interferon gamma

IL	Interleukin
iNOS	Inducible nitric oxide synthase
IV	Intravenous injections
LF	Lactoferrin
LPS	Lipopolysaccharides
LWI	Lung weight index
M1	Macrophage 1
M2	Macrophage 2
MARCO	Macrophage receptor with collagenous structure
MDSC	Myeloid-derived suppressor cells
MHC	Major histocompatibility complex
Mincle	Macrophage inducible Ca2+-dependent lectin receptor
NK	Natural killer cells
NO	Nitric oxide
PBS	Phosphate-buffered saline
PECAM-1	Platelet endothelial cell adhesion molecule (CD31)
rHLF	Recombinant Human Lactoferrin
ROS	Reactive oxygen species
SARS-CoV-2	Severe acute respiratory syndrome coronavirus 2
SIRS	Systemic inflammatory response syndrome
STD	Standard deviation
T cell	T lymphocyte cell

TB	Tuberculosis
TDM	Trehalose 6,6'-dimycolate
TGF-β	Transforming growth factor beta
Th1	Type 1 T helper cells
TLR4	Toll-like receptor 4
TMM	Trehalose monomycolates
TNF-α	Tumor necrosis factor alpha

CHAPTER 1: INTRODUCTION

Tuberculosis disease as an epidemic

It has been over a century since Robert Koch identified the etiological agent of human tuberculosis (TB) [2, 3]. However, to date, this pathogen continues to be a problem for human health. As a single infectious pathogen, *Mycobacterium tuberculosis* (*Mtb*) is one of the top 10 causes of death in middle to low-income countries [4]. In 2020, the Centers for Disease Control and Prevention estimated a fourth of the world's population is infected with TB, with more than 500,000 cases of multidrug-resistant TB reported each year. In the United States alone, about 13 million people currently have latent TB. They show no symptoms of the disease, but have the risk of reactivated infection later in life [5].

Mtb is transmitted between individuals in close proximity by inhalation of *Mtb*-containing droplets from a *Mtb* infected person following coughing, sneezing, or forced respiratory activities [6]. Though most people with latent TB will not develop TB disease in their lifetime, immune compromised individuals, such as HIV-positive people, are at the highest risk to develop active TB infection from the latent TB state [7]. According to the American Lung Association [8], active TB symptoms include, but are not limited to, a persistent coughs that lasts more than three weeks, weight loss, fever, chills, and night sweats. More severe symptoms are fatigue, hemoptysis (coughing up blood), bone pain, and shortness of breath. There are four first-line antimicrobials drugs used in standard TB

treatment regimen: isoniazid, rifampicin, pyrazinamide and ethambutol [9]. Treatment for TB lasts much more than other bacterial infections and takes 180 days of medication in average [5]. However, some *Mtb* strains can display three different types of phenotypic resistance to antibiotics. The first and most familiar is genetic resistance – some *Mtb* strains now possess mutations that produce resistance phenotypes to particular drugs, which is now the biggest threat to human as they continue to evolve while we exhaust our treatment options. The second is when resistance occurs as *Mtb* become dormant, resulting in their refractory to agents that inhibit active metabolic processes. Finally, there is also natural resistance consists of physical barriers and efflux pumps that reject the penetration of antibiotics into these bacteria [6, 10].

Despite extensive research and available low-cost treatments for most *Mtb* strains, *Mtb* remains a major public health threat. Recent forward progress in slowing spread of disease was heavily reversed due to the current Covid-19 pandemic. Currently, approximately 10.0 million active cases and 1.5 million deaths due to *Mtb* were reported in 2020 globally [11]. As SARS-CoV-2 became a more urgent threat to global health, essential resources such as diagnostic equipment, staff, relocation of social care budgets, and even hospital beds were allocated to Covid-19 treatment and inpatient care. Pandemic related lockdowns prevented early diagnostic identification of *Mtb* infection spread, and social distancing guidelines disturbed on-time treatment schedules for *Mtb* patients. Therefore, eradicating efforts are significantly delayed due to the drastic effect on health and society of Covid-19 since early 2020, with world-wide *Mtb* detection efforts have been obstructed

heavily, with WHO's predictions of a 0.2–0.4 million decrease in number of infected individuals receiving treatment by the end of 2020 [11].

Tuberculosis Disease

Mtb was identified in the 1880's through a series of experimental works by Robert Koch as the source for cavitary disease that can lead to chronic lung disorder in human [2]. Tuberculosis manifests disease in two clinical stages [12-14]. The initial stage (primary infection) is readily controlled by individuals with competent immune function. In fact, the majority of individuals exposed to *Mtb* are able to contain and control infection in a matter of weeks without extreme clinical pathology. The primary infection is relatively contained, with a loosely structured granulomatous nodule comprised of central macrophages and surrounding adaptive cells. Most clinical disease is that which is seen during post-primary stages of infection. In this case, re-infection (or reactivation of latent organisms) by *Mtb* induces a pneumonia exudative reaction that can progress to a necrotic lesion [15]. This lesion is hypothesized to be controlled by strong and directed adaptive immune reactivity [16]. The other type of pathology is a relatively contained walled-off nodular tubercle, or caseating granuloma, where organisms may reside and induce continued immune responsiveness [16, 17]. What sets *Mtb* away from other bacterial infections is its silent attack on the human body resulting in granuloma contained organisms in the majority of post-primary infected people, in which they do not display clinical symptoms but still carry either persistent bacteria or strong immune reactivity that reflects on the positive TB skin

test [18-20]. It is easy to imagine a state of latency in which the risk of reactivation, of post-primary *Mtb* infection, later in life due to weakened immune system that fails to continue inhibiting the growth of latent bacilli. Such latent (post-primary) infection causes the majority of TB cases and most of the bacilli transmission [21]. Histologically, post-primary TB is characterized as a lipid pneumonia with foamy macrophages and mostly CD4+ lymphocytes present in the alveoli. A pathological effect is seen when lung tissue ruptures, hypothesized as due to immune reactivity towards an accumulation of mycobacterial mycolic acid antigens [22]. Clinically, this coincides with observed caseating granulomas. Such pulmonary cavitary lesions causes shortness of breath, fatigue, and permanent tissue damages. Immune responses, likely originating from pneumonia, lead to destruction of bronchial passages; subsequent and coughing produces infectious aerosols that can infect a new host [17, 21, 23, 24].

Tuberculosis model – The TDM Granuloma

Much of our observation of disease pathology in humans comes from autopsy of lung disease where pneumonia and caseating granulomas both occur. While the true establishment of mechanisms involved in post-primary infection are still under investigation, it is clear that the granuloma plays a major role in containment of organisms. Our laboratory understood the need to investigate early innate responses that control initial processes during infection. Hence, the study of primary infection relied on the

establishment of animal experimental models which permitted direct investigation into early events that induce the containment response during initial infection.

It is essential to study the disease in an animal model that can mimic the primary signature granulomatous response to Mtb. Early experiments identified a cell wall associated component that was a major factor responsible for the interaction between organisms forming the serpentine cords [24, 25]. This "factor" was later identified as Trehalose 6,6'-dimycolate (TDM), which has been confirmed as the most abundant component of the lipid-rich mycobacterial cell wall. Experimentally, TDM was found to be a useful molecular tool to mimic the primary granulomatous response seen in Mtb infection [26]. Now known as the main mycolic acid of the outer layer of the organism, TDM has been studied for many decades and further identified as the most prevalent virulence factor of Mtb that induces immune pathogenesis. The mouse is an accepted and appropriate animal model system to study how cord factor/TDM initiates the primary granulomatous pathology induce in lung tissue.

Another major property of TDM is that it is known to alter the local microenvironment within macrophages to assist in organism survival [25, 27]. TDM plays a crucial role in Mtb survival; when removed from the organisms, their ability to survive in macrophages is significantly decreased and can be restored when purified TDM is reintroduced [28-30]. Furthermore, TDM has been shown to contribute significantly to the virulence of Mtb by reducing phagosome acidification and fusion with lysosomes. TDM can

also alter the expression of antigen presenting and T-cell activating markers of macrophages such as MHC II, CD40, CD80, and CD86 [30, 31].

TDM's virulent and toxic properties lie within its unique structure. The molecule consists of two trehalose molecules with a long mycolic acid chain of 50-60 carbons, with an extended alpha-carbon branch, that binds to each trehalose molecule. The unique "kinks" in the carbon chains are hypothesized to be responsible for its rigidity and biological activities in a way that allows TDM to be toxic or non-toxic, depending on its presentation [32, 33]. Elimination of this "kink" affects organism virulence [34, 35]. TDM is non-toxic when it is in the form of micelles due to its hydrophobic tails in an aqueous solution, but becomes toxic when forms a monolayer on hydrophobic surfaces. When it is given as an oil-based emulsion that produces roughly 1.0 □m droplets, purified TDM alone can induce innate immune response within the lung tissues where pro-inflammatory cytokines and chemokine productions are increased and immune cells are recruited to establish primary granulomas that mimics primary Mtb infection [36]. Hence, its application in producing primary-infection like pathology in murine lungs has been utilized in studies of primary Mtb infection and granulomas formation [37].

Innate Immune Response to Mtb in Mouse Model

Development of *Mtb* animal models have allowed generations of scientists to investigate *Mtb* primary infection despite the lack of untreated human specimens. Multiple

animal species have been instrumental to investigate *Mtb* pathology [25-30]. For simplicity, this introduction will specifically focus on infections within the mouse model which was used for all parts of this study. Overall, *Mtb* primary infects the lungs and causes major disruption to lung pathology by inducing inflammation structures called granulomas [31, 32]. Granuloma development is the hallmark of *Mtb* infection and plays an essential role in both bacterial containment and symptom development [33]. During primary *Mtb* infection in the mouse, *Mtb* associated factors are involved in the recognition and activation of host cells within the bronchial regions and alveolar sacs, leading to uptake by alveolar macrophages [32, 34]. This interaction triggers a series of immune responses initiated via the production and release of cytokines by infected and responding macrophages [35-38]. For example, TDM, an abundant mycobacterial mycolic acid as introduced earlier, is recognized by Mincle (macrophage-inducible C-type lectin) on the macrophage surface driving *M*. *tuberculosi*s -host recognition [39], which significantly initiates the granulomatous response [21]. Activated macrophages subsequently release pro-inflammatory mediators, such as TNF-α and IL-1β [37], along with additional chemotactic factors to further recruit immune cells to areas of infection [36, 40, 41]. Over time, additional recruited immune cells, such as foamy macrophages, epithelioid cells, and Langhan's giant cells, participate in formation of organized, sphere-shaped primary inflammatory structures at the infected site called granulomas [31, 42]. Disease development can happen even during robust immune response so that, although successfully limit the infection within the granuloma [33], allows bacteria to survive and grow within the infected macrophages [43]. This happens because of various reasons: *Mtb*

have adopted mechanisms to survive within macrophages by persisting without causing inflammation [44], preventing phagolysosome fusion [45, 46], recruited naive macrophages during the immune response can become new potential sites for *Mtb* to shelter and replicate [47], and the dense physical nature of the granuloma limits the penetration of anti-mycobacterial chemotherapy [48, 49]. These factors can lead to the bacterial survival, challenges in treatment efforts, and increase the risk of latent *Mtb* infection. It is believed that mature granulomas is the balance between the arrest of organisms to proliferate due to sufficient adaptive immunity [50] and the survival of intracellular *Mtb* despite killing mechanisms [43, 51].

Macrophages

As a major factor of the innate immunity, macrophages possess mechanisms that allow it to control *Mtb* proliferation. Once activated, macrophages exercise cytotoxic effects that produces nitric oxide (NO) and reactive nitrogen intermediates, which have been shown both *in vitro* and *in vivo* to be important for protection against *Mtb* [52-54]. As an antigen-presenting cell, macrophages also play a key role in presenting digested *Mtb* antigens and produce IL-12 for the initiation of adaptive immune response by lymphocytes [55, 56].

Despite its ability to eliminate *Mtb*, macrophages also contribute to the persistent nature of *Mtb*. Alveolar macrophages play the crucial role of recognizing and phagocytosing

Mtb when first encounter them in the alveoli using mannose receptors, complement receptors, and scavenger receptors [57-59]. Typically, the phagosome then undergoes maturation processes and fuses with lysosome to kill and break down bacteria with organelle acidification and activated lytic enzymes. However, *Mtb* has adapted to survive within the phagosome by using TDM to prevent the phagolysosomal fusion, which allows it to hide within macrophages from other immune factors and even chemotherapies [45, 46, 52].

It has been recently discovered that macrophages can polarize towards the classically activated (M1) or the alternatively activated macrophages (M2). Macrophage polarization is stimulated by the microenvironment surrounding naïve macrophages [60]. M1 macrophages are induced by cytokines such as IFN-γ and TNF-α, and bacterial antigens such as lipopolysaccharide (LPS). Once committing to the M1 phenotype, macrophages produce more pro-inflammatory cytokines such as IFN-γ, TNF-α, and IL-1β, and other molecules important for cytotoxic effects such as reactive oxygen species (ROS) and inducible nitric oxide synthase (iNOS). On the other hand, cytokines such as IL-4, IL-10, and IL-13 can induce M2 polarization in macrophages, resulting in production of anti-inflammatory cytokines such as IL-10 and TGF-β responsible for immune-regulatory and tissue-remodeling [61-63]. In mice, markers for murine M1 macrophages are identified as high expression of CD38 (T-cell receptor) and CD86 (transmembrane protein that both activates and inhibits T-cells), and M2 macrophages have high levels of CD206 (mannose receptor) and EGR2 (transcription factor) [64, 65]. Macrophage populations from *Mtb*

infected mouse lungs show plasticity of response over time [60, 66]. Though it has only been investigated recently, evidence shows that the macrophage polarization is closely related to the pathogenesis of *Mtb* infection and chronic obstructive pulmonary disease. In TB mouse models, the early stages of infection and granuloma establishment are marked with high level of M1 macrophages detected up to 30 days post-infection, while M2 macrophages levels are increased towards the middle and later phases when inflammation is resolved [67-69].

Host-directed therapy in Mtb treatment

As mentioned above, it has been established that *Mtb* can manipulate the immune system to favor its survival at the molecular level [70]. Its adaptation to survive within macrophages after phagocytosis [44-46], an immune cell population that was meant to engulf and digest foreign organisms, was only one piece of the puzzle. Studies have shown that *Mtb* virulence factor alone, TDM, can increase macrophage recruitment to the infected sites for new "hiding" opportunities [47] and induces host cell apoptosis [71]. *Mtb* can also delay the adaptive immune response by limiting stimulated dendritic cells' migration from alveolar spaces in the lungs to lymph nodes, which slows down the initial T-cell activation [72-74]. Therefore, adjunctive treatments aimed at redirecting the immune system are critical alternative approaches to counteract *Mtb* manipulative strategies [75].

Due to the pathological damage and therapeutic challenges caused by *Mtb* adaptation to its survival within granulomas, researchers have been investigating immunotherapy approaches that can improve lung pathology and increase drug penetration to fight hiding bacteria inside granulomas. Novel approaches to *Mtb* treatment include host-directed therapy [75, 76] which focuses on two major fronts; the first sharpens immune response, such as immune-based treatments [77], while the second alters the resultant immunopathology [78]. An example of immune-based treatments includes agents that target the macroautophagic compartment, such as vitamin D and retinoic acid which increase phagocytosis and augment the lysosomal degradative process to increase *Mtb* removal inside macrophages [79]. Ibuprofen, an anti-inflammatory drug, also showed its potential as an adjunct treatment for *Mtb* infection by enhancing mycobactericidal effect of pyrazinamide and alleviate pathological damage in the lungs [77, 80, 81]. These immune-based approaches have significant potential, demonstrating superior disease outcomes in mouse models. However, these approaches face many challenges such as conflicting clinical trial results [82, 83] and drug delivery to macrophages inside established granulomas [84].

On the other hand, therapies that target pathologies are also valid as potential clinical candidates. A well-known example of the immunopathological alteration approach is blocking excess TNF-α, a key pro-inflammatory cytokine required for granuloma formation and proper recruitment of immune cells to form granulomas, to reduce lung pathological damage. TNF-α inhibitors have been used to treat other inflammatory diseases effectively [85-87]. However, its major disadvantage is the increased risk of bacterial dissemination;

abolishing the granuloma containment modality runs the risk of *Mtb* reactivation [88-91]. Another example of the second approach is granuloma modulation by lactoferrin [92]. Lactoferrin, a glycoprotein known for its ability to bind iron, has been extensively studied for its role as an immune modulator in host defense in infected patients and disease models; lactoferrin has been shown to boost immune memory response in vaccine models, while reducing pro-inflammatory response in LPS-exposed mouse models [93-97]. In recent years, research has shown significant modulation of the *Mtb* primary granuloma response using lactoferrin treatments. Bovine lactoferrin significantlly reduced inflammatory pathology in TB-infected mice [98]. Human lactoferrin was also shown effective to limit inflammation in the non-infectious TDM-induce granuloma mouse model [78, 99].

Lactoferrin as a therapeutic approach to TB treatment

Lactoferrin is a single polypeptide chain glycoprotein that consists of about 690 amino acid residues and folds into two globular structures consisting of iron binding sites [100, 101]. It was found primarily as a glycoprotein produced by epithelial cells in mucosal secretions but is also made and stored in neutrophilic granules functioning as an innate immune response component [102]. Overall, lactoferrin has been shown to involve in protection during multiple microbial infections and prevention of systemic inflammation [97, 103-107]. Lactoferrin's biological functions during infections are known as three main effects: first is the bacteriostatic effect by removing the iron supply from environment to slow down bacterial growth, second is the bactericidal effect due to lactoferrin's affinity to

bacterial lipopolysaccharides (LPS) in Gram-negative organisms, and third is the immune modulating effect where it can either boost or downregulate the immune response depending on the current immune status [108-116]. As preventive measures, lactoferrin can also prevent infection by inhibiting binding of pathogens with receptors used for entry on host cells [117-119] and boost immune memory response in vaccine models [94, 95].

Known as an immune modulator, lactoferrin can affect the immune response by modulating several immune cells' functions. During innate immune response, lactoferrin can reduce the production of proinflammatory cytokines produced by activated or infected macrophages such as TNF-α, IL-6, and IL-1β [78, 115, 120] and enhance phagocytic activity of macrophages [120, 121]. Similarly, lactoferrin has been shown to reduce production of stimulation-induced cytokines such as TNF-α, IL-12, and IL-1β in dendritic cells – another key antigen presenting cell population during innate immune response [122, 123]. As infection progresses and leads to the adaptive immune response, lactoferrin has been shown to increase surface expression of CD40 and IL-12 production of macrophages, which are key co-stimulatory factors responsible for activating T-cells and increasing secretion of IFN-γ from T-cells respectively, at the sites of infection [124-126]. In different infectious disease models, lactoferrin can either favored a T-helper 2 response [127, 128] or increase the T-helper 1 response [129]. In murine B-cells, lactoferrin can also promote maturation of B-cells and increase their ability to promote antigen-specific T-cell proliferation [130]. These immune modulating effects are the results of lactoferrin binding to different receptors on immune cells; other than binding to lactoferrin receptor (LfR), which are found on the

surface of monocytes, T-cells, and B-cells [131-134], lactoferrin can also interact with a variety of cell surface receptors such as Toll-like receptor 4 (TLR4) and CD14 on macrophages, and CD22 on mature B-cells [135].

In the case of host anti-*Mtb* response, previous studies have shown its modulating effect during primary infection by reducing proinflammatory response that is responsible for pathological damage in the lung tissues. Latest primary granuloma models show that bovine lactoferrin significantlly reduced inflammatory pathology in TB-infected mice [98] and human lactoferrin can similarly limit inflammation and granuloma size in the non-infectious TDM-induce granuloma mouse model [78, 99]. Such anti-inflammatory response in the lactoferrin-treated mice, along with other data showing lactoferrin reduced pro-inflammatory phenotypes in macrophages [136, 137], suggests that lactoferrin had a modulating pro-inflammatory response on granulomas. This thesis extended theses observations to examine if recombinant-human lactoferrin can modulate granulomatous pathology and its permeability, and if we can utilize such effect to increase drug distribution during innate immune response or granuloma formation. The effect of lactoferrin on the permeability of granulomas to fluoroquinolones is examined in both TDM-challenged and *Mtb*-infected mouse model, while administered as a prophylactic (prior to granuloma formation) or therapeutic (after granuloma establishment) intervention during primary *Mtb* infection. In addition, effects of lactoferrin treatment on the expression of M1/M2 phenotypes as well as endothelial-lined vessel structures are examined within the

granuloma, shedding more light into the potential mechanisms behind the pathological and drug distribution changes.

Summary of Thesis

This thesis explores how macrophages polarize during primary granuloma development and how lactoferrin, as an immune modulator, alters pathogenesis of primary infection in a way that makes increased drug distribution within granulomatous structures a possibility. The first study verified macrophage polarization into M1 phenotype during the innate immune response in the TDM-induced model of primary Mtb granulomatous response (Chapter 2). Once the model is validated, the second study investigated the effect of lactoferrin to alter drug permeability of primary pulmonary mycobacterial-like granulomas (Chapter 3). Mtb infection is a very complex disease that progresses due to both bacterial growth and persistent immune response. Therefore, the effect of lactoferrin to alter drug permeability of primary granulomas was evaluated in the last study by giving Mtb-infected mice lactoferrin prophylactically and therapeutically, as a proof of concept to explore potential differences in effectiveness of each intervention timing (Chapter 4). Finally, the effects of lactoferrin and its immune-modulating mechanisms, as well as future directions, are discussed in Chapter 5.

CHAPTER 2: MYCOBACTERIAL TREHALOSE 6,6'-DIMYCOLATE INDUCED M1-TYPE INFLAMMATION

This work is reprinted from The American Journal of Pathology, Volume 190, Issue 2,Thao K T Nguyen, John d'Aigle, Luis Chinea, Zainab Niaz, Robert L Hunter, Shen-An Hwang, Jeffrey K Actor, Mycobacterial Trehalose 6,6'-Dimycolate-Induced M1-Type Inflammation, Page 286-394, Copyright (2019), with permission from Elsevier.

(https://doi.org/10.1016/j.ajpath.2019.10.006)

Introduction

Dogma in tuberculosis pathology is the notion that induction of a strong T-helper 1 lymphocyte (Th1) phenotype is critical in maintaining protective health during primary mycobacterial infection [138, 139]. Development of this phenotypic outcome is based on critical aspects of the macrophage and its initial interactions with the infectious organism [140-142]. Multiple organism-induced mechanisms have been identified that function to evade host responses [143, 144], essentially limiting effectiveness of this avenue of Th1 lymphocyte response. Many of these evasive properties directly affect macrophage functions [145]. The relatively recent realization that macrophage populations can be subdivided into pro- and anti-inflammatory subsets has sparked a revolution in understanding the complexities of innate responding cells to subsequent immune

outcomes; this has important consequences on ensuing granuloma pathologies post infection [146-148].

The primary stages of mycobacterial infection manifest with a robust pro-inflammatory response in order to effectively mitigate organism dissemination. Indeed, these host responses induce hemorrhagic inflammation and vascular occlusion [149, 150], that coincide with changes to fibrinolytic activity and thrombosis [151], which are in many ways beneficial for limiting spread of microorganisms. Certainly, the establishment of a granuloma is considered protective [43, 152], even though it provides a specialized niche within the lung for organisms to replicate.

A major molecule influencing acute reactivity upon entry of *Mtb* into the host is the mycobacterial cord factor component trehalose-6,6'-dimycolate (TDM). Multiple models of the TDM-induced pulmonary granulomatous response have been studied in mice, all of which have common features to those identified in early acute primary immunopathology of the human host. Initially, Block and Noll (1955) utilized cord factor to mimic pathologies seen in early primary human disease [153], including changes to fibrinolytic activity [149, 150] and thrombosis [151]. Perez, et al., successfully repeated these experiments using purified TDM [154]; Donnachie, et al. [155], and Hwang, et al. [156], built on this using molecular tools to further examine early events in extravascular coagulation. Alternate models of the primary TB response were developed using administered TDM to initiate a synchronized transient granulomatous response [157-159]; these models are extremely

effective to assess monocyte-macrophage factors involved in primary granuloma pathogenesis. Indeed, modifications to this model have allowed further insights into how macrophages utilize required receptors to initiate the cytokine cascades [160], and how these events can push the macrophages to elicit hypersensitive responses [161, 162].

The common link between the different models is the relatively rapid initiated pro-inflammatory macrophage responses elicited *in vivo* by TDM. Here, we desired to further examine the nature of the macrophage phenotype response to TDM, and determine the histopathological evidence to support a hypothesis linking TDM to the presence of recruited macrophage polarization to an M1-like phenotype. Evidence presented in this report uses histologic markers and flow cytometry, immunostaining, and ELISA methods to link TDM as a driver for the M1-like macrophage phenotype during recruited induction of the primary granulomatous pathology.

Materials and Methods

Mice. Female C57BL/6 mice (Envigo, Houston, TX) were five to six weeks of age, and approximately 20g weight, at study initiation. Animal work was performed at the University of Texas Health Science Center (UTHSC) animal welfare committee, according to protocols detailed in approved documents HSC-AWC-16-0140 and HSC-AWC-17-0089.

TDM Induced Lung Pathology. Mycobacterial-derived TDM (cord factor) (Enzo Life Sciences, Farmingdale, NY) was solubilized in hexane:ethanol, at a ratio of 9:1. Material was evaporated by a stream of air. The TDM oil/water emulsion was prepared as previously described [159]. Briefly, evaporated TDM (25 g/mouse) was homogenized in Drakeol (2 l/mouse) (Penreco, Indianapolis, IN). Then 48 l/mouse of DPBS 1x (Dulbeccos' Phosphate Buffered Solution, Cellgro) with 0.2% Tween-80 (Mallinckrodt, Hazelwood, MO) was added; the mixture was homongenized in a glass tube and Teflon pestle for 1 minute to produce an oil/water emulsion. The TDM was intravenously (IV) given at a volume of 100 l per animal. Control mice received material formulated with no addition of TDM in oil. Emulsion only controls did not exhibit inflammation, nor did they exhibit cytokines production, at the times described here, as was previously reported and detailed [158, 163]. All mice were sacrificed at times indicated (7 days after injection of formulated material.

Histological Assessment. Mice were sacrificed, and lungs were immediately perfused with a solution of 1mM EDTA in DPBS. Lungs were weighed, sectioned, and evaluated for pathology and histological results. Tissues were fixed in 10% buffered formalin for histology (Fisher Scientific, Pittsburg, PA). Specimens were processed by the Histology Laboratory at the UTHSC McGovern Medical School (Houston, TX); tissues were embedded in paraffin blocks and then 5 µm thick sections were subsequently stained with hematoxylin (Surgipath, Richmond, IL) and eosin (Richard-Allen Scientific, Kalamazoo, MI).

Lung weight index (LWI). Our laboratory utilizes an accepted lung weight index (LWI) which calculates as an approximation of lung inflammation intensity. The following equation was used for calculation of the gross tissue inflammation due to TDM induced pathology, as used in prior studies [158, 164, 165]:

$$LWI = \frac{\sqrt{\frac{\text{Lung weight (g) x 1000}}{\text{Mouse weight (g) / 10}}}}{10}$$

Computerized analysis. High resolution scanned images of H&E-stained slides were scanned for computerized analysis of lung inflammation using Motic DSAssistant software (Kowloon Bay, Kowloon, HK). Quantitation of inflammation was performed in two steps using ImageJ (Version 1.52o 23 April 2019, National Institutes of Health, Bethesda, MD). Lung area was initially quantified by separation of the image's scale from background. Minimum and maximum values for hue, saturation, and brightness of the image were set as follows: 120, 255; 0, 255; and 0, 255, respectively. Total cell area measurement was calculated using a modified version of the procedure detailed in the online ImageJ stained-sections example directory (https://imagej.nih.gov/ij/docs/examples/stained-sections/index.html; version 1.52a), where peak threshold was set at 164 for all digitized slides analyzed. Methods were similar to published materials [166]. Lung inflammation was calculated as a percentage of total area occupied by cell area; values were averaged within treatment groups and normalized to that of group non-treated controls.

Lung cytokine production. A weighed section of lung was excised, then homogenized, then incubated at 37°C and 5% CO_2 for 4 hours in Dulbecco's Modified Eagle's medium (DMEM) containing 50 µg/ml L-Arginine, 50 µg/ml HEPES, 100 µg/ml penicillin, and 50 µg/ml gentamycin, and 10% fetal bovine serum. Collected supernatants were spun to remove debris, then assessed by enzyme-linked immunoassay (ELISA). Production of TNF-α, IL-1β, IL-12p40, IL-6, TGF-β and IL-10 was determined by manufacturer's instructions (DuoSet kits, R&D Systems, Minneapolis, MN). Supernatants to detect TGF-β were pretreated with 1:5 ratio of 1N HCl, then neutralized with same volume 1.2N NaOH/0.5M HEPES. The average of duplicate wells was determined using a standard curve produced by reactivity to manufacturer's supplied recombinant molecules. Detection sensitivity limit was at least 32 pg/ml, according to manufacturer product details.

Immunohistochemical analysis. The large right lobe of each lung was collected and fixed in 10% buffered formalin. The fixed lung tissue was stained with hematoxylin and eosin (H & E) using standard procedures. Assessment was performed using immunohistochemistry for integrin family member CD11b (Absolute Antibody, Cat# Ab01114-23.0; Wilton, UK) [167], diluted at 1:2000, was performed according to modification of manufacturer's instructions (20 minutes at low pH), and subsequently visualized using standard HRP techniques and DAB chromogen using Dako reagents (Dako, Agilent, Santa Clara, CA). In a similar manner, M1-like marker CD38 (Invitrogen, ThermoFisher, Cat# 14-0381-02), diluted at 1:1000, was used for visualization on serial slide

sections. Henatoxylin counterstained slides were viewed by a trained pathologist, with descriptive results obtained in an experimentally blinded manner.

Flow Cytometry Analysis. Lungs were extracted from WT and TDM treat, homogenized by hand, and underwent a 30-minute Collagenase/Hyaluronidase (StemCell Technologies) and DNAse I (Sigma) incubation in sterile filtered RPMI-1640 with 1% 100X pen/strep and 2.5% HEPES (Thermo Fisher Scientific), and 5% HI FBS 9Corning). Enzymatic digestion was quenched with addition of RPMI mixture before lung tissue was plunged through a 70-micron cell strainer. Cells were pelleted at 4°C for 5 minutes at 450rcf (g). Cell pellets were re-suspended in a 70% GE Healthcare Percoll (Cat# 17-0891-01) gradient and underlaid in 40% Percoll followed by a 20-minute 22°C 500rcf centrifugation with no break and slow acceleration. Cells were collected at the 70-40 Percoll interface before being re-suspended in sterile filtered PBS mixture containing 2% HI FBS and 1mL of 0.5M EDTA (Thermo Fisher Scientific). Surface markers chosen to delineate murine M1-like and M2-like macrophages were based on published data from Jablonski, et al., [65], later detailed by Orecchioni, et al. [168]. Similar findings were identified in human monocyte-derived macrophages [169].Cells were stained in accordance with manufacture recommendation, using Live Dead Aqua (eBioscience, L34966) for 15 minutes, then FC (antibody receptor) blocked with Anti-Mo CD16/CD32 (eBioscience, 14-0161-86) for 15 minutes. Staining used the following antibodies against specific receptors: CD38 (Biolegend, Cat# 102728) APC/Cy7, CD86 (Biolegend, Cat# 105014) PE/Cy7, CD206 (Biolegend, Cat # 141704) FITC, EGR2 (eBioscience, 17-6691-82) APC, CD11b (Biolegend, Cat# 101208) PE, and CD45 (eBioscience,

48-0451-82) eFluor 450 for 20 minutes. Cells were fixed with 2% paraformaldehyde, and evaluated on a Beckmen Coulter Cytoflex S flow cytometer (Model No. B75442). Data was then analyzed using FlowJo V10 (Becton Dickinson).

Statistical Analysis. Collected data was compared across groups, and against naive mice or mice challenged with vehicle formulated without TDM. Analysis used an unpaired *t*-test, or used one-way ANOVA. The differences between means were considered significant at a level of $p \leq 0.05$. Generated data points were compiled using GraphPad Prism (San Diego, CA) and are presented as a representative value obtained from multiple experimental repeats (sets of 2 or 3). Experiments had an N of 4 to 6 mice.

Results

TDM Induced Pathology: Acute Granulomatous Response.

C57BL/6 mice injected with *Mtb* derived TDM (25 □g/mouse) in oil/water given intravenously developed inflammation in lung tissue of (**Figure 1**). Broad lung inflammation was assessed as lung weight index (LWI) at 7 days after IV TDM challenge; This time point reflects peak granulomatous response induced by TDM [158]. Acute treatment increased LWI significantly. TDM treated mice had an average LWI of 1.60 +/- 0.49 units, compared to naïve controls (0.97 +/- 0.03 units; $p \leq 0.05$). The LWI was similar to computerized assessments of lung inflammation. Analysis of digitized lung histograms post TDM

administration confirmed significant parenchymal inflammation and presence of granulomas throughout pulmonary tissue.

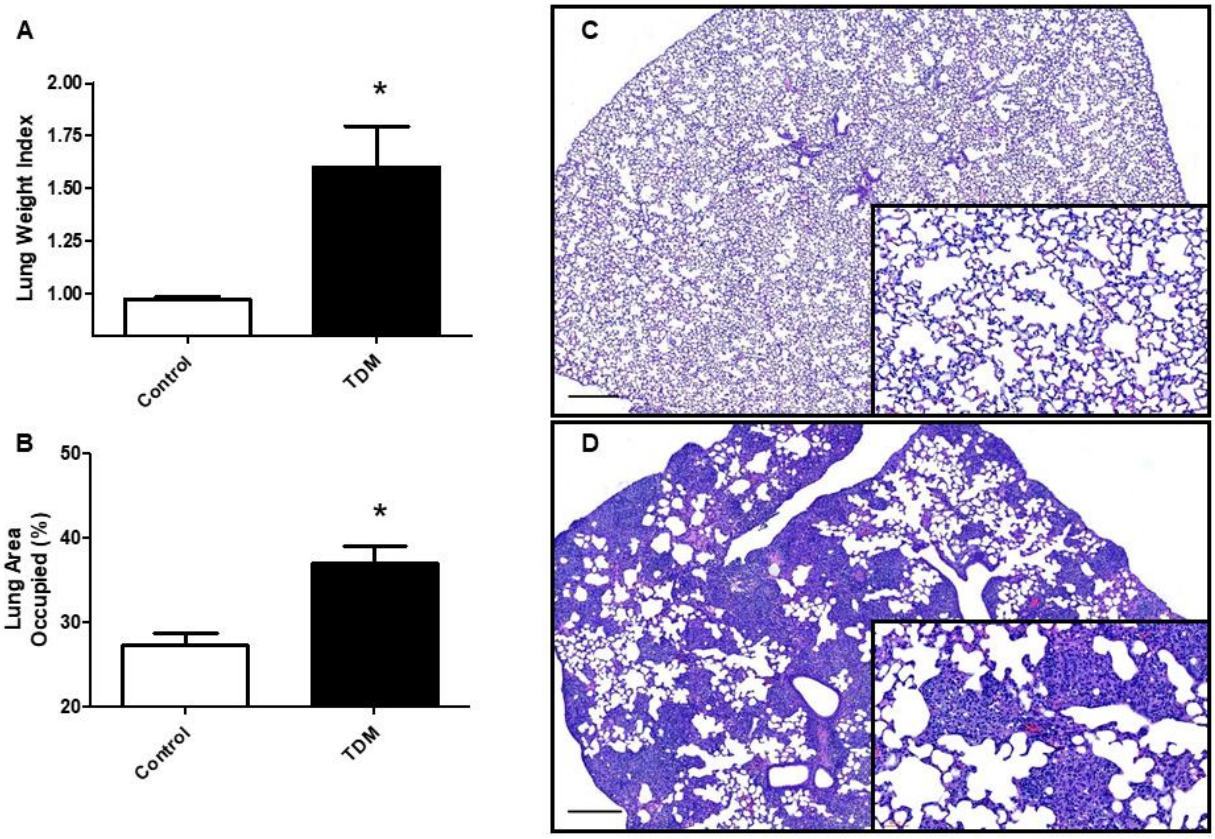

Figure 1. **Comparative Gross Pulmonary Inflammation during TDM Induced Pathology.** Lungs from mice given TDM (25 μg; IV) were assessed after 7 days and compared to control naïve mice. The lung weight index (A) was calculated to quantify gross pulmonary inflammation. Digital analysis of area occupied due to cellularity (B) confirms induction of inflammatory response. Results represent mean ± standard error of the mean (SEM). Similar data was obtained in 3 repeated experiments; 4-6 mice were included per group, per experiment. *; $p \leq 0.05$. Histologic examination of lungs at day 7 post TDM administration revealed acute granulomatous response culminating in high levels of monocytic infiltration, with increased presence of focal macrophages (D), versus non-TDM treated control mouse lungs (C). Higher magnification reveals "foamy" vesiculated macrophages aggregating between regions of relatively normal parenchyma. Formalin fixed lung sections were hematoxylin and eosin stained (H&E); histopathology shown at 10x magnification; inset at 40x, scale bar = 300μm. Sections represent data obtained from repeated experiments. 4-6 mice were in each group, per experiment.

Histological Assessment of TDM Induced Pathology.

Mice administered TDM IV showed a focal accumulation of macrophages at day 7 post injection (**Figure 1**). The pathological reactivity demonstrated widespread inflammation and severely reduced open alveolar space. Small focal hemorrhagic petechiae were present as part of the inflammatory response. Lymphocytic infiltration to lung tissue occurred around regions where granulomas coincided with vasculature. Slight hemorrhage was present throughout the tissue. There was visual evidence of occlusion of intermediate or small sized blood vessels. Activated macrophages with intracellular vesicles were predominant in regions of reactivity; limited to negligible accumulation of lymphocytes occurred within the focal response. General edema was not a major component of the response. Naïve (no TDM) mice did not demonstrate changes to lung architecture. Lungs from control mice exhibited normal pulmonary parenchyma; there were no noticeable cellular infiltrates, and limited presence of monocytic or leukocytic foci.

Pro-inflammatory Response in Pulmonary Tissue of TDM Treated Mice.

It was previously reported that administration of TDM results in a strong pro-inflammatory response [159]. Cytokine assessment was assessed by ELISA to confirm these findings. Lungs were examined at 7 days post administration of TDM. Significant production of pro-inflammatory mediators TNF-α, IL-1β, and IL-12p40 were observed relative to control mice; IL-6 was also elevated in the TDM treated group (**Figure 2**). Anti-inflammatory mediating cytokines were also evaluated; while there was minor increase in production of

TGF-β, it was not a significant change. There was no change, relative to controls, in IL-10 production (**Figure 2**).

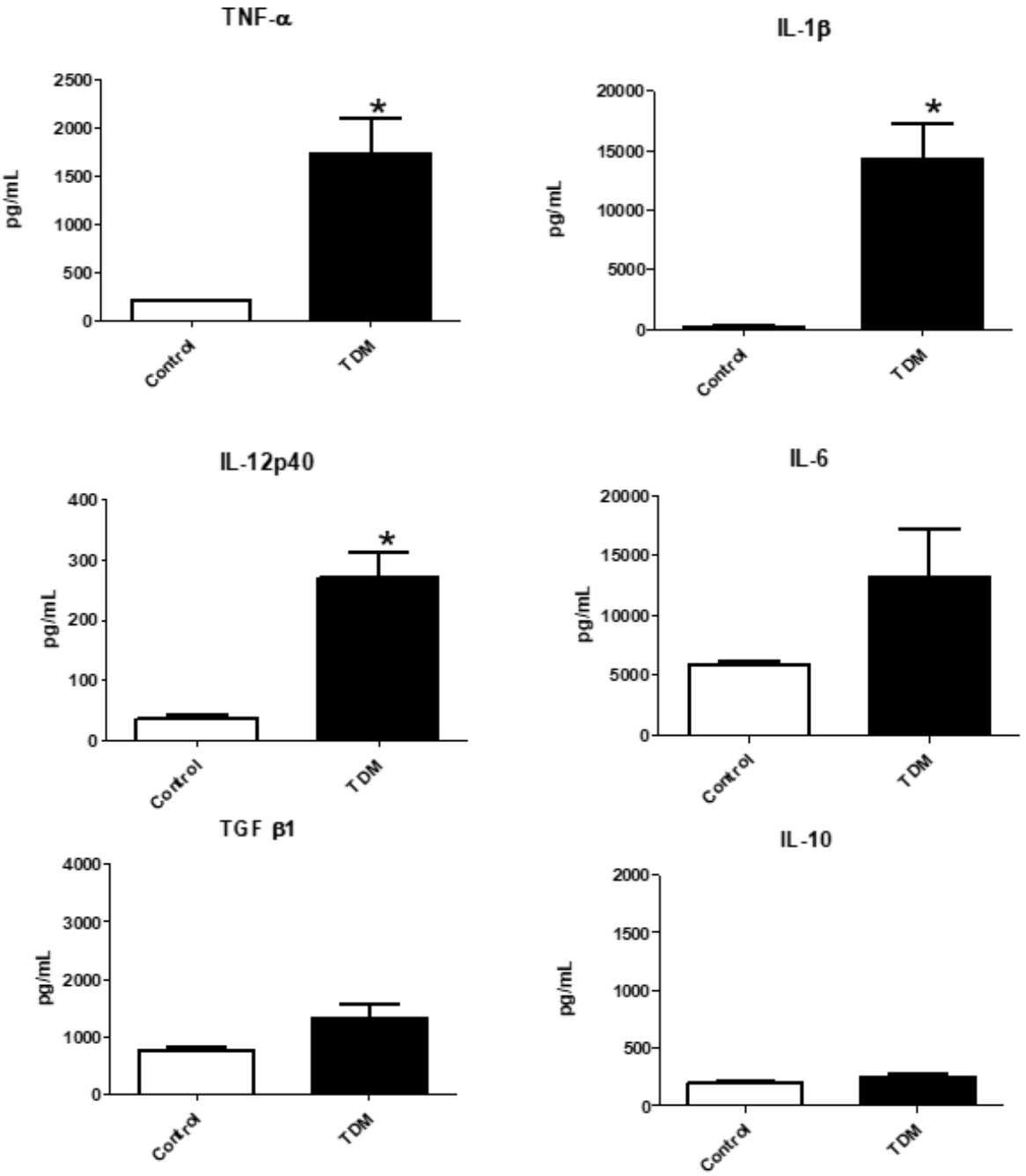

Figure 2. **Pro- and Anti-inflammatory Cytokine Mediators in Lung Tissue during TDM-Induced Response.** ELISA assessment of inflammatory cytokines revealed increase in production of TNF-α, IL-1β, IL-12p40 and IL-6 at day 7 post administration of TDM, compared to non-TDM treated control mice. Lungs of mice receiving TDM did not reveal significant changes in production of TGF-β and IL-10. Results represent mean ± SEM, representative data was collected from 3 independent experiments in which 4-6 mice were in each group per experiment. *; $p \leq 0.05$.

Identification of the M1-like Macrophage Phenotype within Regions of TDM Granulomas.

The extent of macrophage phenotypic polarization was investigated using flow cytometry. Lungs treated with TDM were dissociated, and individual cells were further examined for presence of M1-like and M2-like surface markers. Populations were initially gated on infiltrating monocytic macrophages ($CD11b^{hi}CD45^{hi}$) [170, 171]. **Figure 3** depicts data collected for M1-like markers CD38 and CD86, along with assessment for expression of the M2-like markers CD206 and the early growth response gene-2 (EGR-2). Treatment with TDM resulted in an overall accumulation of $CD11b^{hi}CD45^{hi}$ cells that expressed higher M1-like markers, but not the M2-like surface proteins. Specifically, CD38 was present on 39.50% +/- 3.33% on infiltrating macrophages, which was significantly elevated when compared to the non-treated WT group controls (7.76% +/- 2.24%; $p \leq 0.001$). Additionally, CD86 was present on 19.34% +/- 1.48% macrophages, compared to non-treated controls (5.31% +/- 0.61%; $p \leq 0.001$). **Figure 3** also lists the values for markers examined. CD14 was also highly elevated in this population (57.74% +/- 4.06%; data not shown).

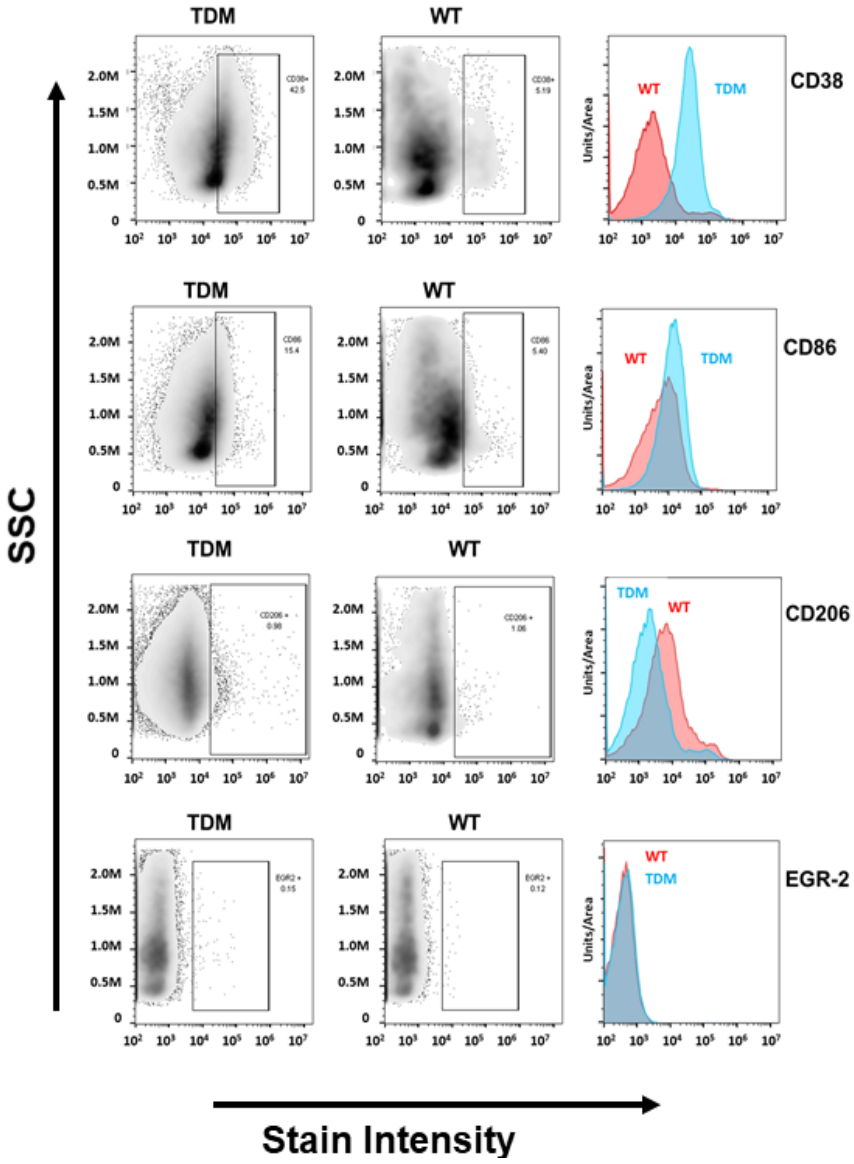

	CD38	CD86
Control		
Avg (%)	7.76	5.31
STDev (%)	2.24	0.61
TDM		
Avg (%)	39.5***	19.34***
STDev (%)	3.33	1.48

	CD206	EGR2
Control		
Avg (%)	1.24	0.11
STDev (%)	0.16	0.05
TDM		
Avg (%)	0.71	0.15
STDev (%)	0.51	0.07

***Figure 3*. Flow Cytometry Assessment of M1/M2-like Markers on Infiltrating Monocyte-Macrophages.** Isolated cells obtained from lungs at 7 days post administration of TDM were examined by flow cytometry for expression of M1-like markers CD38 and CD86 (top), and for M2-like markers CD206 and EGR-2 (bottom). Isolated cells were first gated to identify $CD11b^{hi}CD45^{hi}$ macrophages, then further analyzed for surface expression; Representative histographic plots of data accompany dot plots, side scatter (SSC) shown vs. signal intensity, for TDM treated (blue) or wild type (WT) controls (orange). Analysis on right indicates average (Avg) percent values with standard deviation (STDev) for each marker indicated from 4-6 mice. One Way ANOVA, $p \leq 0.05$, Tukey Post Hoc test for multiple comparisons: $^{**}p \leq 0.001$ for CD86 TDM vs wild type.

Immunohistochemical staining allowed localization of the CD11b+ macrophage population to regions of granulomatous response (**Figure 4A**), and specifically to areas of inflammation. Furthermore, staining for the CD38 surface glycoprotein marker on serial sections demonstrated presence of the M1-like population in a pattern overlapping that for CD11b, coinciding with regions of high macrophage activation within the granuloma's architecture (**Figure 4B**). The CD11b marker is present throughout the inflammatory foci, with diffuse staining in most of the monocytic cells. There is also a number of CD11b+ cells that are heavily stained; the presence of the CD38 marker appears to coincide with cells also expressing the higher levels of CD11b. Of note, not all macrophages within the granuloma exhibit CD38. Cells were also stained with anti-CD206 and anti-EGR-2, however presence of these M2-markers were not detected (data not shown). Taken together with the flow analysis, this suggests that the macrophages recruited to the focal inflammation during the pulmonary granulomatous response induced by the TDM are of the M1-like phenotype.

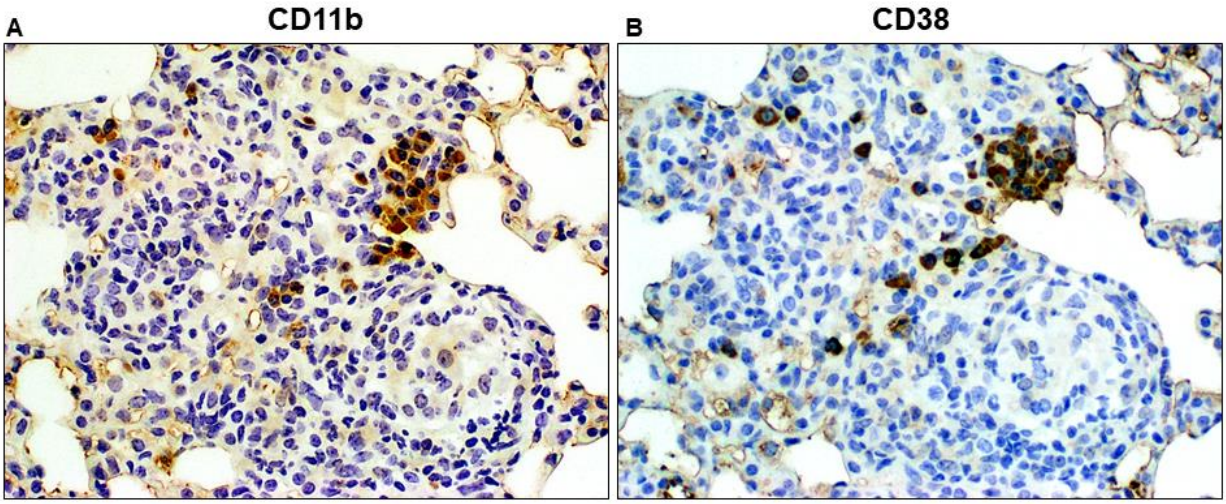

***Figure 4*. Localization of CD11b+ and CD38+ Cells to Pulmonary Regions of Focal TDM-Induced Inflammation.** Serial sections of formalin fixed lung tissue were reacted with antibody to CD11b (A) or CD38 (B), and subsequently visualized by way of standard HRP staining techniques. The acute regions of inflammation demonstrate the overlapping presence of both populations of cells within focal granulomatous regions. Representative section, 100x magnification.

Discussion

The establishment of the *Mtb* induced granuloma is a complex interaction of multiple cell phenotypes responding to a myriad of antigenic stimuli [172]. A multitude of studies have focused on mechanisms underlying development of the induced inflammatory response leading to development of this pathology. Clearly, the influence of any one specific molecule may not form an essential pathological bias *in vivo* during infection. However, a deficiency in production of purified cord factor, trehalose 6,6'-dimycolate [173], or manipulation of its structure [174], has certainly been shown to affect development and morphology of the early granulomatous pathology.

TDM has been identified as an immune mediator of both innate and adaptive inflammatory responses, and has been detailed as a virulence factor in reports focused on animal models [175]. Others have examined its link and relevance to human disease by descriptive comparisons to human pathological manifestations [21]. The nature of the induced pathology is clearly defined by physical parameters [176, 177]. Experiments using deficient mice allowed delineation of events that lead to establishment of the TDM-induced inflammatory granulomatous response [159]. Furthermore, investigators identified innate receptors that trigger distinct immune events [178]. This is the first report to our knowledge that examines the influence of TDM on accumulated M1-like or M2-like phenotype macrophages to the induced pulmonary foci. The results indicate that the presence of the

M1-like surface marker expression was significantly upregulated in TDM treated animals, as opposed to the WT control animals, following the TDM induced granulomatous response.

Our *in vivo* studies show a significant increase of CD86 expression on CD11b+CD45+ cells within pulmonary foci. This population may have been recruited from alveolar spaces, as shown to occur by Cohen, et. al, during *Mtb* infection [179]. At this time, it is unclear if the identified macrophages arrive as a committed M1-like population, or if the environment induces relative M1/M2-like pathology progression once cells arrive to the focus of inflammation. Other groups have identified cellular plasticity in immune cell phenotypes post arrival to pulmonary tissue post infection [180]. This may explain conflicting data from Kan-Sutton, et al., where they found that TDM produced nearly identical strong pro-inflammatory effects in purified BMMs without inducing changes in surface expression of CD86 [46]. Although difficult to compare *in vivo* and *in vitro* effect, it may be that the discrepancy between these studies was due to the nature of the presented TDM. Kan-Sutton used TDM adhered to the surface of beads; this format of exposure to TDM likely measured internalized effects on intracellular mechanisms associated with mycobacterial mycolic acid function, rather than those triggered via extracellular receptors. Our laboratory has also previously shown that TDM impacts intracellular trafficking events [181, 182]. Indeed, the nature of the engagement of macrophage can influence phenotypic and functional outcome [183].

A brief discussion on the evidence for specific cellular receptors for TDM engagement is warranted. Our data, along with previous findings on host macrophage receptors MARCO [160] and Mincle [39, 184, 185], and Mincle-related Clec4d [186], suggest a potential link between the existence of M1-like phenotype and engagement of those putative TDM receptors. An intriguing finding by Bowdish et al., indicated that TDM engagement with MARCO activates the TLR2 signaling pathway, with the end result of production of similar pro-inflammatory cytokines to those identified in our study; macrophages from mice lacking MARCO also produced a significantly reduced amount of TNF-α, IL-6, and IL-1β in response to virulent *Mtb*. In our model of TDM "infection", we observed a similarly strong pro-inflammatory response in lung tissue. However, engagement of the Mincle receptor could just as likely predict an M2-like outcome; Schoenen, et al. elegantly linked Cebpβ and Hif1α nuclear signaling pathways to TDM responsiveness in macrophages, with the end result of EGR (M2-like marker) synthesis [187]. Likely, phenotypic outcome is regulated through multiple receptors. A related Mincle ligand, the shorter chain TDM analog trehalose dibehenate (TDB), was also shown to differentially modulate M1-like (and M2-like) macrophage phenotypes, through Syk signaling processes [188]. Both Syk- and CARD9 pathway interactions have shown to then further engage development of directed hypersensitive responses [189, 190], as well as inflammatory signaling pathways [191]. Perhaps additional experiments comparing trehalose 6-monomycolate (TMM) or galactose-galactose 6,6' dimycolate (GDM) may shed light on the inflammatory response leading to presence of the M1-like phenotype found in this study. However, these molecules have previously shown limits, as they do not induce

MTB-like primary granulomas in oil-in-water emulsions. Nor do they engage macrophages in the same manner as TDM [181, 192]. Therefore, although we might expect little change in M1 markers on recruited cells due to TMM or GDM because of the lack of inflammation, those molecules may provide a handle on pathways related to development of the M1-like phenotype following TDM administration.

The rationale for induction of a strong macrophage pro-inflammatory response has been suggested to promote signals resulting in induction of differentiated hypersensitive populations [193]. *Mtb* has been shown to regulate internal pathways that may dictate polarity of macrophages [194]. Multiple antigens from tuberculosis *spp*, in addition to the mycolic acids, have been shown to trigger strong pro-inflammatory responses, which, again, are likely dependent upon receptor engagement. For example, specific engagement of CD38 affects polarization of Th1 immune responses to *M. avium* [195]. Other molecules, such as ESAT-6, demonstrated a mixed reported transitional function. Refai, et al., demonstrated that ESAT-6 drives macrophages to the M1-like phenotype, although in the presence of TLR-2 engagement it may exert anti-inflammatory M2-like polarization activity [196]. Huang, et al. reported that ESAT-6 contributes to primary innate granuloma formation by inducing an M1-type differentiation, occurring in the presence of strong IFN-γ activity. However, they also indicated that this was likely dependent on the stage of infection in which this molecule was examined (as well as presence of external mediators); ESAT-6 was shown to drive macrophages toward an M2-like phenotype at the later stages of the infection. Regarding *Mtb* antigens "in total", they have been shown to induce a robust M2-like phenotype of

human macrophages over time [197], with a shift away from CD86 towards CD206 surface expression in *in vitro* models. Those findings were consistent with presence of M2-like antigens seen on cells in various stages of post-primary granulomas from infected patients. However, it should be noted that these represent stages of infection occurring well after granuloma formation and Th1 infiltration, which is not seen in our results. Indeed, in our hands, we did not see reactivity to M2-like markers CD206 or EGR-2 in our histological sections. Therefore, the findings discussed do not preclude the results here.

Overall, the results presented support the hypothesis that purified TDM by itself can be a strong inducer of a M1-like polarization of macrophages. As such, it continues to be an effective tool to experimentally define the cross-regulation of inflammatory molecules and cellular recruitment cascades which culminate in pathological changes in models of lung granulomatous disease caused by *Mycobacterium tuberculosis* infection.

CHAPTER 3: LACTOFERRIN REDUCES MYCOBACTERIAL TREHALOSE 6,6'-DIMYCOLATE INDUCED M1-TYPE INFLAMMATION AND PERMITS FLUOROQUINOLONE ENTRY TO GRANULOMAS

This chapter is reprinted from The Biochemistry and Cell Biology Journal, Volume 99, Issue 1, Thao K T Nguyen , Zainab Niaz , John d'Aigle, Shen-An Hwang, Marian L Kruzel, Jeffrey K Actor, "Lactoferrin reduces mycobacterial M1-type inflammation induced with trehalose 6,6'-dimycolate and facilitates the entry of fluoroquinolone into granulomas", Page 73-80, *(https://doi.org/10.1139/bcb-2020-0057)*

Introduction

The *Mycobacterium tuberculosis* (*Mtb*) cell wall cording factor, trehalose 6,6'-dimycolate (TDM), is a physiologically-relevant and useful molecule for modeling early macrophage mediated events during establishment of the tuberculosis-induced granuloma pathogenesis. Recent findings support the hypothesis that this mycobacterial mycolic acid can specifically recruit M1-like polarized macrophages [198], occurring in the absence of a significant M2-like phenotypic response. Many observers hypothesize that the initial strong M1-like biology contributes to creation of a microenvironment essential to limit dissemination of the bacilli [146]. On one hand, this leads to containment of the *Mtb* in infected macrophages within circumscribed granulomas [43]; this is advantageous to the host. However, this containment has the negative effect of also protecting sequestered

organisms from immune-mediated killing by immune effector cells which are unable to effectively penetrate the granulomatous structure [70].

No current therapeutic modalities focus to modulate host immune responses to ameliorate tuberculosis disease [199, 200]. The molecule lactoferrin (LF), a natural iron-binding protein found within neutrophils, is a proven modulator of inflammation [93, 201] which is active in immune functions [202] as well as in host defense [203, 204]. In our hands, bovine-derived LF was able to ameliorate TDM-induced granuloma cohesiveness [205]. This could be clinically advantageous, with potential function for LF to permit recruited cells entry into a densely populated pathological area. Relating this to models of mycobacterial infection, LF was shown to modulate the pulmonary granulomatous response induced during *Mtb* challenge, with no loss of adaptive response or increased dissemination of organisms to tissues peripheral to lungs [206].

Furthermore, organisms within granulomas are isolated from efficiently delivered anti-mycobacterial due to the compact nature of the pathological structure [31, 43, 207]. Thus, an increase in current therapeutic efficacy may be achieved through incorporation of adjunct components that curtail development of aggressive destructive pulmonary pathology. LF was able to mediate a change in cohesiveness of the granulomatous response during model systems of granulomatous response. Therefore, LF may ultimately function as an adjunct therapeutic, serving as a novel strategy for TB disease treatment.

We therefore investigated a recombinant human version of lactoferrin (rhLF) expressed in a CHO cells [208] to modulate the TDM-induced granulomatous pathology.

Experiments were designed to address if LF would serve as an adjunct molecule for increased penetration of anti-mycobacterial agents to regions of granulomatous pathology induced in mice. Furthermore, as an initial investigation into a possible mechanism of action, specific markers of M1- and M2-like macrophages [65] were evaluated to determine if rHLF alters the phenotypic profile of recruited macrophages post induction of the TDM response.

Materials and Methods

Mice. Female C57BL/6 mice (Envigo, Houston, TX) of five to six weeks of age, and approximately 20g weight, were incorporated into the studies. All *in vivo* work was completed at the University of Texas Health Science Center (UTHSC), according to approved protocols (animal welfare ethics committee document HSC-AWC-17-0089). The work was completed under animal welfare ethical guidelines established at the UTHSC, with conditions detailed in the approved animal welfare document.

TDM-Induced Pathology. Mycobacterial-derived trehalose 6,5'-dimycolate (TDM; cord factor) (Enzo Life Sciences, Farmingdale, NY) was given as an oil/water emulsion prepared as described [159, 198], intravenous (IV), at a volume of 100 µl per animal. Control mice received material formulated with no addition of TDM; controls did not exhibit inflammation, as previously reported [158, 163]. All mice were sacrificed at times indicated post injection of formulated material.

Lactoferrin and Ofloxacin. Recombinant human lactoferrin (rHLF; LFH-101; endotoxin <10 EU·mg^{-1}) was kindly provided as lyophilized powder by PharmaReview Corporation (Houston, TX.). Mice were given 1 mg rHLF in a 100 µL volume by oral gavage [209, 210] at day 3 and 6 after TDM injection. The two dose administration schedule was chosen to match the initiation phase and establishment of granuloma development in this model, and levels previously seen effective using bovine derived lactoferrin [209].100 µL volume of 30 mg/ml ofloxacin (Sigma Life Science; O8757-1G), solubilized in DMSO and diluted 1:10 with PBS, was intraperitoneal administered 30 minutes prior to sacrifice.

Pulmonary Cytokines. Lungs were excised, homogenized, and incubated at 37^{o}C and 5% CO_2 for at least 2 hours in Dulbecco's Modified Eagle's medium (DMEM) that contained 50 µg/ml L-Arginine, 100 µg/ml penicillin, 50 µg/ml gentamycin, 50 µg/ml HEPES, and 10% fetal bovine serum. Collected supernatants were examined by enzyme-linked immunoassay (ELISA), as previously detailed [198], for the presence of TNF-α, IL-1β, IL-10 and TGF-β following manufacturer's instructions (DuoSet kits, R&D Systems, Minneapolis, MN). TGF-β samples were pretreated with 1:5 ratio of 1N HCl, then neutralized. Results were calculated by a standard curve produced to manufacturer's recombinant molecules.

Histological Assessment. The mouse lung large right lobe was perfused with 1mM EDTA in phosphate buffered saline, fixed in 10% buffered formalin (Fisher Scientific, Pittsburg, PA), embedded in parafin, sectioned (5 µm thick), and stained with with hematoxylin (Surgipath, Richmond, IL) and eosin (Richard-Allen Scientific, Kalamazoo, MI) as per standard procedures at the Histology Laboratory at the UTHSC McGovern Medical School (Houston, TX). H&E stained slides were then used to capture photos of granulomas under the Olympus

BX51 microscope using the Nuance Cri Multispectral Imaging System FX (PerkinElmer). The granuloma section was first identified and captured under H&E brightfield staining, then Ofloxacin's fluorenscent signals were captured under 40x lens with FITC filter (emmission restriction set between 540nm to 560nm) after 120ms of exposure. All microscopic settings and factors were maintained throughout the photo taking process. All image files have the same dimensions of 1392 x 1040 with 72 dpi resolution.

Computerized Analysis. High resolution scanned images of H&E stained slides were assessed for lung inflammation using Motic DSAssistant software (Kowloon Bay, Kowloon, HK), in a two step process using Fiji ImageJ (Version 1.52o 23 April 2019, National Institutes of Health, Bethesda, MD) with plugin MorphoLibJ [211], described in part in [198]. Minimum and maximum values for hue, saturation, and brightness were set at: 120, 255; 0, 255; and 0, 255, respectively. Total cell area measurement used a modified version detailed elsewhere [212] where peak threshold was set at 164, similar to published examples [166]. Values were averaged within treatment groups and normalized to non-treated controls. For each granuloma, the total fluorescent area (ofloxacin absorption) and the total granuloma area were measured in pixel units using CellProfiler (software version 3.1.5) pipeline algorithm [211], with described modifications [213]. Background was eliminated by the measured average fluorescence signal from control mouse lung H&E-stained histological slides using CellProfiler.

Flow Cytometry Analysis. Flow cytometric assessment was performed as previously done by Nguyen, et al. [198]. Briefly, lungs were extracted from WT, TDM and TDM/LF

treated mice. Homogenized tissue was treated for 30 minutes with Collagenase/Hyaluronidase (StemCell Technologies) and DNAse I (Sigma) in RPMI-1640 with 1% 100X pen/strep and 2.5% HEPES (Thermo Fisher Scientific), and 5% HI FBS (Corning). Cells were purified prior to staining using a 70% GE Healthcare Percoll (Cat# 17-0891-01) gradient Surface markers chosen to delineate murine M1-like and M2-like macrophages were based on published data from Jablonski, et al., [65], later detailed by Orecchioni, et al. [168]. Similar findings were identified in human monocyte-derived macrophages [169]. Cells were stained in accordance with manufacture recommendation, using Live Dead Aqua (eBioscience, L34966) for 15 minutes, then FC (antibody receptor) blocked with Anti-Mo CD16/CD32 (eBioscience, 14-0161-86) for 15 minutes. Staining used the following antibodies against specific receptors: CD38 (Biolegend, Cat# 102728) APC/Cy7, CD86 (Biolegend, Cat# 105014) PE/Cy7, CD206 (Biolegend, Cat # 141704) FITC, EGR2 (eBioscience, 17-6691-82) APC, CD11b (Biolegend, Cat# 101208) PE, and CD45 (eBioscience, 48-0451-82) eFluor 450 for 20 minutes. Cells were fixed with 2% paraformaldehyde, and evaluated on a Beckmen Coulter Cytoflex S flow cytometer (Model No. B75442). Data was then analyzed using FlowJo V10 (Becton Dickinson).

Statistical Analysis. Data presented are a combination of 2-4 experimental repeats. Each experiment incorporated 3-6 mice per group. Data was reported as percent area and compared between groups using a two-tailed t-test in GraphPad Prism, version 5.03. Differences between means were considered statistically significant at a value of $p \leq 0.05$, or otherwise indicated.

Results

Lactoferrin Reduces TDM-Induced Lung Pathology.

Intravenous administration of the mycobacterial mycolic acid TDM, results in development of defined inflammation in C57Bl/6 mice, which mimic many aspects of the granulomatous reactions seen during infectious challenge with virulent *Mycobacterium tuberculosis*. Using the well-defined TDM-induced granuloma model, the histologic accumulation of monocytic cells within the lung readily occurs post TDM administration (**Figure 5**). The number of focal accumulates grow in number, size and complexity through day 7, resulting in occlusion of vascular regions and limitation of open alveolar compartments (**Table 1**). Results are due to treatment with TDM; emulsion vehicle alone was not able to induce morphological change [209]. Oral treatment with 1 mg of recombinant human lactoferrin (rHLF) on days 2 and 4 post TDM administration markedly reduced, but did not completely eliminate, the TDM-induced focal responses. Granulomas were diminished by day 4, with significant reduction in both size and number ($p<0.05$) of inflammatory accumulates at both days 4 and 7 post induction of the response.

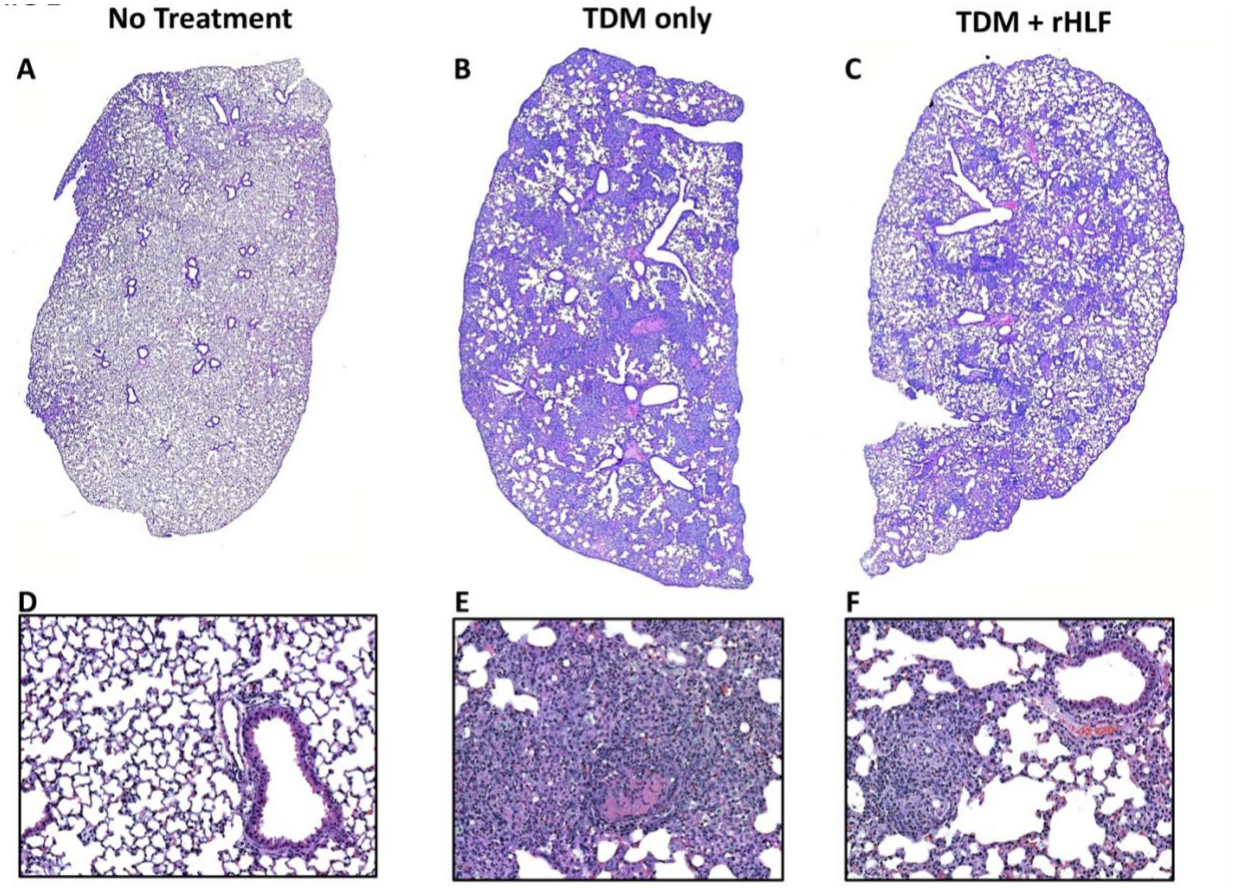

***Figure 5*. Lactoferrin Induced Reduction of Gross Pulmonary Granulomatous Inflammation caused by TDM.** Lungs from mice given TDM (B, E) were assessed after 7 days and compared to control (A, D) or rHLF treated (C, F) animals. Histologic examination revealed acute granulomas with monocytic cell infiltration and presence of focal, "foamy" vesiculated macrophages, and occluded vascular regions. rHLF treatment markedly reduced inflammatory response, with limited pathological damage to lung tissue. Formalin fixed lung sections were hematoxylin and eosin stained; histopathology shown at 10x or 300x magnification. Histographs represent sections obtained from repeated studies with 4 to 6 mice in each group.

	Granulomas/mm^2			Granuloma Size (μm^2)	
	Day 4	**Day 7**		**Day 4**	**Day 7**
TDM					
Avg (%)	3.88	7.79		16.73	40.52
STDev	1.15	1.38		2.23	4.97
TDM + LF					
Avg (%)	2.6	2.04*		12.47	17.74*
STDev	0.47	0.33		2.66	4.39

***Table 1*. Lactoferrin reduction in TDM-induced inflammatory response.** Histological assessment of granulomatous inflammation was assessed at 4 and 7 days post administration of TDM, with or without rHLF treatment. Average number and size of inflammatory foci were measured, with standard deviation shown. N = 4 to 6 mice per group; experiments were repeated at least twice. *$p \leq 0.05$.

Decreased Pro-inflammatory Response in Lungs after Treatment with Lactoferrin.

Administration of TDM results in a strong pro-inflammatory response [214, 215]. The cytokines TNF-α and IL-1β were assessed in lungs by ELISA to examine if the histological changes due to the rHLF administration would also affect responses. Lungs were examined following TDM administration, with or without rHLF treatment. There was significant production of pro-inflammatory mediators TNF-α and IL-1β, which was significantly reduced by the rHLF. (**Figure 6**). The anti-inflammatory cytokines were also examined; there was no change, relative to TDM, in IL-10 production after additional treatment with the rHLF (**Figure 6**). Similarly, there was no production of TGF-β, which was also not altered by addition of rHLF (not shown).

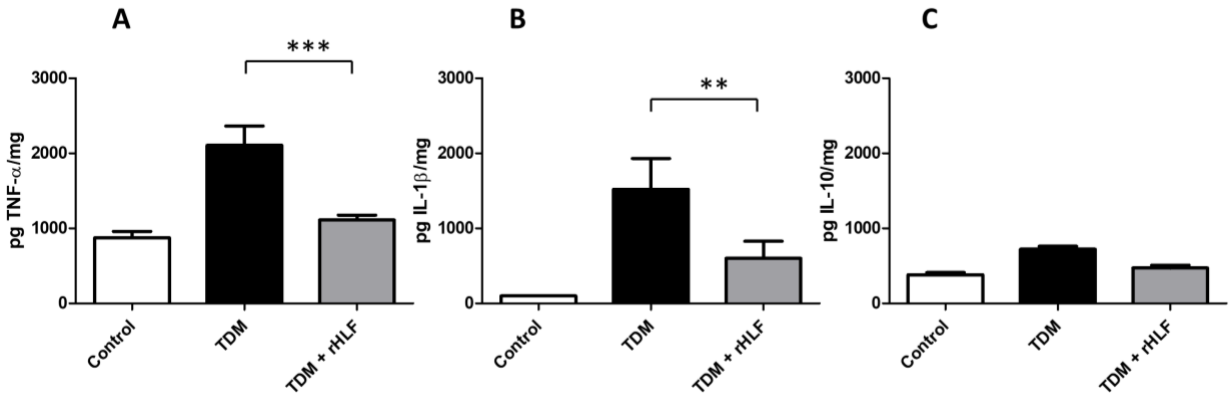

***Figure 6*. Lactoferrin reduced pro-inflammatory cytokines during TDM-induced pathology.** Assessment of inflammatory cytokines post treatment with rHLF revealed decreases in production of TNF-α (left panel, A) and IL-1β (middle panel, B) within lungs at day 7 post administration of TDM, compared to TDM alone treated mice. Mice receiving TDM did not reveal significant changes in production of IL-10 (right panel, C); no alteration of this was apparent in the rHLF treated group. Results represent mean ± standard deviation, data was collected from 2 independent experiments with 4-6 mice in each group per experiment. One Way ANOVA, $p \leq 0.01$, Tukey Post Hoc test for multiple comparisons: $^{**}p \leq 0.01$ for IL-1β TDM+rHLF vs TDM and $^{***}p \leq 0.001$ for TNF-α TDM+rHLF vs TDM.

*Lactoferrin Treatment Increases Ofloxacin Penetration to Inflammatory Foci***.**

The histological complexity of the TDM-induced pathology has been previously reported [214, 215]. Treatment with rHLF markedly altered the inflammatory response, resulting in monocytic foci that were less dense. It was hypothesized that the physical nature of the granulomas were altered in a manner to allow greater permeability of small molecules, such as those useful in treatment of mycobacterial infection. To test this hypothesis, mice were intraperitoneal administered the fluoroquinolone ofloxacin on day 7, just prior to sacrifice. Visualization of lung histological sections prepared from the non-treated mice demonstrated presence of the naturally fluorescent ofloxacin therapeutic agent evenly distributed throughout pulmonary vascular regions (not shown). In contrast, the TDM alone treated mice demonstrated a relative exclusion of fluorescence penetration into regions of inflammatory response (**Figure 7, top left panel**). This was expected, as the compact nature of the granulomatous response results in small blood vessel occlusion [215]; indeed, pockets of fluorescence can be readily visualized in occluded vessels. Of interest, treatment with the rHLF was able to restore ability of the ofloxacin to penetrate evenly throughout regions of granulomatous inflammation (**Figure 7, top right panel**). The relative fluorescence was quantitated via software analysis; the rHLF treatment significantly ($p<0.001$) increased the ability of ofloxacin to penetrate regions of focal inflammation (**Figure 7, bottom panel**).

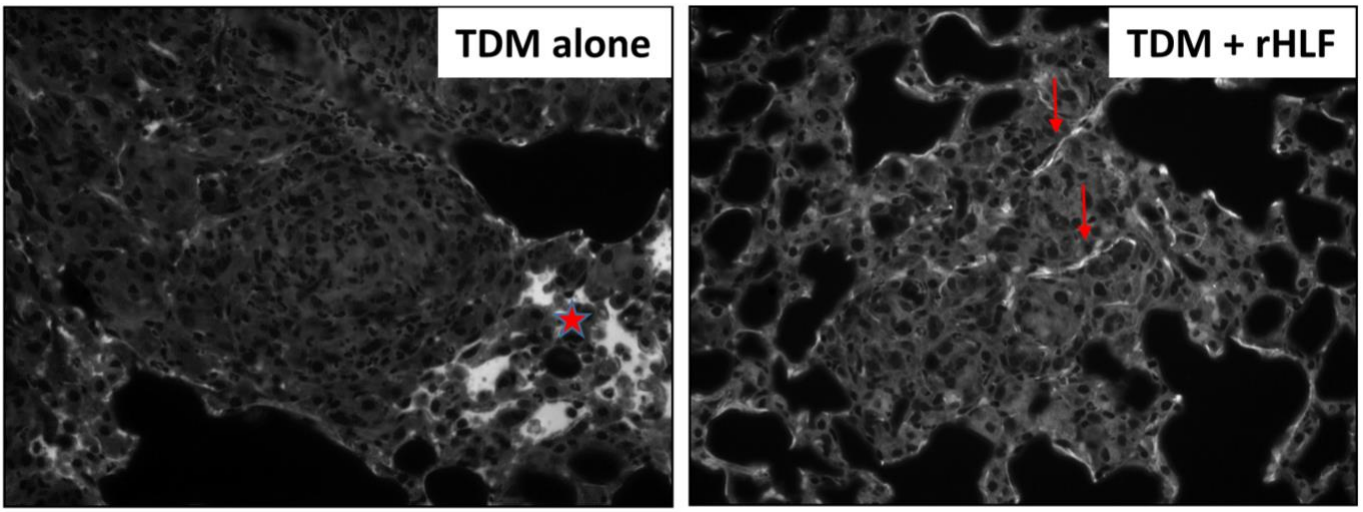
TDM alone
TDM + rHLF

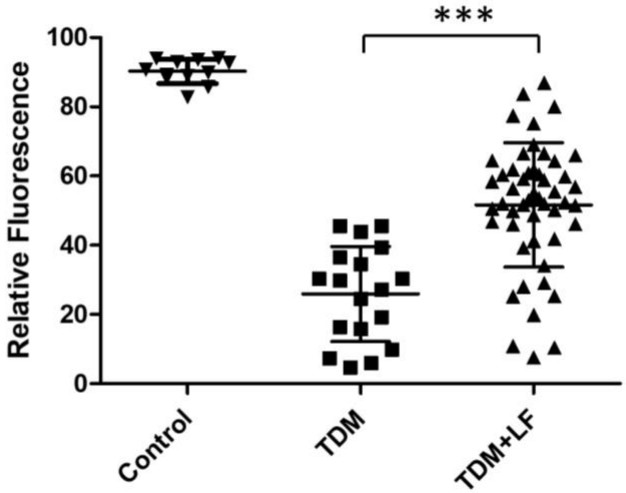
***
Relative Fluorescence
100
80
60
40
20
0
Control
TDM
TDM+LF

***Figure 7*. Increased penetration of ofloxacin to granulomas post lactoferrin treatment.**

Lungs from mice given TDM alone (top, left), or TDM plus rHLF treatment (top, right), were assessed for presence of the fluoroquinolone ofloxacin. Ofloxacin penetration was limited in the TDM alone group, except for regions of high vascular occlusion (red star). The rHLF treated mice permitted entry of ofloxacin via penetrating vasculature (red arrows), and entry within monocytic cells within the pathological foci. Histographs are shown at 40x magnification. Quantitative assessment of relative fluorescence for individual inflammatory foci are represented (bottom), with average and standard deviation included. One Way ANOVA, $p \leq 0.05$, Tukey Post Hoc test for multiple comparisons: $***p \leq 0.001$ for TDM+LF vs TDM.

Lactoferrin Reduces Accumulation of Recruited M1-like Macrophages.

It was recently shown that the TDM-induced granulomatous inflammation was comprised of recruited monocytic macrophages primarily of the M1-like phenotype [198]. Cells were isolated from TDM-induced lungs at 7 days post treatment, and $CD11b^{hi}CD45^{hi}$ macrophages [170, 171] were examined by flow cytometry for presence of M1-like and M2-like surface markers. **Table 2** depicts data collected for M1-like markers CD38 and CD86, and for the M2-like markers CD206 and the early growth response gene-2 (EGR-2). Treatment with TDM resulted in an overall accumulation of $CD11b^{hi}CD45^{hi}$ cells that was approximately 1.77-fold (+/- 0.19-fold) compared to the rHLF treated group. The TDM alone cells expressed higher M1-like markers, but not the M2-like surface proteins. The M1-like marker CD38 was present on 24.70% +/- 11.18% of recruited macrophages. CD86 was present on 12.34% +/- 3.37.48% macrophages. Overall, there were fewer recruited macrophages to the lungs in the rHLF treated mice. In addition, the M1-like markers on these cells were markedly reduced in the rHLF treated group. Specifically, there was a significant reduction in both CD38 (10.19% +/- 1.16%; $p<0.05$) and CD86 (3.98% +/- 0.73%; $p<0.001$). There was a modest (non-significant increase) in M2-like makers in the rHLF treated group compared to TDM alone, however, this was comparable to the non-treated control animals.

	M1-Like Markers		M2-Like Markers	
	CD38	**CD86**	**CD206**	**EGR2**
Control	N=3			
Avg (%)	7.76	5.31	1.24	0.11
STDev	2.24	0.61	0.16	0.05
TDM	N=6			
Avg (%)	24.72	12.34	0.53	0.15
STDev	11.18	3.37	0.35	0.07
TDM + LF	N=4			
Avg (%)	10.19*	3.98**	1.13	0.11
STDev	1.16	0.73	0.71	0.04

***Table 2*. Assessment of M1/M2-like Markers on Infiltrating Monocyte-Macrophages.**

Isolated $CD11b^{hi}CD45^{hi}$ macrophages from lungs at 7 days after administration of TDM were examined for the M1-like markers CD38 and CD86, and for the M2-like markers CD206 and EGR-2. Comparisons are made to rHLF treated mice. Average percent values with standard deviations are given for each marker; control values shown were previously reported [198]. One Way ANOVA, $p \leq 0.05$, Tukey Post Hoc test for multiple comparisons: $*p \leq 0.05$ for C38 TDM+LF vs CD38 TDM and $**p \leq 0.001$ for CD86 TDM+LF vs TDM.

Discussion

The results presented in this study confirm the utility of LF to ameliorate primary granulomatous inflammation [205, 206] and permit entry of therapeutic molecules to sites of macrophage mediated pathology. LF has been extensively examined as a mediator of inflammatory responses (reviewed in [201, 216]), interacting directly with pathogens [217] and controlling host immune homeostasis [218, 219]. Indeed, recombinant human LF is adept at regulating induced macrophage inflammatory responses [220], functioning well as an immune-therapeutic in models of animal sepsis and SIRS [221] and oxidative stress [222]. The experiments outlined here extend our previous findings to show that rHLF can alter MTB-like primary pathology, and specifically modulate TDM-induced inflammation [210] to further allow penetration of therapeutic molecules to sites of immune reactivity.

The TDM-induced granulomatous response is a well-accepted model, if not a simplified model, of the primary pathology seen during mycobacterial infection [21]. Primary tuberculosis infection is defined as a mixed macrophage and adaptive cellular response. Marino, et al., hypothesized that macrophage phenotypes drive the granulomatous response during MTB infection [147], where the initial response is mediated by an M1-like macrophage phenotypic recruitment with balanced contribution from M2-like responders as disease progresses [146]. This fits into known processes for granuloma regulation, where an initial M1-like proinflammatory response characterized by production of TNF-α is required for development of pathology [223, 224]. Marakala, et al., further hypothesized that polarized M1 macrophages are recruited, altering the natural M2-like

anti-inflammatory environment of the alveolar macrophages which first encounter inhaled organisms. This series of events thereby initiates a protective environment to encapsulate bugs into a defined spatial region [142].

The first antigens encountered during mycobacterial infection are likely to be surface mycolic acids [21]. Khan, et al., suggested that these molecules alter the plasticity of macrophages during initiation of the granulomatous response [60]. Although it remains to be determined if macrophages undergo true polarization events during first encounter with mycobacterial antigens, Nguyen, et al., reported that the phenotype of recruited macrophages during the TDM-induced response is of the M1-like phenotype [198]. This phenomenon was reconfirmed in the results presented here. Our results show that the addition of LF during inflammation induced by the TDM mycolic acid led to a decrease in presence of M1-like macrophages. An object of further study would include LF's direct effect on macrophage polarization. Of interest, Gao, et al. used an immunocomplex containing LF to polarize towards M1-like activity [225]. However, that observation was likely due to the construct used, which contained a linked immunoglobulin Fc region that likely interacted with macrophage receptors to alter cellular responsiveness. The results in this report use a purified LF that was not complexed to other molecules.

Host-directed therapies to combat tuberculosis pathology are a promising approach for new treatment modalities [226, 227]. The concept to regulate TNF-α as a method to control mycobacterial infection has been explored in the literature [228]. This is a double-edged sword; too much TNF-α results in tightly packed mycobacterial granulomas, while its

complete absence is detrimental to initiation and development of a protective pathology [214, 224]. LF, as an adjunct host-directed therapeutic, has demonstrated effects on macrophages to limit, but not eliminate, TNF-α [220, 221]. In the studies presented here, LF was useful to decrease the magnitude of the M1-like phenotype, in essence functioning as a host-directed adjunct therapeutic in a non-infectious model of tuberculosis primary infection.

Interest is high in LF as a therapeutic agent to control inflammation and prevent sepsis in neonates, with several clinical trials completed or still in progress [229-233]. Mechanistically, administration of LF may exert anti-inflammatory effects in newborns through modulation of myeloid suppressor cells which are present in high numbers early in life [234]. *In vitro*, LF was able to convert newborn monocytes to MDSCs, with subsequent activity to control inflammatory pathology [235]. The utility of LF to convert cell phenotypes may be similar to alteration of the monocyte phenotypes noticed in this report, however, the concept requires further investigation. At this time, it is not known if the change in recruited macrophage phenotypes is directly due to changes in polarization or in selective recruitment in our model system.

The fact that LF was successful as an oral administered agent is a bonus to future clinical use. At this time, it is unclear how LF functions systemically, since it is known to undergo proteolytic degradation in the gastrointestinal tract by digestive enzymes [236, 237]. It was recently reported that inflammatory pathways identified in transcriptome profiles of oral delivered rHLF significantly overlapped with those of intravenous

administration (M.L. Kruzel, unpublished communication, [238]). While this study was done in rats, it appears that LF-induced effects are systemically transduced, even if the protein is degraded in transit.

Formation of a densely packed granuloma essentially limits efficacy of immune effector cells. Modulation of the magnitude of the granulomatous response could potentially overcome the ability of the organism to escape immune-mediated killing, limiting the compact physical nature of the sequestration of infected cells and allowing effector cell access to the infected nidus. Indeed, oral delivered bovine LF was shown to control pulmonary granulomas in models of MTB infection, without loss of adaptive response or subsequent increase in organism dissemination to other tissues [206, 210]. There are numerous advantages for limited disruption of the primary granuloma during mycobacterial infection, especially if organisms remain contained. Of major interest relative to the findings presented here would be increased drug penetration to sites of compact pathology which harbor infectious agents. The advantages of increased drug penetration to areas where organisms reside include a greater ability to overcome drug resistance development in slowly replicating pathogens, and limitation of toxicity complications with potentially shorter duration of therapeutic treatment times. Ofloxacin, a naturally fluorescent anti-mycobacterial analog of the effective fluoroquinolone therapeutic ciprofloxacin [239, 240], was used in these studies because it permitted detection using a multispectral fluorescent imaging system without addition of modifying tags for detection. LF treatment correlated highly and significantly with the ability of ofloxacin to penetrate into granulomas. It was our subjective impression that while the penetration of ofloxacin

occurred more readily in smaller granulomas, there was increased fluorescence in nearly all inflammatory foci in the LF treated groups, irrespective of granuloma size.

Overall, the recombinant human LF served as an adjunct molecule for increased penetration of anti-mycobacterial agents to regions of induced granulomatous pathology. Mechanistically, this correlated with a shift away from the presence of M1-phenotypic macrophages at the site of pathology. Future studies will investigate the role of LF to alter polarization of inflammatory macrophage phenotypes responding to pathogenic signals. Furthermore, it will be critical to examine LF as an adjunct therapeutic to enhance penetration of antimycobacterial agents during tuberculosis disease, as a way to augment therapeutic treatment to control infectious-related pathology. In addition, the mechanisms of oral delivered lactoferrin must be further investigated.

CHAPTER 4: RECOMBINANT HUMAN LACTOFERRIN REDUCES INFLAMMATION AND INCREASES FLUOROQUINOLONE PENETRATION TO GRANULOMAS DURING MYCOBACTERIAL INFECTION

Introduction

Despite world-wide extensive research and eradicating efforts, *Mycobacterium tuberculosis* (*Mtb*) remains a major infectious pathogen to the human population with approximately 10.0 million infected cases and 1.5 million deaths reported in 2020 globally [241]. The initial host-pathogen interaction, and complex immunological responses, culminate in an inflammatory pathology within pulmonary tissue which is characterized as a primary granulomatous disease [21, 242]. These granulomas and associated lesions obstruct normal pulmonary functions. Active research investigates how *Mtb* directly induces the granulomatous response, focusing on areas of pathological damage and bacterial burden that are most severe during primary infection.

Mtb associated factors are involved in the recognition and activation of host cells within the bronchial regions, leading to uptake by alveolar macrophages [34]. This interaction triggers a series of immune responses via the production and release of cytokines by infected and responding macrophages [243]. For example, trehalose 6'6-dimycolate (TDM), an abundant mycobacterial mycolic acid, directly triggers a granulomatous response [21, 198]. TDM-activated macrophages release pro-inflammatory

mediators, such as TNF-α and IL-1-β, along with additional chemotactic factors, to further recruit immune cells to areas of infection [36, 40, 244]. Over time, additional recruited immune cells participate in formation of organized, sphere-shaped primary inflammatory structures at the infected site [42]. There exists a balance between host and organism; the granulomas formed during active *Mtb* infection contain and limit bacterial dissemination [43], yet organisms have adopted mechanisms to survive and grow inside macrophage host cells. Indeed, recruited naive macrophages can become new potential sites for *Mtb* to shelter and replicate [47].

Clinically, the physical nature of the granuloma also limits penetration of anti-mycobacterial therapeutics; as granulomas mature, reduction in vascularization limits drug delivery to within granulomas where large populations of *Mtb* may reside [48, 49, 70]. The physical nature of the host immune response therefore represents a challenge in treating *Mtb*-infected patients – it contributes to prolongation of treatment while permitting a small population of *Mtb* to escape elimination. The lack of complete penetration of antimycobacterial agents also indirectly increases risk of developing antibiotic-resistance [245-247]. Therefore, multiple lines of investigation currently are aimed at improving drug delivery through focused targeting to either the manipulate the granuloma structure, or to augment immune responses to *Mtb* that lead to granuloma development [248].

Novel approaches to *Mtb* treatment include host-directed therapies [76] which are focused in two major fronts; the first augments immune response using immune-based

treatments [77], while the second alters the resultant immunopathology [78]. Examples of immune-based treatment methods include agents that target the macro-autophagic compartment, such as vitamin D and retinoic acid, which increase phagocytosis to augment the lysosomal degradative processes inside macrophages [79]. Ibuprofen, an anti-inflammatory drug, functions as an adjunct treatment by facilitating pyrazinamide to alleviate pathological damage in the lungs [77, 80, 81]. These immune-based approaches have significant potential, demonstrating superior disease outcomes in clinical trial results [249, 250]. While promising, the obstacle in drug delivery to macrophages inside established granulomas persists [84]. Therefore, therapies that target pathologies, in addition to antimycobacterial function, may subsequently be more useful as clinical tools. A well-known example of the immunopathological alteration approach is blocking excess TNF-α, a key pro-inflammatory cytokine required for granuloma formation [224, 251]. TNF-α inhibitors have been used to treat other inflammatory diseases effectively [85-87]. However, its current downside is that TNF-α inhibitors can lead to increased bacterial dissemination; abolishing the granuloma containment modality runs the risk of *Mtb* reactivation [88-91].

Lactoferrin, a glycoprotein known for its ability to bind iron, has been extensively studied for its role as an immune modulator in host defense in disease models [219, 252]. It falls into the category of “immune modulators”, and has been identified to reduce pathology of the tuberculoid granuloma [92]. In addition, lactoferrin has been shown to boost immune memory response in vaccine models, while reducing pro-inflammatory

response in lipopolysaccharide (LPS) exposed mouse models [93, 94, 96, 97, 253]. Relative to the study described in this report, bovine lactoferrin significantlly reduced inflammatory pathology in TB-infected mice [98]. Both human and bovine lactoferrins were also shown effective to limit inflammation in the non-infectious TDM-induce granuloma mouse model [78, 99].

Lactoferrin treatment reduced the M1 phenotypic response to TDM, and limited pathological damage in murine lungs [78, 198]. The lactoferrin treatment also significantly increased penetration of the second-line anti-mycobacterial agent Fluoroquinolone into TDM-induced granulomas [78]. Such anti-inflammatory response in the lactoferrin-treated mice, along with other data showing lactoferrin reduces pro-inflammatory phenotypes in macrophages [136, 137], suggests that lactoferrin had a modulating pro-inflammatory response on granulomas. The studies presented here extend theses observations to examine if lactoferrin can modulate granuloma permeability and drug distribution during active *Mtb* infection. Here, the effect of lactoferrin on the permeability of granulomas to fluoroquinolones is examined in the *Mtb*-infected mouse model, when administered as a prophylactic (prior to granuloma formation) or therapeutic (after granuloma establishment) intervention. These experiments shed light on mechanisms underlying changes to the *Mtb* pathological events due to lactoferrin adjunct treatment.

Materials and Methods

Mice. Five-week-old female C57BL/6 mice were purchased from Envigo (Houston, TX) with 18-20 grams initial body mass. Eight to ten mice were used per group, per time each point indicated. All *Mtb* infections occurred in biosafety level 3 facilities under the University of Texas Health Science Center at Houston institutional guidelines (IBC-18-014), with approval from the animal ethics committee (AWC-17-0089).

Recombinant human lactoferrin and ofloxacin, and delivery to mice. CHO-expressed recombinant human lactoferrin (rHLF; >98% purity; <10% iron saturated; <0.5 EU·mg^{-1}; Cat# LFH-101) was kindly provided as lyophilized powder by PharmaReview Corporation (Houston, TX) [254, 255]. The rHLF was reconstituted in dH_2O to a concentration of 1 0 mg·mL^{-1}. From day 14 to day 28 after *Mtb* infection, mice were given 1 mg·(100 µL)$^{-1}$·mouse^{-1} of rHLF by oral gavage every other day as prophylatic treatment, similar to reported use in models of mycobacterial granulomatous responses [92, 209, 210]. 1 mg/ml was found to be more productive than a 100 µg/ml dose (**Figure 8**). From day 21 to day 28 after *Mtb* infection, another group of mice were given 1 mg·(100 µL)$^{-1}$·mouse^{-1} of recombinant human lactoferrin by oral gavage every other day as therapeutic treatment. Ofloxacin (Sigma Life Science; O8757-1G) was given at 100 µL of 30 mg·mL^{-1}·mouse^{-1}, solubilized in DMSO and diluted 1:10 with PBS, was intraperitoneal administered 30 minutes prior to sacrifice [256].

No Treatment

A

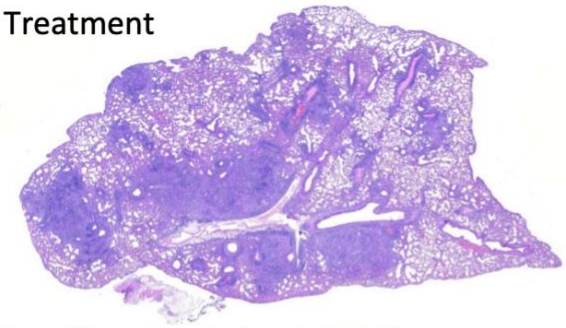

LF, 1mg/day, Prophylactic (D14)

B

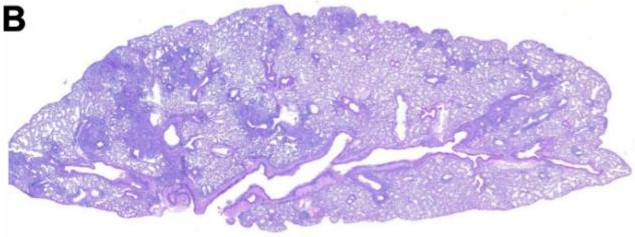

LF, 100µg/day, Prophylactic (D14)

C

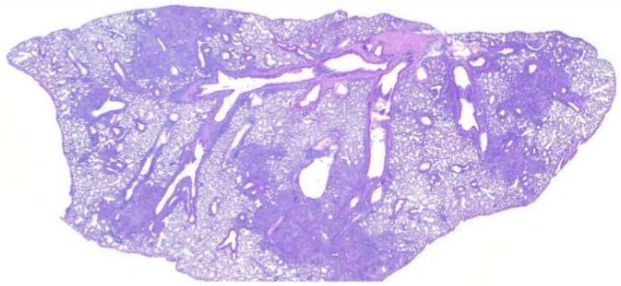

LF, 1mg/day, Therapeutic (D21)

D

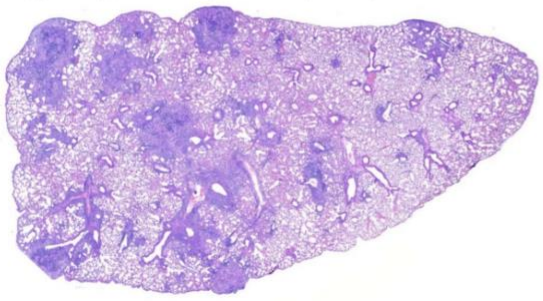

LF, 100µg/day, Therapeutic (D21)

E

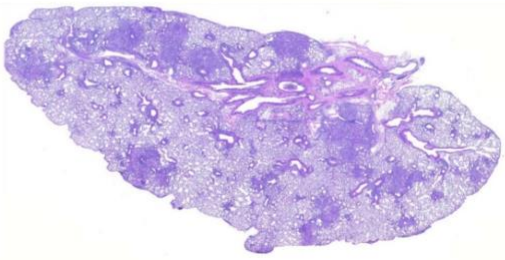

***Figure 8*. Lactoferrin treatment reduces pulmonary inflammation post infectious challenge with *Mtb* in a dose dependent response.** Lungs from *Mtb* infected mice were assessed at day 28 post aerosol infection (A) and compared to animals given bovine LF in the prophylactic group (B,C) or therapeutic group (D,E). Histologic assessment revealed primary granulomatous response with monocytic cell infiltration, dense cellular foci, and occluded vascular regions in control infected mice. Both prophylactic and therapeutic rHLF treatment reduced inflammatory response resulting in modest inflammatory foci and reduced pathological damage to lung tissue. While both doses (100 μg and 1 mg levels) were productive in limiting focal inflammation, the higher dose was more consistent between treatment groups. Hematoxylin and eosin stained histographs represent formalin fixed lung sections at 10x magnification obtained with 8 to 10 mice in each group; study representative of repeat experiments.

Mtb infection. Aerosol infections were done as previously reported [253, 257], using Mycobacterium tuberculosis, strain Erdman (TMC 107, American Type Cell Culture). Organisms were cultured in Middlebrook 7H9 broth with 10% supplement (5% bovine serum albumin, 2% dextrose, and 0.5% Tween 20 in distilled water) to log phase. Pelleted bacteria were resuspended in phosphate buffered saline (PBS) and diluted to 3×10^8 colony forming units (CFU) per ml using McFarland standards. Bacteria were sonicated to disperse aggregates. The bacterial CFUs for each time point, including day 1 post infection, were confirmed by plating serial dilutions on Middlebrook 7H11 agar plates (Hardy Diagnostics, Santa Maria, CA) using the large right lobe of the mouse lung that was weighed and homogenized into 2 mL PBS, which were incubated at 37 °C for 3 – 4 weeks. Mice were infected for 4 weeks, with treatments described above, using the protocol shown in **Figure 9**. Bovine lactoferrin, shown to have biological equivalency to the rHLF [92] was used for analysis of CFU dissemination to other organs and to reconfirm bioequivalence in dose response treatments (**Figure 10**).

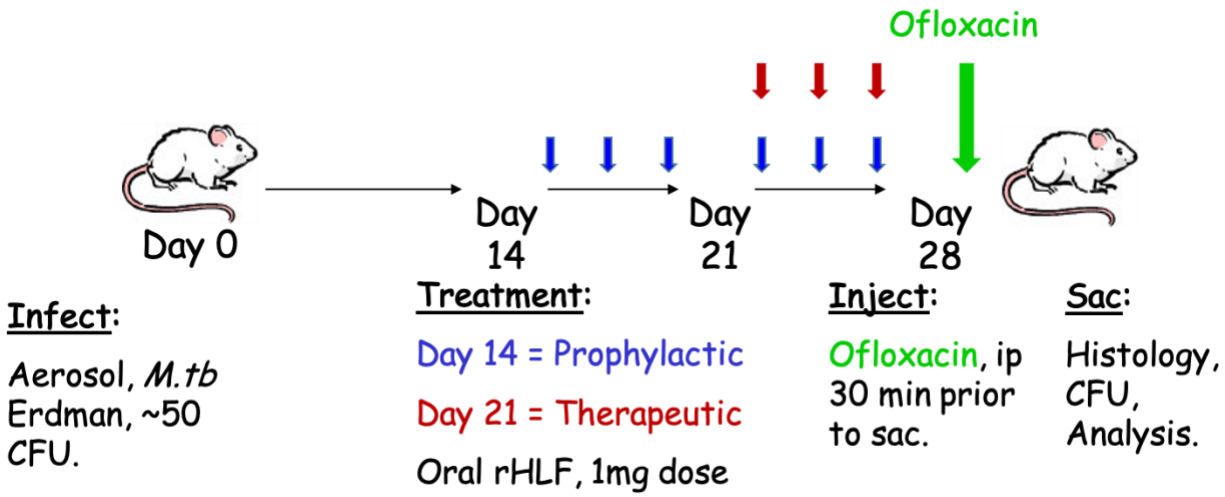

***Figure 9*. *Mtb* infection and lactoferrin treatment scheme.** C57Bl/6 mice were aerosol challenged with *Mtb* and treated with rHLF administered every other day orally beginning on day 14 (prophylactic; 6 total doses), or beginning on day 21 post infection (therapeutic; 3 total doses). Mice were intravenous injected with ofloxacin 30 minutes prior to sacrifice, at 28 days post initial infectious challenge.

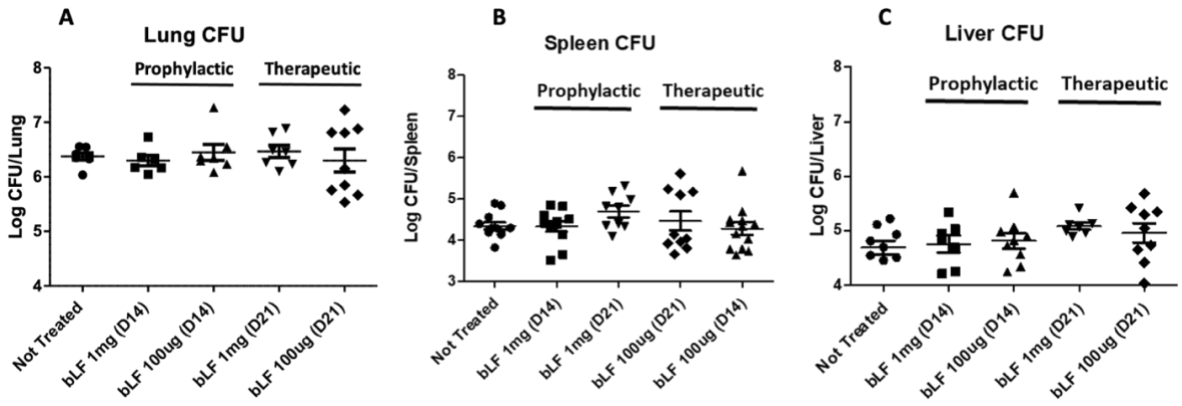

***Figure 10*. Mycobacterial burden in lactoferrin treated mice.** C57Bl/6 mice were aerosol challenged with Mtb, strain Erdman, and treated with bovine lactoferrin (bLF) given as 100 µg or as 1 mg dose administered every other day orally beginning on day 14 (prophylactic treatment), or beginning on day 21 (therapeutic treatment) post infection. Lung (A), spleen (B) and liver (C) were removed on day 28 post infection; tissues were assessed for bacterial CFUs confirmed by plating serial dilutions on Middlebrook 7H11 agar plates using the large right lobe of the mouse lung that was weighed and homogenized into 2 mL PBS, which were subsequently incubated at 37 °C for 3 to 4 weeks and represented as CFU burden per organ. Data are presented as individual mice with the mean and SEM indicated, $n \geq 6$ mice per group. One Way ANOVA, $p \geq 0.05$, Tukey Post Hoc test for multiple comparisons.

Histological assessment. The small left lobe of the mouse lung was collected and fixed in 10% buffered formalin. For histologic analysis, the lung was sectioned (5 µm thick) and stained with hematoxylin and eosin (H&E) and acid-fast staining as per standard procedures [253]. The histological assessment of the lung tissue following aerosol infection was done as previously reported [257]. Multiple sections from at least 6 mice per group were analyzed using Motic DSAssistant digital software (version 1.0.7.44; Kowloon Bay, Kowloon, HK) [78]. H&E stained and acid-fast stained slides were viewed by a trained pathologist, with descriptive results obtained in an experimentally blinded manner.

Immunohistochemistry. Fixed lung was embedded in paraffin, sectioned, and stained for immunohistochemical examination, similar to methods described [258], diluted at 1:2000, was performed according to manufacturer's instructions with a modification of 20 minutes at low pH for antigen retrival, and visualized using standard HRP techniques and DAB chromogen using Dako reagents (Dako, Agilent, Santa Clara, CA). In a similar manner, M1-like marker CD38 (Invitrogen, ThermoFisher, Cat# 14-0381-02), diluted at 1:1000, M2-like marker CD 206 (Bioss, Cat# bs-4727R), diluted at 1:1000, and endothelial cell marker CD31/PECAM-1 (Cell Signaling, Cat# 77699T) diluted at 1:200 was used for visualization on serial slide sections. Hematoxylin counterstained slides were viewed by a trained pathologist, with descriptive results obtained in an experimentally blinded manner.

Quantitative assessment of pulmonary inflammation. High resolution scanned images of H&E-stained slides were assessed for lung inflammation and granulomas using

Motic DSAssistant software (Kowloon Bay, Kowloon, HK), in a two-step process using Fiji ImageJ (version 1.52o 23 April 2019, National Institutes of Health, Bethesda, MD) with plugin MorphoLibJ (McQuin et al. 2018), described in part in [78]. Minimum and maximum values for hue, saturation, and brightness were set at: 120, 255; 0, 255; and 0, 255, respectively. Total cell area measurement used a modified equation detailed elsewhere where peak threshold was set at 164 [166]. Values were averaged within treatment groups and normalized to non-treated controls. H&E-stained slides were also used to capture photos of granulomas under the Olympus BX51 microscope using the Nuance Cri Multispectral Imaging System FX (PerkinElmer). The granuloma section was first identified and captured under H&E brightfield scope, then ofloxacin's fluorescent signals were captured under 40x lens with FITC filter (emission restriction set between 540nm to 560nm) after 120ms of exposure. All microscopic settings and factors were maintained throughout the photo taking process with image files having the same dimensions of 1392 x 1040 with 72 dpi resolution. For each granuloma, the total fluorescent area or ofloxacin absorption area and the total granuloma area were measured in pixel units using CellProfiler (software version 3.1.5) pipeline algorithm [211], with described modifications [213]. Background was eliminated by the measured average fluorescence signal from control mouse lung H&E-stained histological slides using CellProfiler. The measurement on the selected lung section is reported as percent area that represents the ratio of ofloxacin absorption over the total granuloma area. All data was graphed and statistical analyzed in GraphPad Prism (version 5.03).

Statistical analysis. *Data obtained was compared across groups then analyzed using a paired Student* **t**-*test or one-way ANOVA with a Tukey post-hoc test; differences between means were considered statistically significant at a value of* $\mathbf{p} \leq 0.05$. *Data are presented are a combination of 2-3 experimental repeats. Each experiment incorporated 8-10 mice per group.*

Results

Oral administration of recombinant human lactoferrin alleviates pulmonary inflammation post Mtb infection.

Previous studies using bovine derived lactoferrin given in drinking water demonstrated that continuous-access oral delivery during *Mycobacterium tuberculosis* infection could reduce inflammation-related primary granulomatous pathology in mice [98]. A defined protocol was adopted to determine if recombinant human lactoferrin (rHLF) would initiate a similar protective response (**Figure 9**). Mice were aerosol infected with *Mtb*, strain Erdman, and rHLF was given by oral gavage beginning either prior to (prophylactic), or post (therapeutic) expected initiation of granulomatous responses. Histological assessment (**Figure 8 and Figure 11**) revealed marked reduction of pulmonary inflammation in both the prophylactic and therapeutic rHLF treated groups, in a similar manner to that previously reported with the bovine LF treatment. Specifically, the rHLF treatments demonstrated reduced complexity of granulomatous responses, smaller foci of inflammation, with less cellular accumulation and density in areas of inflammation. Quantitative measurement of inflammation confirmed histological reduction in pathology due to the rHLF treatments.

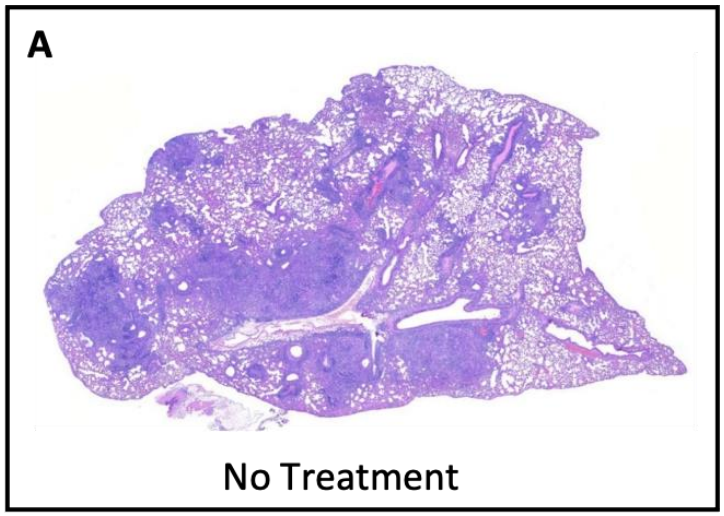
A
No Treatment

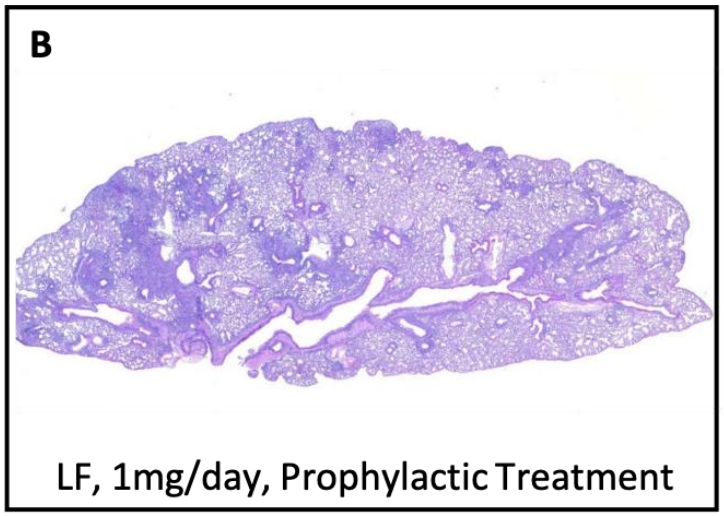
B
LF, 1mg/day, Prophylactic Treatment

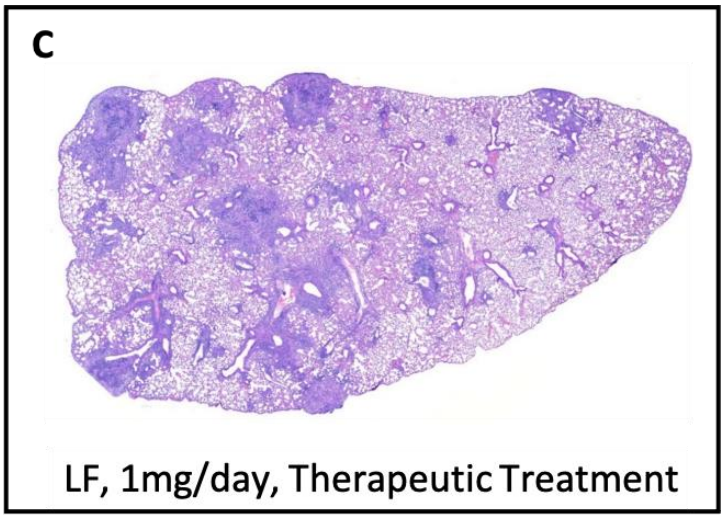
C
LF, 1mg/day, Therapeutic Treatment

***Figure 11*. Lactoferrin treatment reduces pulmonary inflammation post infectious challenge with *Mtb*.** Figure contains identical histographs from Figure 8 for text discussion**.** Lungs from *Mtb* infected mice were assessed at day 28 post aerosol infection (A) and compared to animals given rHLF in the prophylactic group (B) or therapeutic group (C). Histologic assessment revealed primary granulomatous response with monocytic cell infiltration, dense cellular foci, and occluded vascular regions in control infected mice. Both prophylactic and therapeutic rHLF treatment reduced inflammatory response resulting in modest inflammatory foci and reduced pathological damage to lung tissue. Hematoxylin and eosin stained histographs represent formalin fixed lung sections at 10x magnification obtained from repeated studies with 8 to 10 mice in each group; study representative of repeat experiments.

Whole right lobes of mouse lung were collected at 4 weeks post infections and processed for quantitative assessment of primary granulomatous response. Serial sections of H&E-stained tissue sections were high resolution scanned to assess area occupied by inflammation (**Figure 12**). The *Mtb* infected group had the largest occluded regions, with 24.79% ± 4.2% relative area occupied by inflammatory response. Both lactoferrin treatment modalities resulted in reduction of pathology. The prophylactic treatment resulted in reduction of granuloma area to 21.42% ± 4.1% of lung sections observed, while the therapeutic treatment significantly reduced occupied space to 17.36% ± 4.9% ($p<0.001$). Of interest, there was no change in CFU in the treated group in lung, liver or spleen tissue at 4 weeks post infection (**Figure 10 and Figure 12**), suggesting that (1) the short-term administration of lactoferrin did not alter pathogenic burden, and (2) the alteration due to treatments did not result in significant net dissemination to other tissues.

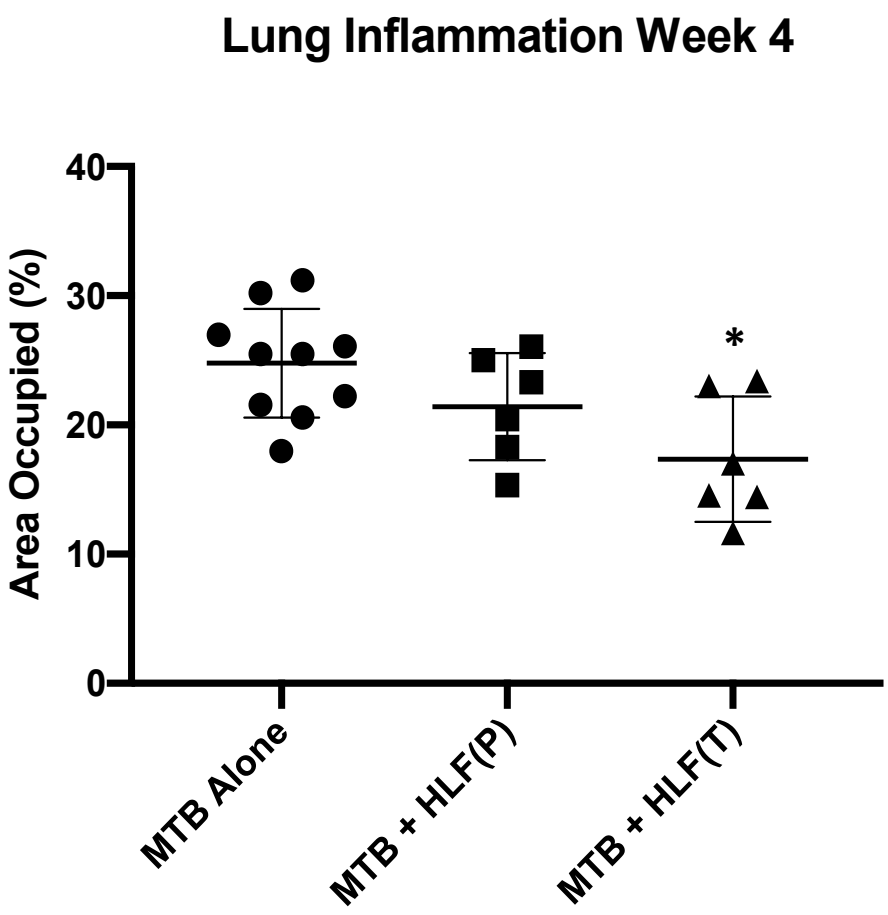

***Figure 12*. Decreased inflammatory response in lactoferrin treated mice.** *Mtb* infected mice were assessed by digital analysis for cellularity and inflammation. Area occupied of pulmonary scanned sections is shown for individual mice, with and without recombinant HLF treatments. Results represent mean ± standard deviation of the mean. Similar data was obtained in repeated experiments; 6-10 mice were included per group, per experiment. Prophylactic treatment, P; therapeutic treatment, T. One Way ANOVA, $p \leq 0.05$, Tukey Post Hoc test for multiple comparisons: $p \leq 0.05$ for MTB vs MTB+HLF(T).

Increased penetration of fluoroquinolone to inflammatory foci after treatment with rHLF.

The altered pathology of less dense granulomatous structures raised the hypothesis that vascular structure would be maintained in the rHLF treated groups, which could subsequently result in enhanced penetration of mycobacterial therapeutic agents to within regions of inflammation. To test this, the naturally fluorescent fluoroquinolone, ofloxacin, was intravenous administered to mice 30 minutes prior to sacrifice at the 28 days post infection time point. **Figure 13** reveals the penetration patterns of ofloxacin to within regions of pulmonary granulomatous response. The histologically dense inflammatory response in the *Mtb* alone group did not permit penetration of the fluoroquinolone, with little to no signal entering granulomatous foci. In contrast, both the prophylactic and the therapeutic rHLF treatment protocols resulted in granulomas that were permissible to ofloxacin penetration. Assessment of serial sections by high resolution scanning revealed significant differences between groups (**Figure 14**). The *Mtb* alone infected group had a relative fluorescent distribution of signal 13.76% ± 7.5%, confirming the relative difficulty in penetration of ofloxacin to within inflammatory regions. For comparison, the relative fluorescence of normal mouse lung had an average of 90.25% ± 3.5% penetration, reflecting antibiotic distribution to the lung at 30 minutes post delivery. Of interest, in alignment with visual observations described above, both rHLF treated groups demonstrated elevated ofloxacin penetration within granulomas. The prophylactic treatment permitted relative increases to 21.68% ± 14.1%, and the therapeutic treatment showed significant increase at 47.15% ± 14.9% presence of fluorescent signal. Furthermore, high power observation of

signal revealed accumulation of ofloxacin correlating with presence of activated foamy macrophages (**Figure 15**).

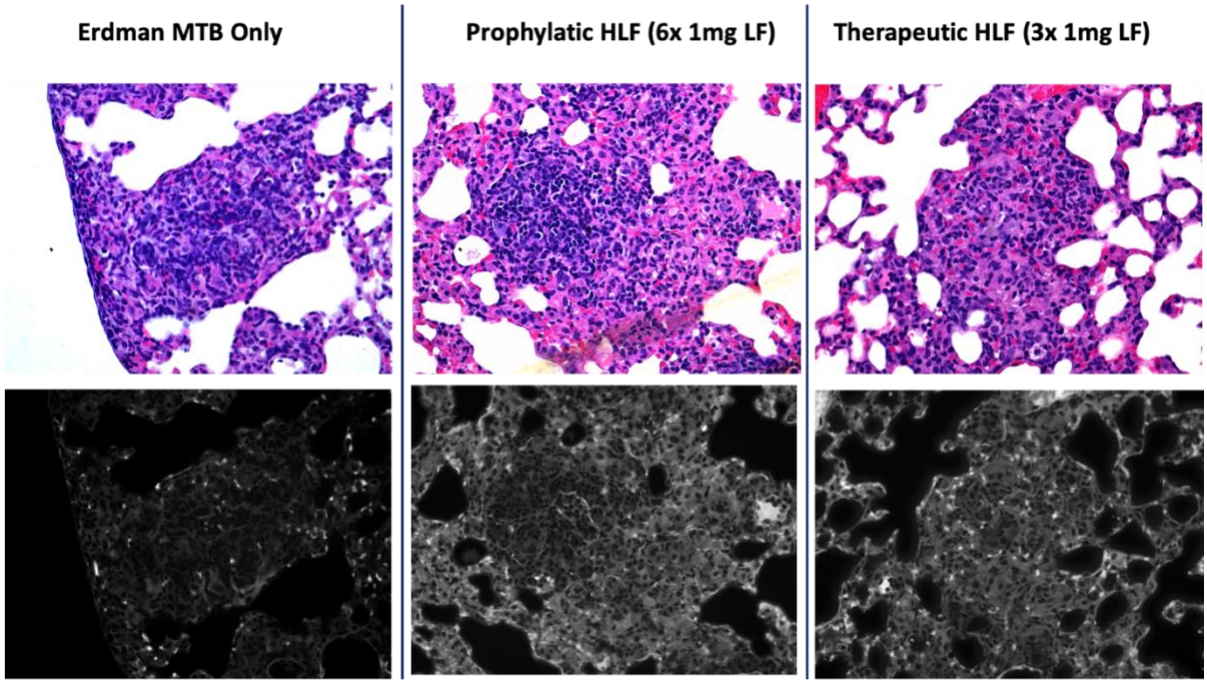

Figure 13. **Increased fluoroquinolone penetration to primary granulomas after treatment with lactoferrin.** Lungs from *Mtb* infected mice alone (left), or rHLF treated prophylactically (P; middle) or therapeutically (T; right) were assessed for presence of ofloxacin within granulomatous inflammation. Ofloxacin penetration was primarily excluded from inflammatory foci in the *Mtb* infected alone group, while both rHLF treated mice permitted entry of ofloxacin into regions of pathology. Top panels represent hematoxylin & eosin (H&E) brightfield stained histographs (40x magnification) with matching fluorescence captured using multispectral imaging (bottom).

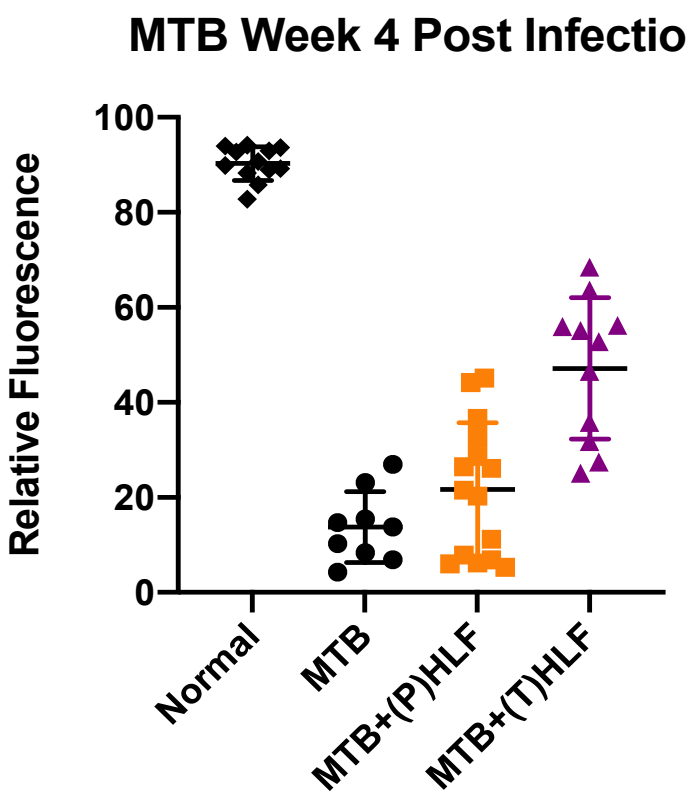

***Figure 14*. Relative fluorescence for individual inflammatory foci post lactoferrin treatment.** Quantitative assessment of ofloxacin penetration into granulomas in lactoferrin treated mice are compared to non-treated infected animals. Individual scans are represented from at least 8 mice per group; average values and standard deviation included. Prophylactic treatment, P; therapeutic treatment, T. One Way ANOVA, $p \leq 0.05$, Tukey Post Hoc test for multiple comparisons: *$p \leq 0.001$ for MTB vs MTB+(T)HLF and $p \leq 0.001$ for MTB vs Normal.

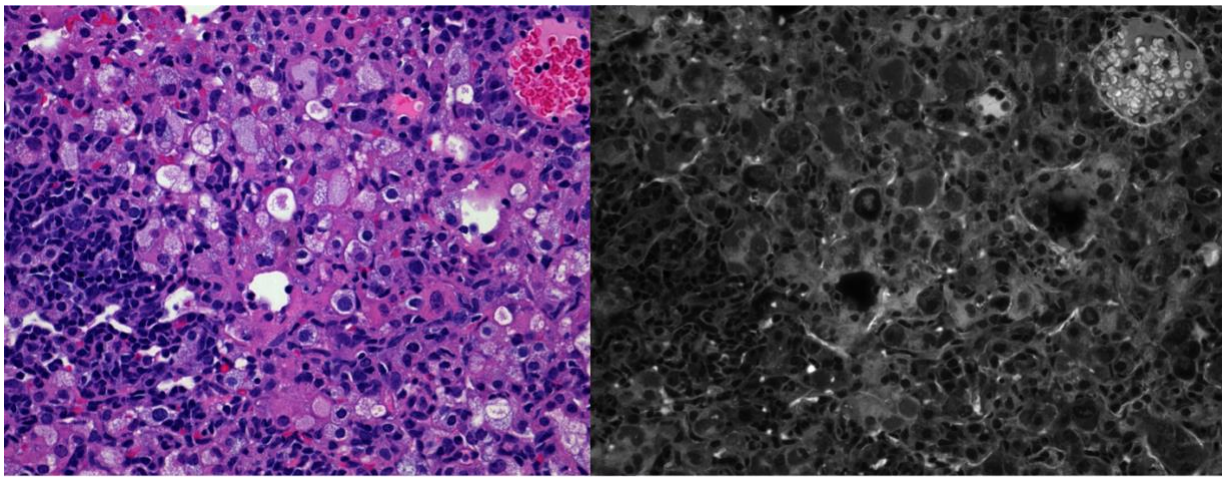

***Figure 15*. Accumulation of ofloxacin signal in activated macrophages in lactoferrin treated *Mtb* infected mice.** H&E staining of inflammatory foci within rHLF therapeutically treated mouse lung revealed acute regions of highly activated "foamy" macrophage-phenotypic cells. Mutispectral imaging correlates the presence of fluorescence which overlaps presence of activated cells, located within the focal granulomatous regions. Representative section, 100x magnification.

rHLF treatment correlates with retention of endothelial integrity in regions of pulmonary inflammation.

The *Mtb* alone infected group demonstrated responses consistent with pulmonary disruption to alveolar structure and associated vascular tissue. To further examine the effect of the rHLF treatment on vascular structure, histological sections were stained with PECAM-1. Granulomas in the *Mtb* alone group demonstrated collapsed alveoli with central accumulation of immune cells in regions that disrupt blood distribution (**Figure 16**). Central foci in these mice were devoid of staining, representing reduced vascularization to regions where organisms are expected to reside. In contrast, the rHLF treated mice demonstrated retention of vascularized structures within areas of inflammation, which also corresponded in matched sections to regions demonstrating ofloxacin penetration.

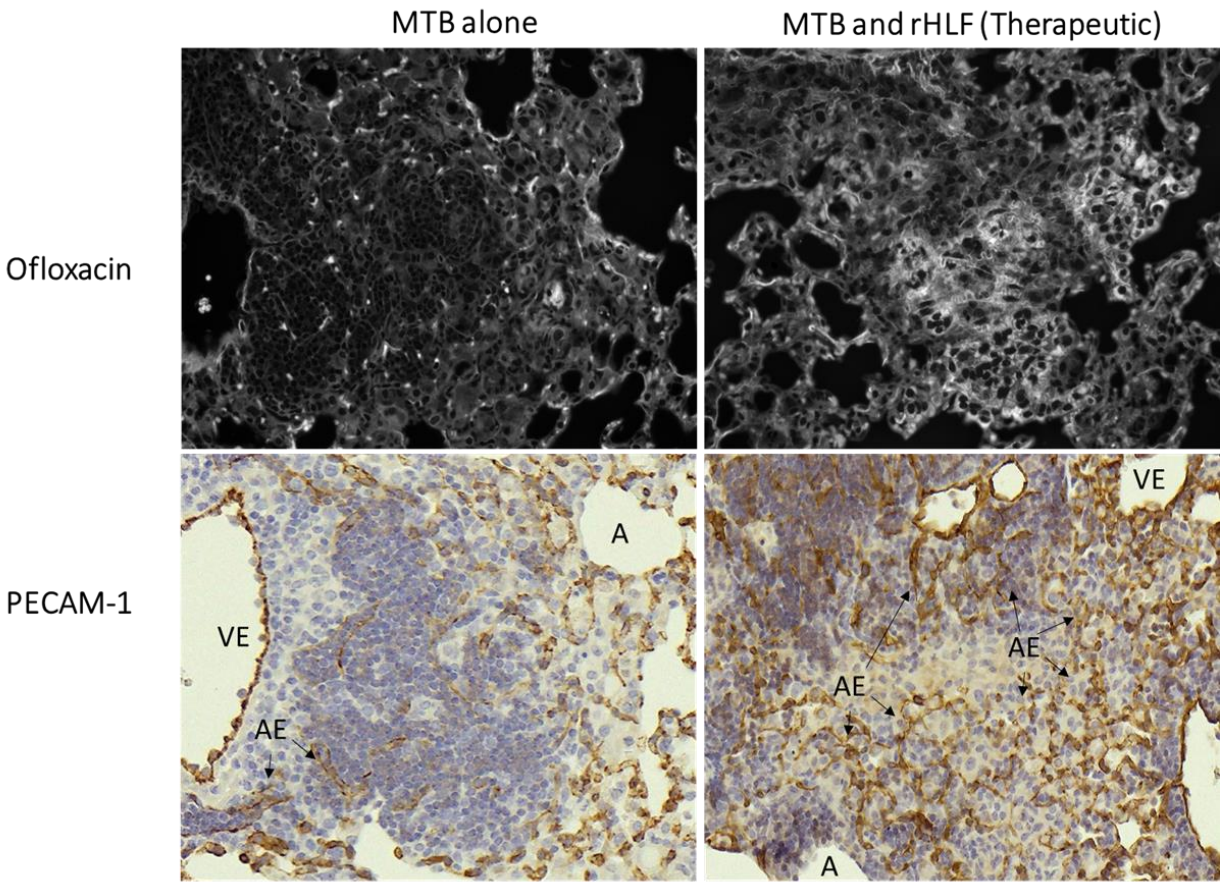

***Figure 16*. Retention of vascularized structures within regions of inflammation in lactoferrin treated *Mtb*-infected mice.** Serial sections compared presence of maintained vascular structure within inflammatory foci in *Mtb* infected mice (left side) or in *Mtb* infected mice treated therapeutically with rHLF (right side). Fluorescence patterns obtained using multispectral imaging (top panels) were compared with serial lung sections that were immunohistochemically stained for PECAM-1 to identify vascular endothelial populations within inflammatory foci (bottom panels). VE, vascular endothelium; AE, alveolar capillary endothelium; A, alveolus.

Altered localization of M1/M2-like macrophages in primary granulomas following rHLF treatment.

Recent reports demonstrated altered distribution of macrophage populations within primary granulomas, which may dictate pathological outcomes [259]. Therefore, sections were also immunohistochemically stained for general M1-like and M2-like antigens. **Figure 17** depicts immunohistochemical staining for the M1-like marker CD38 and for the M2-like marker CD206. The non-treated *Mtb* infected lungs revealed a concentrated pattern of staining demonstrating high presence of both M1-like and M2-like macrophages, primarily cuffing vascular regions surrounding regions of inflammation. Limited numbers of M2-like cells were visible (diffuse staining) within the granuloma itself. In contrast, the rHLF treated mice exhibited primarily only M2-like macrophages, which were evenly distributed throughout the primary granulomatous pathology; M1-like cells were not readily apparent.

MTB (Week 4)

MTB + (P) HLF (Week 4)

CD38
M1 Marker

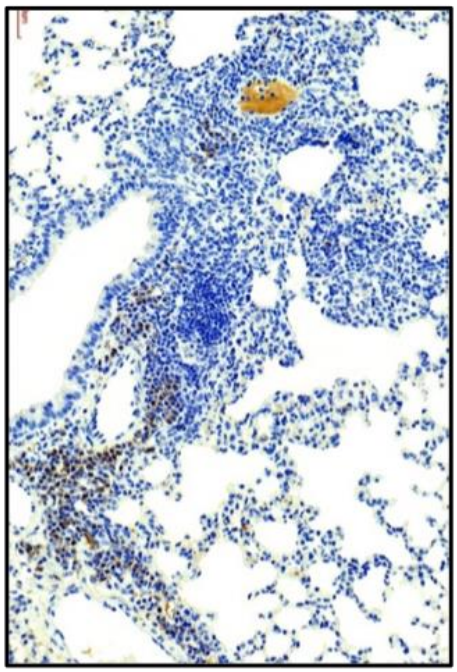

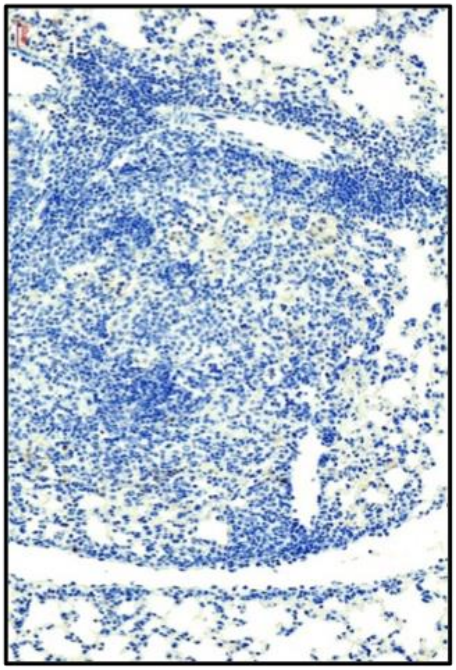

CD206
M2 Marker

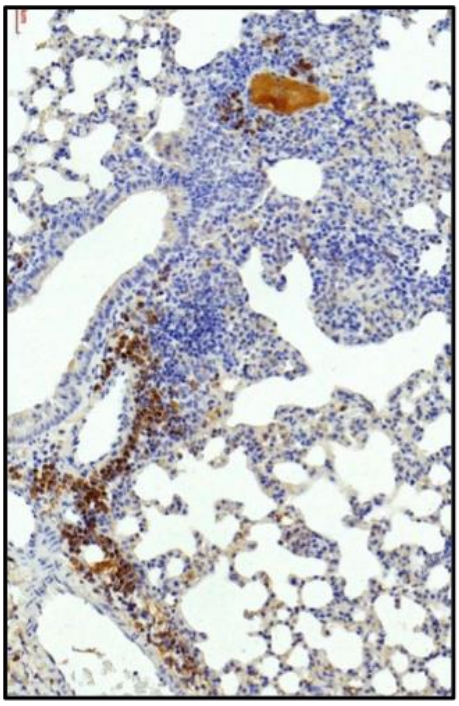

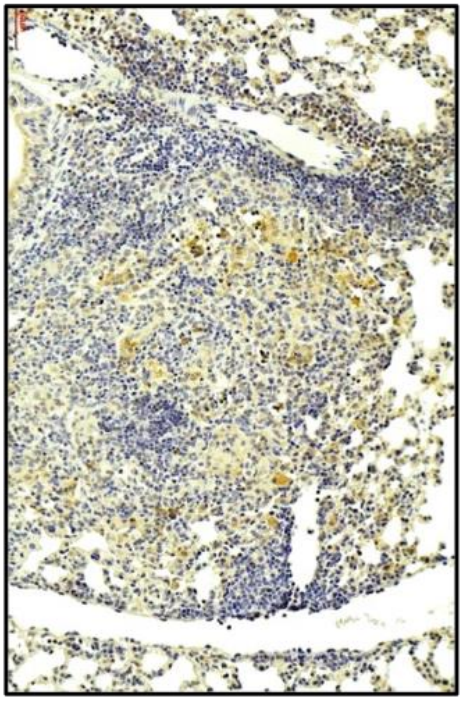

***Figure 17*. Altered localization of M1-like and M2-like populations following lactoferrin treatment of *Mtb* infected mice.** Serial sections of formalin fixed lung tissue were reacted with antibody to CD38 (top) or CD206 (bottom), for either *Mtb* alone (left side) or *Mtb* infected mice treated therapeutically with rHLF (right side). *Mtb* alone infected mice demonstrate accumulation of both M1- and M2-like phenotypic cells in a cuffing pattern surrounding blood vessels adjacent to granulomatous inflammation. A different pattern appears in the rHLF treated group, with minimal presence of M1-like phenotype and a primarily diffuse distribution of M2-like cells throughout the inflammatory foci.

Summary of Chapter

Infection with *Mtb* results in the primary formation of a densely packed inflammatory foci that limits entry of therapeutic agents into pulmonary sites where organisms reside. No current therapeutic regimens exist that modulate host immune responses to permit increased drug penetration to regions of pathological damage during tuberculosis disease. Lactoferrin is a natural iron-binding protein previously demonstrated to modulate inflammation and granuloma cohesiveness, while maintaining control of pathogenic burden. Studies were designed to continue examination of recombinant human lactoferrin (rHLF) to modulate histological progression of Mtb-induced pathology. The rHLF was oral administered prophylactically, at times corresponding to initiation of primary granulomatous response, or as a therapeutic intervention during granuloma maintenance. Treatment with rHLF demonstrated significant reduction in size of primary inflammatory foci following Mtb challenge, and permitted penetration of ofloxacin fluoroquinolone therapeutic to sites of pathological disruption where activated (foamy) macrophages reside. Increased drug penetration was accompanied by retention of endothelial cell integrity within pulmonary parenchyma. Finally, preliminary examination by immunohistochemistry revealed altered patterns of M1-like and M2-like phenotypic cell localization post infectious challenge, with increased presence of M2-like markers found evenly distributed throughout regions of pulmonary inflammatory foci in rHLF treated mice.

CHAPTER 5: DISCUSSION AND FUTURE DIRECTIONS

Discussion

The research for host-directed therapeutics is intended to increase the success of Tuberculosis treatment by affecting the immune response to modulate its function towards a protective response. Immune-based therapeutics is an intervention to orchestrate the reduction of non-productive inflammation in a way that redirects the immune response during infection in a manner that benefits the host. In contrast, immunomodulation is intended to lie within the framework of harmonizing with anti-TB treatment regimens against drug susceptible- and drug resistant-TB to improve the entire recovery process and promote absolute cure. Host-directed therapeutics are, therefore, considered necessary to reach the goals set by the World Health Organization (WHO) to end TB by 2035. Repurposed compounds and molecules are increasingly being used in human clinical trials investigating new host-directed therapeutics [260]. In this regard, lactoferrin, a well-known immune modulator that has been investigated in many clinical trials for protection and prevention of infections, came to be a promising candidate. In this thesis, lactoferrin is used as an immunomodulating therapeutic, given orally during the innate immune response, to both lessen the development of disease pathology and to improve drug distribution in granulomas. Overall, this strategy would benefit host pathology resulting in limiting the growth and spread of *Mtb*.

This thesis represents the first report that recombinant human lactoferrin can modulate the granulomatous response during primary *Mtb* infection in mice, in a manner nearly identical to that reported for bovine lactoferrin [98]. The results presented indicate utility for human lactoferrin administered orally as a therapeutic approach to limit pathological damage during primary granuloma development. The intervention led to increased penetration of ofloxacin to regions where *Mtb* typically reside. The observations in these thesis studies verified effects in both non-infectious, examining induced granulomas using purified mycobacterial mycolic acid TDM [78], and primary TB model, delivered via aerosol infection, where administration of rHLF achieved inflammation reduction in the lungs and greater ofloxacin distribution throughout granulomatous structures after treatment.

Lactoferrin-induced modulation in inflammatory response within mycobacterial-induced granulomas is likely the result of two concurrent events; that of significantly less proinflammatory cytokine production and reduction in recruited M1-like macrophages [78]. Alveolar macrophages uptake *Mtb* during primary infection and become essentially the key cell phenotype to recruit and activate additional naïve macrophages to the sites of infection [34, 140]. Classically activated macrophages polarize to the M1-like phenotype and exhibit functional phagocytosis and killing of bacteria. As a pathological by-product, they initiate immune cell recruitment via secreted proinflammatory cytokines which aid in the establishment of granulomatous tissue structures. Temporally, the subsequent recruitment and introduction of M2-like macrophages allows immune modification of the aggressive

inflammatory response, permitting an immunological “brake” to an overwhelming pathological response [21, 147, 197, 198, 261]. While further investigation is required, it is theorized that a balance in the presence of macrophage phenotypes within the granulomatous structures is essential to control pathological mediators by innate immune cells [66], which is critical to regulation of IL-1β (T cell activation and migration) [262] and TNF-α (vasodilatation and leukocyte adhesion to epithelium) [263] necessary as a response to control bacterial growth.

A major observation of this study was that the second-line mycobacterial therapeutic fluoroquinolone was able to penetrate within inflammatory foci. Similar to results using the TDM non-infectious model of pathology, significant amount of ofloxacin was found within granulomas following treatment with human lactoferrin, especially, but not limited to, regions of reduced inflammation. Concurrently, the lactoferrin-treated mice exhibited granulomatous responses with maintained vascular structures and open alveolar spaces. Acute inflammation and reactivity during *Mtb* infection occurs primarily peripheral to vascular regions, coinciding with destruction in continuity of endothelial lined blood vessels [258, 264]. In the experiments presented in this thesis, lactoferrin treatment allowed greater regions of lung tissue, and alveolar spaces, to remain unobstructed, as evident using the PECAM-1 endothelial surface marker. This coincided with observational retention of blood vessels within regions of pathology. The lessened pathological damage in the lactoferrin treated animals, along with significant maintenance of vascular architecture, likely permitted ofloxacin transport inside of granulomas, as evident by the drug’s

fluorescent signal observed within and around the endothelial-lined vessels. This raises the hypothesis for use of lactoferrin as a safe adjuvant molecule to increase delivery of standard *Mtb* therapeutics. This may also have the potential to reduce overall treatment times, limit drug sensitivity development, and reduce antibiotic side effects in patients undergoing treatment.

A major concern with current host-directed therapy is the increase of bacterial dissemination during treatment, such as seen when TNF-αblockers are used [88-91]. It is crucial that the role of established granulomas is maintained throughout the anti-mycobacterial treatment; specifically, the activation of recruited immune cells must be maintained to limit organism spread to other tissues. The observations in this thesis demonstrated no increase in lung CFUs in the treated group and no change in levels of detected organisms in liver and spleen. Such observations align with previous studies using bovine lactoferrin in a similar *Mtb* infectious model [98]. This shows potential therapeutic application of recombinant human lactoferrin to reduce pathological damage due to infection. And it does so without the major side effect of other host-directed therapies, including the compromising of *Mtb* confinement at the site of initial inflammation.

Lactoferrin immune-modulating effects in the *Mtb* infectious model are consistent with other infectious models reported [115, 265, 266]. And its utility as a host-directed therapeutic has been demonstrated in other diseases where host inflammation plays a key role in pathology development [115, 267]. Lactoferrin was used successfully in clinical trials

a prophylactic to prevent development of enterocolitis and sepsis [107, 268, 269]. In a similar manner, the prophylactic administration presented here was done prior to the establishment of granulomatous pathology. However, significant results were surprisingly identified when lactoferrin was given as a therapeutic at day 21 post infection at a time after granulomas have initiated in the lungs. Of clinical importance, when lactoferrin was used therapeutically it both decreased overall lung inflammation and increased ofloxacin distribution in granulomas.

The results in this thesis also brought to light the underlying functional activity of a relatively novel recombinant human lactoferrin. Most previous studies investigating the immune-modulating effects of lactoferrin used bovine lactoferrin due to its considerable availability and affordable pricing as a byproduct of cow milk. Though experiment and clinical trials on bovine lactoferrin immunomodulating effects show great potential as a therapeutic component, there is roughly a 30% difference in sequence identity between bovine and human lactoferrin [270]. In terms of amino acid composition, there are 696 amino acids in bovine lactoferrin compared with 691 amino acids in the human molecule [271, 272]. Since there are differences in their structure, though not major, there remains a gap where species compatibility might affect optimalization of modulating properties against human diseases, which is rarely observed and explored. In these sets of experiments, the consistent immunomodulating effects in the treated groups, in both TDM and *Mtb* models, shed light into this unexplored area. This was achievable due to the novel production of recombinant human lactoferrin using a stable Chinese hamster ovary cell line

(CHO) that is widely accepted as a leading mammalian platform in pharmaceutical production [273], thus allowing the use of recombinant human lactoferrin to be much more affordable and accessible in research. The recombinant human lactoferrin that was used in these studies possesses human-like glycosylation patterns, sequence identity, and antibacterial functions that are similar to that found in breast milk derived human lactoferrin [273].

Mechanistically, lactoferrin can induce dendritic cell activation and maturation, specifically supporting functions of antigen presenting cell (APC) populations that act as to bridge innate and adaptive immunity [274-278]. Lactoferrin can directly enhance the antigen presenting activity and T-cell stimulation function in mycobacterial-infected macrophages [279]. Lactoferrin can also modulate T-cell activities in multiple ways [115]. *In vitro*, T-cell maturation and expression of T-cell ζ-chain, a component of T-cell receptor (TCR) complex involved in receptor signaling pathways, can be increased upon treatment with lactoferrin [280-282]; T-cell adhesive molecules involved in cell-to-cell contact are also increased in the presence of lactoferrin [283]. Bovine lactoferrin administered orally increased IFN-γ Th1 T-cell responses [284] and NK cell activity in mice [285] likely by increasing IL-12 and related cytokines [285, 286]. Together, these suggest possible modulations of T cell activities, combined with enhanced antigen-presenting cell maturation and macrophage recruitment effects, which theoretically shift the overall outcome of granulomas to successful containment of pathogens

The observations using the TDM-induced granuloma model demonstrated that lactoferrin could lessen the presence of inflammatory mediators post initiation of pathology [78], as well as preferentially recruit M2-like cells to granulomas [78]. It is reasonable to infer that similar reductions using human lactoferrin at 4 weeks post *Mtb* infection would occur, since TDM is significantly released from mycobacteria [21, 287]. This also suggests an important mechanistic link between macrophage recruitment and lactoferrin treatment during *Mtb* infection, perhaps via the alteration of surface adhesion markers on monocytes that would permit increased interaction with endothelial cells [288, 289]. However, it remains unknown if lactoferrin can differentially affect M1-like versus M2-like activities; such experiments have only been explored on classical M1-like activated monocytes [198, 279]. This suggests a premise that macrophage polarization could occur in the presence of lactoferrin, perhaps via the reduction of locally produced proinflammatory cytokines [78, 97, 261, 290, 291].

Future Directions

The studies presented here set a foundation to further investigate usage of human lactoferrin in combination with standard treatments for *Mtb* infection. Bacterial dissemination in later time points after infection, and prolonged treatments, should be studied to understand the full potential of its use as a host-directed therapeutic. It remains unknown if lactoferrin treatment, when limited to the duration of early innate immune responses (such as was done in our models), is enough to significantly amplify the

bactericidal effect of Ofloxacin when given as a standard TB treatment regimen. In reality, it is not clinically feasible to identify individuals prior to development of pathology and granuloma formation. Therefore, more experiments are needed to determine the extent of human lactoferrin on the adaptive immune response when treatments begin after exposure at the primary granuloma establishment and maintenance stages.

The understanding of how Lactoferrin exerts its immunomodulating effect to the granulomatous response remains to be explored. The molecule is known to interact with "danger signal" receptors in addition to the lactoferrin receptor [252], therefore, it is remains unclear where such interactions happen physically during the granulomatous response. Future studies are needed to determine if lactoferrin works from within the granuloma structure as it penetrates the dense inflammatory tissues or indirectly by interacting with recruited immune cells in blood vessels and normal lung tissue (with secondary effects culminating in altered granuloma structure). In the non-infectious model where macrophages are responsible for the majority of inflammatory response, it is unclear how lactoferrin modulated the macrophage immune response. It has been established that bovine lactoferrin improved antigen-presentation in BCG infected bone marrow-derived macrophages by increasing surface expression of Class II (I-A^b) [120]. Therefore, more investigation is needed to confirm such effect, as well as other unknown changes in phenotype and intercellular signaling, in macrophages caused by lactoferrin during the primary immune response to *Mtb* infection.

Though a significant modulation of granulomatous response was achieved by giving lactoferrin orally, further investigation is needed for a thorough analysis of how much recombinant human lactoferrin was absorbed through the gut, and whether its intact structure and glycosylation presence within the circulating blood and lung tissue survives degradation in the digestive system.It is expected that bioavailability is affected by protein degradation and absorption. Recent studies by Kruzel, et al [292] suggest that up-regulation of specific genes involved in oxidative stress and inflammation occur after oral delivery. Future in-depth studies can extend comparisons of efficiency of different delivery methods when lactoferrin is given as a therapeutic for TB, such as when given orally, deposited on mucosal surfaces, or injected intravenously. In this study, the modulating effect of lactoferrin during the establishment of granulomas was investigated, which was not maintained after 4 weeks of ending lactoferrin treatment (8 weeks post Mtb infection). Therefore, future studies using lactoferrin in a longer term and more persistent manner is needed to discover the extent of its effect, long-term consequences, and the appropriate exposure to lactoferrin for optimized treatments.

Overall, a role for clinical utility of human lactoferrin to modify the aggressive immune function during primary *Mtb* infection may exist, which would allow greater efficacy of treatments. In turn, this would potentially reduce standard treatment duration, antibiotic side effects, and overall pathological damage in patients.

BIBLIOGRAPHY

1. Actor, J.K., Nguyen, T.K., D'Aigle, J., Hwang, S.-A., Wasik-Smietana, A., Kruzel, M.L., *Lactoferrin Treatment alters macrophage phenotypes and permits drug penetration to mycobacterial granulomas*, in *The 14th International Conference on Lactoferrin Structure, Function and Applications*. 2019: Lima, Peru.
2. Koch, R., *A Further Communication on a Remedy for Tuberculosis.* Ind Med Gaz, 1891. **26**(3): p. 85-87.
3. Keshavjee, S. and P.E. Farmer, *Tuberculosis, drug resistance, and the history of modern medicine.* N Engl J Med, 2012. **367**(10): p. 931-6.
4. WHO. *The top 10 causes of death*. 2020 December 9, 2020 [cited 2021 Febuary 15]; Available from: https://www.who.int/news-room/fact-sheets/detail/the-top-10-causes-of-death.
5. CDC. *Tuberculosis - Data and Statistics*. 2020 October 29, 2020 [cited 2021 Febuary 15]; Available from: https://www.cdc.gov/tb/statistics/default.htm.
6. Fogel, N., *Tuberculosis: a disease without boundaries.* Tuberculosis (Edinb), 2015. **95**(5): p. 527-31.
7. CDC. *TB and HIV Coinfection*. 2016 March 15, 2016 [cited 2021 Febuary 15]; Available from: https://www.cdc.gov/tb/topic/basics/tbhivcoinfection.htm.
8. *Tuberculosis Symptoms and Diagnosis*. 2020 March 9, 2020 [cited 2021 Febuary 15]; Available from: https://www.lung.org/lung-health-diseases/lung-disease-lookup/tuberculosis/symptoms-diagnosis.

9. Pai, M., M.A. Behr, D. Dowdy, K. Dheda, M. Divangahi, C.C. Boehme, A. Ginsberg, S. Swaminathan, M. Spigelman, H. Getahun, D. Menzies, and M. Raviglione, *Tuberculosis.* Nat Rev Dis Primers, 2016. **2**: p. 16076.

10. Jarlier, V. and H. Nikaido, *Mycobacterial cell wall: structure and role in natural resistance to antibiotics.* FEMS Microbiol Lett, 1994. **123**(1-2): p. 11-8.

11. Katherine Floyd, A.B., Marie-Christine Bar- tens, Anna Dean, Hannah Monica Dias, Dennis Falzon, Inés Garcia Baena, Nebiat Gebreselas- sie, Philippe Glaziou, Marek Lalli, Irwin Law, Nobuyuki Nishikiori, Gita Parwati, Charalambos Sismanidis, Lana Syed, Hazim Timimi. *Global tuberculosis report 2020*. 2020 14 October Available from: https://apps.who.int/iris/bitstream/handle/10665/336069/9789240013131-eng.pdf.

12. Hunter, R.L., J.K. Actor, S.-A. Hwang, V. Karev, and C. Jagannath, *Pathogenesis of post primary tuberculosis: immunity and hypersensitivity in the development of cavities.* Annals of Clinical & Laboratory Science, 2014. **44**(4): p. 365-387.

13. Hunter, R.L., J.K. Actor, S.-A. Hwang, A. Khan, M.E. Urbanowski, D. Kaushal, and C. Jagannath, *Pathogenesis and animal models of post-primary (bronchogenic) tuberculosis, a review.* Pathogens, 2018. **7**(1): p. 19.

14. Hunter, R.L., C. Jagannath, and J.K. Actor, *Pathology of postprimary tuberculosis in humans and mice: contradiction of long-held beliefs.* Tuberculosis, 2007. **87**(4): p. 267-278.

15. Hunter, R.L., *The Pathogenesis of Tuberculosis: The Early Infiltrate of Post-primary (Adult Pulmonary) Tuberculosis: A Distinct Disease Entity.* Front Immunol, 2018. **9**: p. 2108.

16. Hunter, R.L., *Tuberculosis as a three-act play: A new paradigm for the pathogenesis of pulmonary tuberculosis.* Tuberculosis (Edinb), 2016. **97**: p. 8-17.

17. Hunter, R.L., C. Jagannath, and J.K. Actor, *Pathology of postprimary tuberculosis in humans and mice: contradiction of long-held beliefs.* Tuberculosis (Edinb), 2007. **87**(4): p. 267-78.

18. Bloom, B.R. and C.J. Murray, *Tuberculosis: commentary on a reemergent killer.* Science, 1992. **257**(5073): p. 1055-64.

19. Parrish, N.M., J.D. Dick, and W.R. Bishai, *Mechanisms of latency in Mycobacterium tuberculosis.* Trends Microbiol, 1998. **6**(3): p. 107-12.

20. Vynnycky, E. and P.E. Fine, *Lifetime risks, incubation period, and serial interval of tuberculosis.* Am J Epidemiol, 2000. **152**(3): p. 247-63.

21. Hunter, R.L., M.R. Olsen, C. Jagannath, and J.K. Actor, *Multiple roles of cord factor in the pathogenesis of primary, secondary, and cavitary tuberculosis, including a revised description of the pathology of secondary disease.* Ann Clin Lab Sci, 2006. **36**(4): p. 371-86.

22. Hunter, R.L., *The Pathogenesis of Tuberculosis-The Koch Phenomenon Reinstated.* Pathogens, 2020. **9**(10).

23. Welsh, K.J., S.A. Risin, J.K. Actor, and R.L. Hunter, *Immunopathology of postprimary tuberculosis: increased T-regulatory cells and DEC-205-positive foamy macrophages in cavitary lesions.* Clin Dev Immunol, 2011. **2011**: p. 307631.

24. Rahman, S., B. Gudetta, J. Fink, A. Granath, S. Ashenafi, A. Aseffa, M. Derbew, M. Svensson, J. Andersson, and S.G. Brighenti, *Compartmentalization of immune responses in human tuberculosis: few CD8+ effector T cells but elevated levels of FoxP3+ regulatory t cells in the granulomatous lesions.* Am J Pathol, 2009. **174**(6): p. 2211-24.

25. Rhoades, E.R., A.A. Frank, and I.M. Orme, *Progression of chronic pulmonary tuberculosis in mice aerogenically infected with virulent Mycobacterium tuberculosis.* Tuber Lung Dis, 1997. **78**(1): p. 57-66.

26. Orme, I.M., *The mouse as a useful model of tuberculosis.* Tuberculosis (Edinb), 2003. **83**(1-3): p. 112-5.

27. Manabe, Y.C., A.K. Kesavan, J. Lopez-Molina, C.L. Hatem, M. Brooks, R. Fujiwara, K. Hochstein, M.L. Pitt, J. Tufariello, J. Chan, D.N. McMurray, W.R. Bishai, A.M. Dannenberg, Jr., and S. Mendez, *The aerosol rabbit model of TB latency, reactivation and immune reconstitution inflammatory syndrome.* Tuberculosis (Edinb), 2008. **88**(3): p. 187-96.

28. Cronan, M.R. and D.M. Tobin, *Fit for consumption: zebrafish as a model for tuberculosis.* Dis Model Mech, 2014. **7**(7): p. 777-84.

29. Scanga, C.A. and J.L. Flynn, *Modeling tuberculosis in nonhuman primates.* Cold Spring Harb Perspect Med, 2014. **4**(12): p. a018564.

30. Turner, O.C., R.J. Basaraba, and I.M. Orme, *Immunopathogenesis of pulmonary granulomas in the guinea pig after infection with Mycobacterium tuberculosis.* Infect Immun, 2003. **71**(2): p. 864-71.

31. Russell, D.G., P.J. Cardona, M.J. Kim, S. Allain, and F. Altare, *Foamy macrophages and the progression of the human tuberculosis granuloma.* Nat Immunol, 2009. **10**(9): p. 943-8.

32. Cooper, A.M., *Mouse model of tuberculosis.* Cold Spring Harb Perspect Med, 2014. **5**(2): p. a018556.

33. Saunders, B.M. and A.M. Cooper, *Restraining mycobacteria: role of granulomas in mycobacterial infections.* Immunol Cell Biol, 2000. **78**(4): p. 334-41.

34. Akira, S., S. Uematsu, and O. Takeuchi, *Pathogen recognition and innate immunity.* Cell, 2006. **124**(4): p. 783-801.

35. Domingo-Gonzalez, R., O. Prince, A. Cooper, and S.A. Khader, *Cytokines and Chemokines in Mycobacterium tuberculosis Infection.* Microbiol Spectr, 2016. **4**(5).

36. Monin, L. and S.A. Khader, *Chemokines in tuberculosis: the good, the bad and the ugly.* Semin Immunol, 2014. **26**(6): p. 552-8.

37. Cooper, A.M., K.D. Mayer-Barber, and A. Sher, *Role of innate cytokines in mycobacterial infection.* Mucosal Immunol, 2011. **4**(3): p. 252-60.

38. Orme, I.M. and A.M. Cooper, *Cytokine/chemokine cascades in immunity to tuberculosis.* Immunol Today, 1999. **20**(7): p. 307-12.

39. Ishikawa, E., T. Ishikawa, Y.S. Morita, K. Toyonaga, H. Yamada, O. Takeuchi, T. Kinoshita, S. Akira, Y. Yoshikai, and S. Yamasaki, *Direct recognition of the*

mycobacterial glycolipid, trehalose dimycolate, by C-type lectin Mincle. J Exp Med, 2009. **206**(13): p. 2879-88.

40. Welsh, K.J., A.N. Abbott, S.A. Hwang, J. Indrigo, L.Y. Armitige, M.R. Blackburn, R.L. Hunter, and J.K. Actor, *A role for tumour necrosis factor-alpha, complement C5 and interleukin-6 in the initiation and development of the mycobacterial cord factor trehalose 6,6'-dimycolate induced granulomatous response.* Microbiology (Reading), 2008. **154**(Pt 6): p. 1813-1824.

41. Torrado, E. and A.M. Cooper, *Cytokines in the balance of protection and pathology during mycobacterial infections.* Adv Exp Med Biol, 2013. **783**: p. 121-40.

42. Martin, C.J., A.F. Carey, and S.M. Fortune, *A bug's life in the granuloma.* Semin Immunopathol, 2016. **38**(2): p. 213-20.

43. Russell, D.G., *Who puts the tubercle in tuberculosis?* Nat Rev Microbiol, 2007. **5**(1): p. 39-47.

44. Hunter, R.L., S.A. Hwang, C. Jagannath, and J.K. Actor, *Cord factor as an invisibility cloak? A hypothesis for asymptomatic TB persistence.* Tuberculosis (Edinb), 2016. **101S**: p. S2-S8.

45. Goren, M.B., P. D'Arcy Hart, M.R. Young, and J.A. Armstrong, *Prevention of phagosome-lysosome fusion in cultured macrophages by sulfatides of Mycobacterium tuberculosis.* Proc Natl Acad Sci U S A, 1976. **73**(7): p. 2510-4.

46. Kan-Sutton, C., C. Jagannath, and R.L. Hunter, Jr., *Trehalose 6,6'-dimycolate on the surface of Mycobacterium tuberculosis modulates surface marker expression for*

antigen presentation and costimulation in murine macrophages. Microbes Infect, 2009. **11**(1): p. 40-8.

47. Davis, J.M. and L. Ramakrishnan, *The role of the granuloma in expansion and dissemination of early tuberculous infection.* Cell, 2009. **136**(1): p. 37-49.

48. Driver, E.R., G.J. Ryan, D.R. Hoff, S.M. Irwin, R.J. Basaraba, I. Kramnik, and A.J. Lenaerts, *Evaluation of a mouse model of necrotic granuloma formation using C3HeB/FeJ mice for testing of drugs against Mycobacterium tuberculosis.* Antimicrob Agents Chemother, 2012. **56**(6): p. 3181-95.

49. Dartois, V., *The path of anti-tuberculosis drugs: from blood to lesions to mycobacterial cells.* Nat Rev Microbiol, 2014. **12**(3): p. 159-67.

50. Robinson, R.T., I.M. Orme, and A.M. Cooper, *The onset of adaptive immunity in the mouse model of tuberculosis and the factors that compromise its expression.* Immunol Rev, 2015. **264**(1): p. 46-59.

51. Bold, T.D. and J.D. Ernst, *Who benefits from granulomas, mycobacteria or host?* Cell, 2009. **136**(1): p. 17-9.

52. Flynn, J.L. and J. Chan, *Immunology of tuberculosis.* Annu Rev Immunol, 2001. **19**: p. 93-129.

53. MacMicking, J., Q.W. Xie, and C. Nathan, *Nitric oxide and macrophage function.* Annu Rev Immunol, 1997. **15**: p. 323-50.

54. Shiloh, M.U. and C.F. Nathan, *Reactive nitrogen intermediates and the pathogenesis of Salmonella and mycobacteria.* Curr Opin Microbiol, 2000. **3**(1): p. 35-42.

55. Schmitt, E., P. Hoehn, C. Huels, S. Goedert, N. Palm, E. Rude, and T. Germann, *T helper type 1 development of naive CD4+ T cells requires the coordinate action of interleukin-12 and interferon-gamma and is inhibited by transforming growth factor-beta.* Eur J Immunol, 1994. **24**(4): p. 793-8.

56. Seder, R.A., R. Gazzinelli, A. Sher, and W.E. Paul, *Interleukin 12 acts directly on CD4+ T cells to enhance priming for interferon gamma production and diminishes interleukin 4 inhibition of such priming.* Proc Natl Acad Sci U S A, 1993. **90**(21): p. 10188-92.

57. Brown, E.J., *Complement receptors and phagocytosis.* Curr Opin Immunol, 1991. **3**(1): p. 76-82.

58. Schlesinger, L.S., *Entry of Mycobacterium tuberculosis into mononuclear phagocytes.* Curr Top Microbiol Immunol, 1996. **215**: p. 71-96.

59. Pieters, J., *Entry and survival of pathogenic mycobacteria in macrophages.* Microbes Infect, 2001. **3**(3): p. 249-55.

60. Khan, A., V.K. Singh, R.L. Hunter, and C. Jagannath, *Macrophage heterogeneity and plasticity in tuberculosis.* J Leukoc Biol, 2019. **106**(2): p. 275-282.

61. Arora, S., K. Dev, B. Agarwal, P. Das, and M.A. Syed, *Macrophages: Their role, activation and polarization in pulmonary diseases.* Immunobiology, 2018. **223**(4-5): p. 383-396.

62. Murray, P.J., *Macrophage Polarization.* Annu Rev Physiol, 2017. **79**: p. 541-566.

63. Saradna, A., D.C. Do, S. Kumar, Q.L. Fu, and P. Gao, *Macrophage polarization and allergic asthma.* Transl Res, 2018. **191**: p. 1-14.

64. Misharin, A.V., L. Morales-Nebreda, G.M. Mutlu, G.R. Budinger, and H. Perlman, *Flow cytometric analysis of macrophages and dendritic cell subsets in the mouse lung.* Am J Respir Cell Mol Biol, 2013. **49**(4): p. 503-10.

65. Jablonski, K.A., S.A. Amici, L.M. Webb, D. Ruiz-Rosado Jde, P.G. Popovich, S. Partida-Sanchez, and M. Guerau-de-Arellano, *Novel Markers to Delineate Murine M1 and M2 Macrophages.* PLoS One, 2015. **10**(12): p. e0145342.

66. Pisu, D., L. Huang, B.N. Rin Lee, J.K. Grenier, and D.G. Russell, *Dual RNA-Sequencing of Mycobacterium tuberculosis-Infected Cells from a Murine Infection Model.* STAR Protoc, 2020. **1**(3): p. 100123.

67. Redente, E.F., D.M. Higgins, L.D. Dwyer-Nield, I.M. Orme, M. Gonzalez-Juarrero, and A.M. Malkinson, *Differential polarization of alveolar macrophages and bone marrow-derived monocytes following chemically and pathogen-induced chronic lung inflammation.* J Leukoc Biol, 2010. **88**(1): p. 159-68.

68. Lugo-Villarino, G., C. Verollet, I. Maridonneau-Parini, and O. Neyrolles, *Macrophage polarization: convergence point targeted by mycobacterium tuberculosis and HIV.* Front Immunol, 2011. **2**: p. 43.

69. Yamasaki, K. and S.F.V. Eeden, *Lung Macrophage Phenotypes and Functional Responses: Role in the Pathogenesis of COPD.* Int J Mol Sci, 2018. **19**(2).

70. Paige, C. and W.R. Bishai, *Penitentiary or penthouse condo: the tuberculous granuloma from the microbe's point of view.* Cell Microbiol, 2010. **12**(3): p. 301-9.

71. Ozeki, Y., K. Kaneda, N. Fujiwara, M. Morimoto, S. Oka, and I. Yano, *In vivo induction of apoptosis in the thymus by administration of mycobacterial cord factor (trehalose 6,6'-dimycolate).* Infect Immun, 1997. **65**(5): p. 1793-9.

72. Wolf, A.J., L. Desvignes, B. Linas, N. Banaiee, T. Tamura, K. Takatsu, and J.D. Ernst, *Initiation of the adaptive immune response to Mycobacterium tuberculosis depends on antigen production in the local lymph node, not the lungs.* J Exp Med, 2008. **205**(1): p. 105-15.

73. Divangahi, M., D. Desjardins, C. Nunes-Alves, H.G. Remold, and S.M. Behar, *Eicosanoid pathways regulate adaptive immunity to Mycobacterium tuberculosis.* Nat Immunol, 2010. **11**(8): p. 751-8.

74. Griffiths, K.L., M. Ahmed, S. Das, R. Gopal, W. Horne, T.D. Connell, K.D. Moynihan, J.K. Kolls, D.J. Irvine, M.N. Artyomov, J. Rangel-Moreno, and S.A. Khader, *Targeting dendritic cells to accelerate T-cell activation overcomes a bottleneck in tuberculosis vaccine efficacy.* Nat Commun, 2016. **7**: p. 13894.

75. Krug, S., S. Parveen, and W.R. Bishai, *Host-Directed Therapies: Modulating Inflammation to Treat Tuberculosis.* Front Immunol, 2021. **12**: p. 660916.

76. Ndlovu, H. and M.J. Marakalala, *Granulomas and Inflammation: Host-Directed Therapies for Tuberculosis.* Front Immunol, 2016. **7**: p. 434.

77. Vilaplana, C., E. Marzo, G. Tapia, J. Diaz, V. Garcia, and P.J. Cardona, *Ibuprofen therapy resulted in significantly decreased tissue bacillary loads and increased survival in a new murine experimental model of active tuberculosis.* J Infect Dis, 2013. **208**(2): p. 199-202.

78. Nguyen, T.K.T., Z. Niaz, J. d'Aigle, S.A. Hwang, M.L. Kruzel, and J.K. Actor, *Lactoferrin reduces mycobacterial M1-type inflammation induced with trehalose 6,6'-dimycolate and facilitates the entry of fluoroquinolone into granulomas.* Biochem Cell Biol, 2021. **99**(1): p. 73-80.

79. Estrella, J.L., C. Kan-Sutton, X. Gong, M. Rajagopalan, D.E. Lewis, R.L. Hunter, N.T. Eissa, and C. Jagannath, *A Novel in vitro Human Macrophage Model to Study the Persistence of Mycobacterium tuberculosis Using Vitamin D(3) and Retinoic Acid Activated THP-1 Macrophages.* Front Microbiol, 2011. **2**: p. 67.

80. Byrne, S.T., S.M. Denkin, and Y. Zhang, *Aspirin and ibuprofen enhance pyrazinamide treatment of murine tuberculosis.* J Antimicrob Chemother, 2007. **59**(2): p. 313-6.

81. Eisen, D.P., E.S. McBryde, and A. Walduck, *Low-dose aspirin and ibuprofen's sterilizing effects on Mycobacterium tuberculosis suggest safe new adjuvant therapies for tuberculosis.* J Infect Dis, 2013. **208**(11): p. 1925-7.

82. Martineau, A.R., P.M. Timms, G.H. Bothamley, Y. Hanifa, K. Islam, A.P. Claxton, G.E. Packe, J.C. Moore-Gillon, M. Darmalingam, R.N. Davidson, H.J. Milburn, L.V. Baker, R.D. Barker, N.J. Woodward, T.R. Venton, K.E. Barnes, C.J. Mullett, A.K. Coussens, C.M. Rutterford, C.A. Mein, G.R. Davies, R.J. Wilkinson, V. Nikolayevskyy, F.A. Drobniewski, S.M. Eldridge, and C.J. Griffiths, *High-dose vitamin D(3) during intensive-phase antimicrobial treatment of pulmonary tuberculosis: a double-blind randomised controlled trial.* Lancet, 2011. **377**(9761): p. 242-50.

83. Daley, P., V. Jagannathan, K.R. John, J. Sarojini, A. Latha, R. Vieth, S. Suzana, L. Jeyaseelan, D.J. Christopher, M. Smieja, and D. Mathai, *Adjunctive vitamin D for*

treatment of active tuberculosis in India: a randomised, double-blind, placebo-controlled trial. Lancet Infect Dis, 2015. **15**(5): p. 528-34.

84. Gupta, A., A. Misra, and V. Deretic, *Targeted pulmonary delivery of inducers of host macrophage autophagy as a potential host-directed chemotherapy of tuberculosis.* Adv Drug Deliv Rev, 2016. **102**: p. 10-20.

85. Lv, S., M. Han, R. Yi, S. Kwon, C. Dai, and R. Wang, *Anti-TNF-alpha therapy for patients with sepsis: a systematic meta-analysis.* Int J Clin Pract, 2014. **68**(4): p. 520-8.

86. Zhang, H., N. Shi, Z. Diao, Y. Chen, and Y. Zhang, *Therapeutic potential of TNFalpha inhibitors in chronic inflammatory disorders: Past and future.* Genes Dis, 2021. **8**(1): p. 38-47.

87. Skerry, C., J. Harper, M. Klunk, W.R. Bishai, and S.K. Jain, *Adjunctive TNF inhibition with standard treatment enhances bacterial clearance in a murine model of necrotic TB granulomas.* PLoS One, 2012. **7**(6): p. e39680.

88. Keane, J., S. Gershon, R.P. Wise, E. Mirabile-Levens, J. Kasznica, W.D. Schwieterman, J.N. Siegel, and M.M. Braun, *Tuberculosis associated with infliximab, a tumor necrosis factor alpha-neutralizing agent.* N Engl J Med, 2001. **345**(15): p. 1098-104.

89. Wallis, R.S., M.S. Broder, J.Y. Wong, M.E. Hanson, and D.O. Beenhouwer, *Granulomatous infectious diseases associated with tumor necrosis factor antagonists.* Clin Infect Dis, 2004. **38**(9): p. 1261-5.

90. Chakravarty, S.D., G. Zhu, M.C. Tsai, V.P. Mohan, S. Marino, D.E. Kirschner, L. Huang, J. Flynn, and J. Chan, *Tumor necrosis factor blockade in chronic murine tuberculosis*

enhances granulomatous inflammation and disorganizes granulomas in the lungs. Infect Immun, 2008. **76**(3): p. 916-26.

91. Fernandez-Ruiz, M. and J.M. Aguado, *Risk of infection associated with anti-TNF-alpha therapy.* Expert Rev Anti Infect Ther, 2018. **16**(12): p. 939-956.

92. Hwang, S.A., M.L. Kruzel, and J.K. Actor, *Oral recombinant human or mouse lactoferrin reduces Mycobacterium tuberculosis TDM induced granulomatous lung pathology.* Biochem Cell Biol, 2017. **95**(1): p. 148-154.

93. Legrand, D., *Lactoferrin, a key molecule in immune and inflammatory processes.* Biochem Cell Biol, 2012. **90**(3): p. 252-68.

94. Hwang, S.A., R. Arora, M.L. Kruzel, and J.K. Actor, *Lactoferrin enhances efficacy of the BCG vaccine: comparison between two inbred mice strains (C57BL/6 and BALB/c).* Tuberculosis (Edinb), 2009. **89 Suppl 1**: p. S49-54.

95. Crucian, B.E., S.-A. Hwang, J.K. Actor, H. Quiriarte, and C.F. Sams, *Altered Innate and Lymphocytic Immunity in Murine Splenocytes Following Short-Duration Spaceflight.* 2011.

96. Crouch, S.P., K.J. Slater, and J. Fletcher, *Regulation of cytokine release from mononuclear cells by the iron-binding protein lactoferrin.* Blood, 1992. **80**(1): p. 235-40.

97. Kruzel, M.L., Y. Harari, D. Mailman, J.K. Actor, and M. Zimecki, *Differential effects of prophylactic, concurrent and therapeutic lactoferrin treatment on LPS-induced inflammatory responses in mice.* Clin Exp Immunol, 2002. **130**(1): p. 25-31.

98. Welsh, K.J., S.A. Hwang, S. Boyd, M.L. Kruzel, R.L. Hunter, and J.K. Actor, *Influence of oral lactoferrin on Mycobacterium tuberculosis induced immunopathology.* Tuberculosis (Edinb), 2011. **91 Suppl 1**: p. S105-13.

99. Welsh, K.J., S.A. Hwang, R.L. Hunter, M.L. Kruzel, and J.K. Actor, *Lactoferrin modulation of mycobacterial cord factor trehalose 6-6'-dimycolate induced granulomatous response.* Transl Res, 2010. **156**(4): p. 207-15.

100. Legrand, D., A. Pierce, E. Elass, M. Carpentier, C. Mariller, and J. Mazurier, *Lactoferrin structure and functions.* Adv Exp Med Biol, 2008. **606**: p. 163-94.

101. Baker, E.N. and H.M. Baker, *Molecular structure, binding properties and dynamics of lactoferrin.* Cell Mol Life Sci, 2005. **62**(22): p. 2531-9.

102. Baggiolini, M., C. De Duve, P.L. Masson, and J.F. Heremans, *Association of lactoferrin with specific granules in rabbit heterophil leukocytes.* J Exp Med, 1970. **131**(3): p. 559-70.

103. Sanchez, L., M. Calvo, and J.H. Brock, *Biological role of lactoferrin.* Arch Dis Child, 1992. **67**(5): p. 657-61.

104. Lonnerdal, B. and S. Iyer, *Lactoferrin: molecular structure and biological function.* Annu Rev Nutr, 1995. **15**: p. 93-110.

105. Clare, D.A., G.L. Catignani, and H.E. Swaisgood, *Biodefense properties of milk: the role of antimicrobial proteins and peptides.* Curr Pharm Des, 2003. **9**(16): p. 1239-55.

106. Baveye, S., E. Elass, J. Mazurier, G. Spik, and D. Legrand, *Lactoferrin: a multifunctional glycoprotein involved in the modulation of the inflammatory process.* Clin Chem Lab Med, 1999. **37**(3): p. 281-6.

107. Ochoa, T.J., A. Pezo, K. Cruz, E. Chea-Woo, and T.G. Cleary, *Clinical studies of lactoferrin in children.* Biochem Cell Biol, 2012. **90**(3): p. 457-67.

108. Ellison, R.T., 3rd and T.J. Giehl, *Killing of gram-negative bacteria by lactoferrin and lysozyme.* J Clin Invest, 1991. **88**(4): p. 1080-91.

109. Vorland, L.H., *Lactoferrin: a multifunctional glycoprotein.* APMIS, 1999. **107**(11): p. 971-81.

110. Farnaud, S. and R.W. Evans, *Lactoferrin--a multifunctional protein with antimicrobial properties.* Mol Immunol, 2003. **40**(7): p. 395-405.

111. Ward, P.P., E. Paz, and O.M. Conneely, *Multifunctional roles of lactoferrin: a critical overview.* Cell Mol Life Sci, 2005. **62**(22): p. 2540-8.

112. Orsi, N., *The antimicrobial activity of lactoferrin: current status and perspectives.* Biometals, 2004. **17**(3): p. 189-96.

113. Valenti, P. and G. Antonini, *Lactoferrin: an important host defence against microbial and viral attack.* Cell Mol Life Sci, 2005. **62**(22): p. 2576-87.

114. Weinberg, E.D., *Antibiotic properties and applications of lactoferrin.* Curr Pharm Des, 2007. **13**(8): p. 801-11.

115. Actor, J.K., S.A. Hwang, and M.L. Kruzel, *Lactoferrin as a natural immune modulator.* Curr Pharm Des, 2009. **15**(17): p. 1956-73.

116. Legrand, D., *Overview of Lactoferrin as a Natural Immune Modulator.* J Pediatr, 2016. **173 Suppl**: p. S10-5.

117. Kawasaki, Y., S. Tazume, K. Shimizu, H. Matsuzawa, S. Dosako, H. Isoda, M. Tsukiji, R. Fujimura, Y. Muranaka, and H. Isihida, *Inhibitory effects of bovine lactoferrin on the*

adherence of enterotoxigenic Escherichia coli to host cells. Biosci Biotechnol Biochem, 2000. **64**(2): p. 348-54.

118. Drobni, P., J. Naslund, and M. Evander, *Lactoferrin inhibits human papillomavirus binding and uptake in vitro.* Antiviral Res, 2004. **64**(1): p. 63-8.

119. Ochoa, T.J., M. Noguera-Obenza, and T.G. Cleary, *Lactoferrin blocks the initial host cell attachment mechanism of Enteropathogenic E. coli (EPEC).* Adv Exp Med Biol, 2004. **554**: p. 463-6.

120. Wilk, K.M., S.A. Hwang, and J.K. Actor, *Lactoferrin modulation of antigen-presenting-cell response to BCG infection.* Postepy Hig Med Dosw (Online), 2007. **61**: p. 277-82.

121. Tanida, T., F. Rao, T. Hamada, E. Ueta, and T. Osaki, *Lactoferrin peptide increases the survival of Candida albicans-inoculated mice by upregulating neutrophil and macrophage functions, especially in combination with amphotericin B and granulocyte-macrophage colony-stimulating factor.* Infect Immun, 2001. **69**(6): p. 3883-90.

122. Cumberbatch, M., M. Bhushan, R.J. Dearman, I. Kimber, and C.E. Griffiths, *IL-1beta-induced Langerhans' cell migration and TNF-alpha production in human skin: regulation by lactoferrin.* Clin Exp Immunol, 2003. **132**(2): p. 352-9.

123. Mikkelsen, T.L., S. Bakman, E.S. Sorensen, V. Barkholt, and H. Frokiaer, *Sialic acid-containing milk proteins show differential immunomodulatory activities independent of sialic acid.* J Agric Food Chem, 2005. **53**(20): p. 7673-80.

124. Curran, C.S., K.P. Demick, and J.M. Mansfield, *Lactoferrin activates macrophages via TLR4-dependent and -independent signaling pathways.* Cell Immunol, 2006. **242**(1): p. 23-30.

125. Murphy, E.E., G. Terres, S.E. Macatonia, C.S. Hsieh, J. Mattson, L. Lanier, M. Wysocka, G. Trinchieri, K. Murphy, and A. O'Garra, *B7 and interleukin 12 cooperate for proliferation and interferon gamma production by mouse T helper clones that are unresponsive to B7 costimulation.* J Exp Med, 1994. **180**(1): p. 223-31.

126. Gately, M.K., L.M. Renzetti, J. Magram, A.S. Stern, L. Adorini, U. Gubler, and D.H. Presky, *The interleukin-12/interleukin-12-receptor system: role in normal and pathologic immune responses.* Annu Rev Immunol, 1998. **16**: p. 495-521.

127. Fischer, R., H. Debbabi, M. Dubarry, P. Boyaka, and D. Tome, *Regulation of physiological and pathological Th1 and Th2 responses by lactoferrin.* Biochem Cell Biol, 2006. **84**(3): p. 303-11.

128. Zimecki, M., J. Mazurier, G. Spik, and J.A. Kapp, *Lactoferrin inhibits proliferative response and cytokine production of TH1 but not TH2 cell lines.* Arch Immunol Ther Exp (Warsz), 1996. **44**(1): p. 51-6.

129. Guillen, C., I.B. McInnes, D.M. Vaughan, S. Kommajosyula, P.H. Van Berkel, B.P. Leung, A. Aguila, and J.H. Brock, *Enhanced Th1 response to Staphylococcus aureus infection in human lactoferrin-transgenic mice.* J Immunol, 2002. **168**(8): p. 3950-7.

130. Zimecki, M., J. Mazurier, G. Spik, and J.A. Kapp, *Human lactoferrin induces phenotypic and functional changes in murine splenic B cells.* Immunology, 1995. **86**(1): p. 122-7.

131. Mazurier, J., J. Montreuil, and G. Spik, *Visualization of lactotransferrin brush-border receptors by ligand-blotting.* Biochim Biophys Acta, 1985. **821**(3): p. 453-60.

132. Suzuki, Y.A., V. Lopez, and B. Lonnerdal, *Mammalian lactoferrin receptors: structure and function.* Cell Mol Life Sci, 2005. **62**(22): p. 2560-75.

133. Van Snick, J.L. and P.L. Masson, *The binding of human lactoferrin to mouse peritoneal cells.* J Exp Med, 1976. **144**(6): p. 1568-80.

134. Legrand, D., E. Elass, M. Carpentier, and J. Mazurier, *Interactions of lactoferrin with cells involved in immune function.* Biochem Cell Biol, 2006. **84**(3): p. 282-90.

135. Zimecki, M., J. Artym, M. Kocieba, M. Duk, and M.L. Kruzel, *The effect of carbohydrate moiety structure on the immunoregulatory activity of lactoferrin in vitro.* Cell Mol Biol Lett, 2014. **19**(2): p. 284-96.

136. Hwang, S.A., M.L. Kruzel, and J.K. Actor, *Recombinant human lactoferrin modulates human PBMC derived macrophage responses to BCG and LPS.* Tuberculosis (Edinb), 2016. **101S**: p. S53-S62.

137. Wisgrill, L., I. Wessely, A. Spittler, E. Forster-Waldl, A. Berger, and K. Sadeghi, *Human lactoferrin attenuates the proinflammatory response of neonatal monocyte-derived macrophages.* Clin Exp Immunol, 2018. **192**(3): p. 315-324.

138. Orme, I.M., R.T. Robinson, and A.M. Cooper, *The balance between protective and pathogenic immune responses in the TB-infected lung.* Nat Immunol, 2015. **16**(1): p. 57-63.

139. Jasenosky, L.D., T.J. Scriba, W.A. Hanekom, and A.E. Goldfeld, *T cells and adaptive immunity to Mycobacterium tuberculosis in humans.* Immunol Rev, 2015. **264**(1): p. 74-87.

140. McClean, C.M. and D.M. Tobin, *Macrophage form, function, and phenotype in mycobacterial infection: lessons from tuberculosis and other diseases.* Pathog Dis, 2016. **74**(7).

141. BoseDasgupta, S. and J. Pieters, *Macrophage-microbe interaction: lessons learned from the pathogen Mycobacterium tuberculosis.* Semin Immunopathol, 2018. **40**(6): p. 577-591.

142. Marakalala, M.J., F.O. Martinez, A. Pluddemann, and S. Gordon, *Macrophage Heterogeneity in the Immunopathogenesis of Tuberculosis.* Front Microbiol, 2018. **9**: p. 1028.

143. Goldberg, M.F., N.K. Saini, and S.A. Porcelli, *Evasion of Innate and Adaptive Immunity by Mycobacterium tuberculosis.* Microbiol Spectr, 2014. **2**(5).

144. Hmama, Z., S. Pena-Diaz, S. Joseph, and Y. Av-Gay, *Immunoevasion and immunosuppression of the macrophage by Mycobacterium tuberculosis.* Immunol Rev, 2015. **264**(1): p. 220-32.

145. Upadhyay, S., E. Mittal, and J.A. Philips, *Tuberculosis and the art of macrophage manipulation.* Pathog Dis, 2018. **76**(4).

146. Hao, W., L.S. Schlesinger, and A. Friedman, *Modeling Granulomas in Response to Infection in the Lung.* PLoS One, 2016. **11**(3): p. e0148738.

147. Marino, S., N.A. Cilfone, J.T. Mattila, J.J. Linderman, J.L. Flynn, and D.E. Kirschner, *Macrophage polarization drives granuloma outcome during Mycobacterium tuberculosis infection.* Infect Immun, 2015. **83**(1): p. 324-38.

148. Khan, A., V.K. Singh, R.L. Hunter, and C. Jagannath, *Macrophage heterogeneity and plasticity in tuberculosis.* J Leukoc Biol, 2019.

149. Turken, O., E. Kunter, M. Sezer, E. Solmazgul, K. Cerrahoglu, E. Bozkanat, A. Ozturk, and A. Ilvan, *Hemostatic changes in active pulmonary tuberculosis.* Int J Tuberc Lung Dis, 2002. **6**(10): p. 927-32.

150. Sezer, M., A. Ozturk, A. Ilvan, M. Ozkan, and N. Uskent, *The Hemostatic Changes in Active Pulmonary Tuberculosis.* Turk J Haematol, 2001. **18**(2): p. 95-100.

151. Kager, L.M., D.C. Blok, I.O. Lede, W. Rahman, R. Afroz, P. Bresser, J.S. van der Zee, A. Ghose, C.E. Visser, M.D. de Jong, M.W. Tanck, A.S. Zahed, K.M. Alam, M. Hassan, A. Hossain, R. Lutter, C.V. Veer, A.M. Dondorp, J.C. Meijers, and T. van der Poll, *Pulmonary tuberculosis induces a systemic hypercoagulable state.* J Infect, 2015. **70**(4): p. 324-34.

152. Dorhoi, A., S.T. Reece, and S.H. Kaufmann, *For better or for worse: the immune response against Mycobacterium tuberculosis balances pathology and protection.* Immunol Rev, 2011. **240**(1): p. 235-51.

153. Bloch, H. and H. Noll, *Studies on the virulence of Tubercle bacilli; the effect of cord factor on murine tuberculosis.* Br J Exp Pathol, 1955. **36**(1): p. 8-17.

154. Perez, R.L., J. Roman, G.W. Staton, Jr., and R.L. Hunter, *Extravascular coagulation and fibrinolysis in murine lung inflammation induced by the mycobacterial cord*

factor trehalose-6,6'-dimycolate. Am J Respir Crit Care Med, 1994. **149**(2 Pt 1): p. 510-8.

155. Donnachie, E., E.P. Fedotova, and S.A. Hwang, *Trehalose 6,6-Dimycolate from Mycobacterium tuberculosis Induces Hypercoagulation.* Am J Pathol, 2016. **186**(5): p. 1221-33.

156. Hwang, S.A., C.D. Byerly, and J.K. Actor, *Mycobacterial trehalose 6,6'-dimycolate induced vascular occlusion is accompanied by subendothelial inflammation.* Tuberculosis (Edinb), 2019.

157. Geisel, R.E., K. Sakamoto, D.G. Russell, and E.R. Rhoades, *In vivo activity of released cell wall lipids of Mycobacterium bovis bacillus Calmette-Guerin is due principally to trehalose mycolates.* J Immunol, 2005. **174**(8): p. 5007-15.

158. Perez, R.L., J. Roman, S. Roser, C. Little, M. Olsen, J. Indrigo, R.L. Hunter, and J.K. Actor, *Cytokine message and protein expression during lung granuloma formation and resolution induced by the mycobacterial cord factor trehalose-6,6'-dimycolate.* J Interferon Cytokine Res, 2000. **20**(9): p. 795-804.

159. Welsh, K.J., A.N. Abbott, S.A. Hwang, J. Indrigo, L.Y. Armitige, M.R. Blackburn, R.L. Hunter, Jr., and J.K. Actor, *A role for tumour necrosis factor-alpha, complement C5 and interleukin-6 in the initiation and development of the mycobacterial cord factor trehalose 6,6'-dimycolate induced granulomatous response.* Microbiology, 2008. **154**(Pt 6): p. 1813-24.

160. Bowdish, D.M., K. Sakamoto, M.J. Kim, M. Kroos, S. Mukhopadhyay, C.A. Leifer, K. Tryggvason, S. Gordon, and D.G. Russell, *MARCO, TLR2, and CD14 are required for*

macrophage cytokine responses to mycobacterial trehalose dimycolate and Mycobacterium tuberculosis. PLoS Pathog, 2009. **5**(6): p. e1000474.

161. Guidry, T.V., R.L. Hunter, Jr., and J.K. Actor, *Mycobacterial glycolipid trehalose 6,6'-dimycolate-induced hypersensitive granulomas: contribution of CD4+ lymphocytes.* Microbiology, 2007. **153**(Pt 10): p. 3360-9.

162. Yamagami, H., T. Matsumoto, N. Fujiwara, T. Arakawa, K. Kaneda, I. Yano, and K. Kobayashi, *Trehalose 6,6'-dimycolate (cord factor) of Mycobacterium tuberculosis induces foreign-body- and hypersensitivity-type granulomas in mice.* Infect Immun, 2001. **69**(2): p. 810-5.

163. Guidry, T.V., M. Olsen, K.S. Kil, R.L. Hunter, Jr., Y.J. Geng, and J.K. Actor, *Failure of CD1D-/- mice to elicit hypersensitive granulomas to mycobacterial cord factor trehalose 6,6'-dimycolate.* J Interferon Cytokine Res, 2004. **24**(6): p. 362-71.

164. Pelletier, M., A. Forget, D. Bourassa, P. Gros, and E. Skamene, *Immunopathology of BCG infection in genetically resistant and susceptible mouse strains.* J Immunol, 1982. **129**(5): p. 2179-85.

165. Collins, F.M., C.C. Congdon, and N.E. Morrison, *Growth of mycobacterium bovis (BCG) in T lymphocyte-depleted mice.* Infect Immun, 1975. **11**(1): p. 57-64.

166. Schneider, C.A., W.S. Rasband, and K.W. Eliceiri, *NIH Image to ImageJ: 25 years of image analysis.* Nat Methods, 2012. **9**(7): p. 671-5.

167. Yue, Y., W. Huang, J. Liang, J. Guo, J. Ji, Y. Yao, M. Zheng, Z. Cai, L. Lu, and J. Wang, *IL4I1 Is a Novel Regulator of M2 Macrophage Polarization That Can Inhibit T Cell*

Activation via L-Tryptophan and Arginine Depletion and IL-10 Production. PLoS One, 2015. **10**(11): p. e0142979.

168. Orecchioni, M., Y. Ghosheh, A.B. Pramod, and K. Ley, *Macrophage Polarization: Different Gene Signatures in M1(LPS+) vs. Classically and M2(LPS-) vs. Alternatively Activated Macrophages.* Front Immunol, 2019. **10**: p. 1084.

169. Amici, S.A., N.A. Young, J. Narvaez-Miranda, K.A. Jablonski, J. Arcos, L. Rosas, T.L. Papenfuss, J.B. Torrelles, W.N. Jarjour, and M. Guerau-de-Arellano, *CD38 Is Robustly Induced in Human Macrophages and Monocytes in Inflammatory Conditions.* Front Immunol, 2018. **9**: p. 1593.

170. Koeniger, T. and S. Kuerten, *Splitting the "Unsplittable": Dissecting Resident and Infiltrating Macrophages in Experimental Autoimmune Encephalomyelitis.* Int J Mol Sci, 2017. **18**(10).

171. Sheng, J., C. Ruedl, and K. Karjalainen, *Most Tissue-Resident Macrophages Except Microglia Are Derived from Fetal Hematopoietic Stem Cells.* Immunity, 2015. **43**(2): p. 382-93.

172. Dorhoi, A. and S.H. Kaufmann, *Versatile myeloid cell subsets contribute to tuberculosis-associated inflammation.* Eur J Immunol, 2015. **45**(8): p. 2191-202.

173. Copenhaver, R.H., E. Sepulveda, L.Y. Armitige, J.K. Actor, A. Wanger, S.J. Norris, R.L. Hunter, and C. Jagannath, *A mutant of Mycobacterium tuberculosis H37Rv that lacks expression of antigen 85A is attenuated in mice but retains vaccinogenic potential.* Infect Immun, 2004. **72**(12): p. 7084-95.

174. Glickman, M.S., J.S. Cox, and W.R. Jacobs, Jr., *A novel mycolic acid cyclopropane synthetase is required for cording, persistence, and virulence of Mycobacterium tuberculosis.* Mol Cell, 2000. **5**(4): p. 717-27.

175. Ryll, R., Y. Kumazawa, and I. Yano, *Immunological properties of trehalose dimycolate (cord factor) and other mycolic acid-containing glycolipids--a review.* Microbiol Immunol, 2001. **45**(12): p. 801-11.

176. Schabbing, R.W., A. Garcia, and R.L. Hunter, *Characterization of the trehalose 6,6'-dimycolate surface monolayer by scanning tunneling microscopy.* Infect Immun, 1994. **62**(2): p. 754-6.

177. Syed, S.S. and R.L. Hunter, Jr., *Studies on the toxic effects of quartz and a mycobacterial glycolipid, trehalose 6,6'-dimycolate.* Ann Clin Lab Sci, 1997. **27**(5): p. 375-83.

178. Ishikawa, E., D. Mori, and S. Yamasaki, *Recognition of Mycobacterial Lipids by Immune Receptors.* Trends Immunol, 2017. **38**(1): p. 66-76.

179. Cohen, S.B., B.H. Gern, J.L. Delahaye, K.N. Adams, C.R. Plumlee, J.K. Winkler, D.R. Sherman, M.Y. Gerner, and K.B. Urdahl, *Alveolar Macrophages Provide an Early Mycobacterium tuberculosis Niche and Initiate Dissemination.* Cell Host Microbe, 2018. **24**(3): p. 439-446 e4.

180. Davis, M.J., T.M. Tsang, Y. Qiu, J.K. Dayrit, J.B. Freij, G.B. Huffnagle, and M.A. Olszewski, *Macrophage M1/M2 polarization dynamically adapts to changes in cytokine microenvironments in Cryptococcus neoformans infection.* MBio, 2013. **4**(3): p. e00264-13.

181. Indrigo, J., R.L. Hunter, Jr., and J.K. Actor, *Cord factor trehalose 6,6'-dimycolate (TDM) mediates trafficking events during mycobacterial infection of murine macrophages.* Microbiology, 2003. **149**(Pt 8): p. 2049-59.

182. Indrigo, J., R.L. Hunter, Jr., and J.K. Actor, *Influence of trehalose 6,6'-dimycolate (TDM) during mycobacterial infection of bone marrow macrophages.* Microbiology, 2002. **148**(Pt 7): p. 1991-8.

183. Rajaram, M.V., B. Ni, C.E. Dodd, and L.S. Schlesinger, *Macrophage immunoregulatory pathways in tuberculosis.* Semin Immunol, 2014. **26**(6): p. 471-85.

184. Schoenen, H., B. Bodendorfer, K. Hitchens, S. Manzanero, K. Werninghaus, F. Nimmerjahn, E.M. Agger, S. Stenger, P. Andersen, J. Ruland, G.D. Brown, C. Wells, and R. Lang, *Cutting edge: Mincle is essential for recognition and adjuvanticity of the mycobacterial cord factor and its synthetic analog trehalose-dibehenate.* J Immunol, 2010. **184**(6): p. 2756-60.

185. Matsunaga, I. and D.B. Moody, *Mincle is a long sought receptor for mycobacterial cord factor.* J Exp Med, 2009. **206**(13): p. 2865-8.

186. Miyake, Y., K. Toyonaga, D. Mori, S. Kakuta, Y. Hoshino, A. Oyamada, H. Yamada, K. Ono, M. Suyama, Y. Iwakura, Y. Yoshikai, and S. Yamasaki, *C-type lectin MCL is an FcRgamma-coupled receptor that mediates the adjuvanticity of mycobacterial cord factor.* Immunity, 2013. **38**(5): p. 1050-62.

187. Schoenen, H., A. Huber, N. Sonda, S. Zimmermann, J. Jantsch, B. Lepenies, V. Bronte, and R. Lang, *Differential control of Mincle-dependent cord factor recognition and*

macrophage responses by the transcription factors C/EBPbeta and HIF1alpha. J Immunol, 2014. **193**(7): p. 3664-75.

188. Kodar, K., J.L. Harper, M.J. McConnell, M.S.M. Timmer, and B.L. Stocker, *The Mincle ligand trehalose dibehenate differentially modulates M1-like and M2-like macrophage phenotype and function via Syk signaling.* Immun Inflamm Dis, 2017. **5**(4): p. 503-514.

189. Zhao, X.Q., L.L. Zhu, Q. Chang, C. Jiang, Y. You, T. Luo, X.M. Jia, and X. Lin, *C-type lectin receptor dectin-3 mediates trehalose 6,6'-dimycolate (TDM)-induced Mincle expression through CARD9/Bcl10/MALT1-dependent nuclear factor (NF)-kappaB activation.* J Biol Chem, 2014. **289**(43): p. 30052-62.

190. LeibundGut-Landmann, S., O. Gross, M.J. Robinson, F. Osorio, E.C. Slack, S.V. Tsoni, E. Schweighoffer, V. Tybulewicz, G.D. Brown, J. Ruland, and C. Reis e Sousa, *Syk- and CARD9-dependent coupling of innate immunity to the induction of T helper cells that produce interleukin 17.* Nat Immunol, 2007. **8**(6): p. 630-8.

191. Schweneker, K., O. Gorka, M. Schweneker, H. Poeck, J. Tschopp, C. Peschel, J. Ruland, and O. Gross, *The mycobacterial cord factor adjuvant analogue trehalose-6,6'-dibehenate (TDB) activates the Nlrp3 inflammasome.* Immunobiology, 2013. **218**(4): p. 664-73.

192. Behling, C.A., R.L. Perez, M.R. Kidd, G.W. Staton, Jr., and R.L. Hunter, *Induction of pulmonary granulomas, macrophage procoagulant activity, and tumor necrosis factor-alpha by trehalose glycolipids.* Ann Clin Lab Sci, 1993. **23**(4): p. 256-66.

193. Tomioka, H., Y. Tatano, W.W. Maw, C. Sano, Y. Kanehiro, and T. Shimizu, *Characteristics of suppressor macrophages induced by mycobacterial and protozoal infections in relation to alternatively activated M2 macrophages.* Clin Dev Immunol, 2012. **2012**: p. 635451.

194. Shen, P., Q. Li, J. Ma, M. Tian, F. Hong, X. Zhai, J. Li, H. Huang, and C. Shi, *IRAK-M alters the polarity of macrophages to facilitate the survival of Mycobacterium tuberculosis.* BMC Microbiol, 2017. **17**(1): p. 185.

195. Viegas, M.S., A. do Carmo, T. Silva, F. Seco, V. Serra, M. Lacerda, and T.C. Martins, *CD38 plays a role in effective containment of mycobacteria within granulomata and polarization of Th1 immune responses against Mycobacterium avium.* Microbes Infect, 2007. **9**(7): p. 847-54.

196. Refai, A., S. Gritli, M.R. Barbouche, and M. Essafi, *Mycobacterium tuberculosis Virulent Factor ESAT-6 Drives Macrophage Differentiation Toward the Pro-inflammatory M1 Phenotype and Subsequently Switches It to the Anti-inflammatory M2 Phenotype.* Front Cell Infect Microbiol, 2018. **8**: p. 327.

197. Huang, Z., Q. Luo, Y. Guo, J. Chen, G. Xiong, Y. Peng, J. Ye, and J. Li, *Mycobacterium tuberculosis-Induced Polarization of Human Macrophage Orchestrates the Formation and Development of Tuberculous Granulomas In Vitro.* PLoS One, 2015. **10**(6): p. e0129744.

198. Nguyen, T.K.T., J. d'Aigle, L. Chinea, Z. Niaz, R.L. Hunter, S.A. Hwang, and J.K. Actor, *Mycobacterial Trehalose 6,6'-Dimycolate-Induced M1-Type Inflammation.* Am J Pathol, 2020. **190**(2): p. 286-294.

199. Zumla, A., M. Rao, E. Dodoo, and M. Maeurer, *Potential of immunomodulatory agents as adjunct host-directed therapies for multidrug-resistant tuberculosis.* BMC Med, 2016. **14**: p. 89.

200. Palucci, I. and G. Delogu, *Host Directed Therapies for Tuberculosis: Future Strategies for an Ancient Disease.* Chemotherapy, 2018. **63**(3): p. 172-180.

201. Kruzel, M.L., M. Zimecki, and J.K. Actor, *Lactoferrin in a context of inflammation-induced pathology.* Frontiers in immunology, 2017. **8**: p. 1438.

202. Legrand, D. and J. Mazurier, *A critical review of the roles of host lactoferrin in immunity.* Biometals, 2010. **23**(3): p. 365-76.

203. Vogel, H.J., *Lactoferrin, a bird's eye view.* Biochem Cell Biol, 2012. **90**(3): p. 233-44.

204. Siqueiros-Cendon, T., S. Arevalo-Gallegos, B.F. Iglesias-Figueroa, I.A. Garcia-Montoya, J. Salazar-Martinez, and Q. Rascon-Cruz, *Immunomodulatory effects of lactoferrin.* Acta Pharmacol Sin, 2014. **35**(5): p. 557-66.

205. Actor, J.K., *Lactoferrin: a modulator for immunity against tuberculosis related granulomatous pathology.* Mediators of inflammation, 2015. **2015:409596**.

206. Hwang, S.-A., M.L. Kruzel, and J.K. Actor, *Oral recombinant human or mouse lactoferrin reduces Mycobacterium tuberculosis TDM induced granulomatous lung pathology.* Biochemistry and Cell Biology, 2016. **95**(1): p. 148-154.

207. Reece, S.T. and S.H. Kaufmann, *Floating between the poles of pathology and protection: can we pin down the granuloma in tuberculosis?* Curr Opin Microbiol, 2012. **15**(1): p. 63-70.

208. Zimecki, M., J. Artym, M. Kocieba, K. Kaleta-Kuratewicz, P. Kuropka, J. Kuryszko, and M. Kruzel, *Homologous lactoferrin triggers mobilization of the myelocytic lineage of bone marrow in experimental mice.* Stem Cells Dev, 2013. **22**(24): p. 3261-70.

209. Welsh, K.J., S.-A. Hwang, R.L. Hunter, M.L. Kruzel, and J.K. Actor, *Lactoferrin modulation of mycobacterial cord factor trehalose 6-6'-dimycolate induced granulomatous response.* Translational Research, 2010. **156**(4): p. 207-215.

210. Welsh, K.J., S.-A. Hwang, S. Boyd, M.L. Kruzel, R.L. Hunter, and J.K. Actor, *Influence of oral lactoferrin on Mycobacterium tuberculosis induced immunopathology.* Tuberculosis, 2011. **91**: p. S105-S113.

211. McQuin, C., A. Goodman, V. Chernyshev, L. Kamentsky, B.A. Cimini, K.W. Karhohs, M. Doan, L. Ding, S.M. Rafelski, D. Thirstrup, W. Wiegraebe, S. Singh, T. Becker, J.C. Caicedo, and A.E. Carpenter, *CellProfiler 3.0: Next-generation image processing for biology.* PLoS Biol, 2018. **16**(7): p. e2005970.

212. Rasband, W.S. *Image J*. 1997-2018; Available from: https://imagej.nih.gov/ij/.

213. Diem, K., A. Magaret, A. Klock, L. Jin, J. Zhu, and L. Corey, *Image analysis for accurately counting CD4+ and CD8+ T cells in human tissue.* J Virol Methods, 2015. **222**: p. 117-21.

214. Welsh, K.J., A.N. Abbott, S.-A. Hwang, J. Indrigo, L.Y. Armitige, M.R. Blackburn, R.L. Hunter Jr, and J.K. Actor, *A role for tumour necrosis factor-α, complement C5 and interleukin-6 in the initiation and development of the mycobacterial cord factor trehalose 6, 6'-dimycolate induced granulomatous response.* Microbiology (Reading, England), 2008. **154**(Pt 6): p. 1813.

215. Hwang, S.-A., C.D. Byerly, and J.K. Actor, *Mycobacterial trehalose 6, 6'-dimycolate induced vascular occlusion is accompanied by subendothelial inflammation.* Tuberculosis (Edinb), 2019(116S): p. S118-S122.

216. Lepanto, M.S., L. Rosa, R. Paesano, P. Valenti, and A. Cutone, *Lactoferrin in Aseptic and Septic Inflammation.* Molecules, 2019. **24**(7).

217. Latorre, D., F. Berlutti, P. Valenti, S. Gessani, and P. Puddu, *LF immunomodulatory strategies: mastering bacterial endotoxin.* Biochem Cell Biol, 2012. **90**(3): p. 269-78.

218. Cutone, A., L. Rosa, M.S. Lepanto, M.J. Scotti, F. Berlutti, M.C. Bonaccorsi di Patti, G. Musci, and P. Valenti, *Lactoferrin Efficiently Counteracts the Inflammation-Induced Changes of the Iron Homeostasis System in Macrophages.* Front Immunol, 2017. **8**: p. 705.

219. Rosa, L., A. Cutone, M.S. Lepanto, R. Paesano, and P. Valenti, *Lactoferrin: A Natural Glycoprotein Involved in Iron and Inflammatory Homeostasis.* Int J Mol Sci, 2017. **18**(9).

220. Hwang, S.-A., M.L. Kruzel, and J.K. Actor, *Recombinant human lactoferrin modulates human PBMC derived macrophage responses to BCG and LPS.* Tuberculosis, 2016. **101**: p. S53-S62.

221. Hwang, S.-A., M.L. Kruzel, and J.K. Actor, *Immunomodulatory effects of recombinant lactoferrin during MRSA infection.* International immunopharmacology, 2014. **20**(1): p. 157-163.

222. Kruzel, M.L., J.K. Actor, M. Zimecki, J. Wise, P. Płoszaj, S. Mirza, M. Kruzel, S.-A. Hwang, X. Ba, and I. Boldogh, *Novel recombinant human lactoferrin: differential*

activation of oxidative stress related gene expression. Journal of biotechnology, 2013. **168**(4): p. 666-675.

223. Kindler, V., A.P. Sappino, G.E. Grau, P.F. Piguet, and P. Vassalli, *The inducing role of tumor necrosis factor in the development of bactericidal granulomas during BCG infection.* Cell, 1989. **56**(5): p. 731-40.

224. Flynn, J.L., M.M. Goldstein, J. Chan, K.J. Triebold, K. Pfeffer, C.J. Lowenstein, R. Schreiber, T.W. Mak, and B.R. Bloom, *Tumor necrosis factor-alpha is required in the protective immune response against Mycobacterium tuberculosis in mice.* Immunity, 1995. **2**(6): p. 561-72.

225. Gao, C.H., H.L. Dong, L. Tai, and X.M. Gao, *Lactoferrin-Containing Immunocomplexes Drive the Conversion of Human Macrophages from M2- into M1-like Phenotype.* Front Immunol, 2018. **9**: p. 37.

226. Tobin, D.M., *Host-Directed Therapies for Tuberculosis.* Cold Spring Harb Perspect Med, 2015. **5**(10).

227. Tomioka, H., C. Sano, and Y. Tatano, *Host-Directed Therapeutics against Mycobacterial Infections.* Curr Pharm Des, 2017. **23**(18): p. 2644-2656.

228. Dorhoi, A. and S.H. Kaufmann, *Tumor necrosis factor alpha in mycobacterial infection.* Semin Immunol, 2014. **26**(3): p. 203-9.

229. Pammi, M. and G. Suresh, *Enteral lactoferrin supplementation for prevention of sepsis and necrotizing enterocolitis in preterm infants.* Cochrane Database Syst Rev, 2020. **3**: p. CD007137.

230. Embleton, N.D. and J.E. Berrington, *Clinical Trials of Lactoferrin in the Newborn: Effects on Infection and the Gut Microbiome.* Nestle Nutr Inst Workshop Ser, 2020. **94**: p. 1-11.

231. Ochoa, T.J., J. Zegarra, S. Bellomo, C.P. Carcamo, L. Cam, A. Castaneda, A. Villavicencio, J. Gonzales, M.S. Rueda, C.G. Turin, A. Zea-Vera, D. Guillen, M. Campos, L. Ewing-Cobbs, and N.R. Group, *Randomized Controlled Trial of Bovine Lactoferrin for Prevention of Sepsis and Neurodevelopment Impairment in Infants Weighing Less Than 2000 Grams.* J Pediatr, 2020. **219**: p. 118-125 e5.

232. Manzoni, P., M.A. Militello, S. Rizzollo, E. Tavella, A. Messina, M. Pieretto, E. Boano, M. Carlino, E. Tognato, R. Spola, A. Perona, M.M. Maule, R. Garcia Sanchez, M. Meyer, I. Stolfi, L. Pugni, H. Messner, S. Cattani, P.M. Betta, L. Memo, L. Decembrino, L. Bollani, M. Rinaldi, M. Fioretti, M. Quercia, C. Tzialla, N. Laforgia, F. Mosca, R. Magaldi, M. Mostert, D. Farina, W. Tarnow-Mordi, I. Italian Task Force for the Study Prevention of Neonatal Fungal, and N. the Italian Society of, *Is Lactoferrin More Effective in Reducing Late-Onset Sepsis in Preterm Neonates Fed Formula Than in Those Receiving Mother's Own Milk? Secondary Analyses of Two Multicenter Randomized Controlled Trials.* Am J Perinatol, 2019. **36**(S 02): p. S120-S125.

233. Martin, A., A. Ghadge, P. Manzoni, K. Lui, R. Brown, W. Tarnow-Mordi, and L.C.S. Group, *Protocol for the Lactoferrin Infant Feeding Trial (LIFT): a randomised trial of adding lactoferrin to the feeds of very-low birthweight babies prior to hospital discharge.* BMJ Open, 2018. **8**(10): p. e023044.

234. Gervassi, A., N. Lejarcegui, S. Dross, A. Jacobson, G. Itaya, E. Kidzeru, S. Gantt, H. Jaspan, and H. Horton, *Myeloid derived suppressor cells are present at high frequency in neonates and suppress in vitro T cell responses.* PLoS One, 2014. **9**(9): p. e107816.

235. Liu, Y., M. Perego, Q. Xiao, Y. He, S. Fu, J. He, W. Liu, X. Li, Y. Tang, X. Li, W. Yuan, W. Zhou, F. Wu, C. Jia, Q. Cui, G.S. Worthen, E.A. Jensen, D.I. Gabrilovich, and J. Zhou, *Lactoferrin-induced myeloid-derived suppressor cell therapy attenuates pathologic inflammatory conditions in newborn mice.* J Clin Invest, 2019. **129**(10): p. 4261-4275.

236. Wang, B., Y.P. Timilsena, E. Blanch, and B. Adhikari, *Lactoferrin: Structure, function, denaturation and digestion.* Crit Rev Food Sci Nutr, 2019. **59**(4): p. 580-596.

237. Furlund, C.B., E.K. Ulleberg, T.G. Devold, R. Flengsrud, M. Jacobsen, C. Sekse, H. Holm, and G.E. Vegarud, *Identification of lactoferrin peptides generated by digestion with human gastrointestinal enzymes.* J Dairy Sci, 2013. **96**(1): p. 75-88.

238. Kruzel, M.L., S.-A. Hwang, P. Olszewska, and J.K. Actor, *Systemic effects of oral lactoferrin*, in *The 14th International Conference on Lactoferrin Structure, Function and Applications*. 2019: Lima, Peru.

239. Pranger, A.D., T.S. van der Werf, J.G.W. Kosterink, and J.W.C. Alffenaar, *The Role of Fluoroquinolones in the Treatment of Tuberculosis in 2019.* Drugs, 2019. **79**(2): p. 161-171.

240. Das, S., T. Garg, N. Srinivas, A. Dasgupta, and S. Chopra, *Targeting DNA Gyrase to Combat Mycobacterium tuberculosis: An Update.* Curr Top Med Chem, 2019. **19**(8): p. 579-593.

241. *Global tuberculosis report 2020*. 2020, Geneva: World Health Organization.

242. Adams, D.O., *The granulomatous inflammatory response. A review.* Am J Pathol, 1976. **84**(1): p. 164-92.

243. Hossain, M.M. and M.N. Norazmi, *Pattern recognition receptors and cytokines in Mycobacterium tuberculosis infection--the double-edged sword?* Biomed Res Int, 2013. **2013**: p. 179174.

244. Khader, S.A., J. Rangel-Moreno, J.J. Fountain, C.A. Martino, W.W. Reiley, J.E. Pearl, G.M. Winslow, D.L. Woodland, T.D. Randall, and A.M. Cooper, *In a murine tuberculosis model, the absence of homeostatic chemokines delays granuloma formation and protective immunity.* J Immunol, 2009. **183**(12): p. 8004-14.

245. Kaplan, G., F.A. Post, A.L. Moreira, H. Wainwright, B.N. Kreiswirth, M. Tanverdi, B. Mathema, S.V. Ramaswamy, G. Walther, L.M. Steyn, C.E. Barry, 3rd, and L.G. Bekker, *Mycobacterium tuberculosis growth at the cavity surface: a microenvironment with failed immunity.* Infect Immun, 2003. **71**(12): p. 7099-108.

246. Sotgiu, G., R. Centis, L. D'Ambrosio, and G.B. Migliori, *Tuberculosis treatment and drug regimens.* Cold Spring Harb Perspect Med, 2015. **5**(5): p. a017822.

247. Schito, M., G.B. Migliori, H.A. Fletcher, R. McNerney, R. Centis, L. D'Ambrosio, M. Bates, G. Kibiki, N. Kapata, T. Corrah, J. Bomanji, C. Vilaplana, D. Johnson, P. Mwaba, M. Maeurer, and A. Zumla, *Perspectives on Advances in Tuberculosis Diagnostics, Drugs, and Vaccines.* Clin Infect Dis, 2015. **61Suppl 3**: p. S102-18.

248. Kaplan, G., *Tuberculosis control in crisis-causes and solutions.* Prog Biophys Mol Biol, 2020. **152**: p. 6-9.

249. Hayford, F.E.A., R.C. Dolman, R. Blaauw, A. Nienaber, C.M. Smuts, L. Malan, and C. Ricci, *The effects of anti-inflammatory agents as host-directed adjunct treatment of tuberculosis in humans: a systematic review and meta-analysis.* Respir Res, 2020. **21**(1): p. 223.

250. Zhang, R., X. Xi, C. Wang, Y. Pan, C. Ge, L. Zhang, S. Zhang, and H. Liu, *Therapeutic effects of recombinant human interleukin 2 as adjunctive immunotherapy against tuberculosis: A systematic review and meta-analysis.* PLoS One, 2018. **13**(7): p. e0201025.

251. Plessner, H.L., P.L. Lin, T. Kohno, J.S. Louie, D. Kirschner, J. Chan, and J.L. Flynn, *Neutralization of tumor necrosis factor (TNF) by antibody but not TNF receptor fusion molecule exacerbates chronic murine tuberculosis.* J Infect Dis, 2007. **195**(11): p. 1643-50.

252. Kruzel, M.L., M. Zimecki, and J.K. Actor, *Lactoferrin in a Context of Inflammation-Induced Pathology.* Front Immunol, 2017. **8**: p. 1438.

253. Hwang, S.A., K.J. Welsh, S. Boyd, M.L. Kruzel, and J.K. Actor, *Comparing efficacy of BCG/lactoferrin primary vaccination versus booster regimen.* Tuberculosis (Edinb), 2011. **91 Suppl 1**: p. S90-5.

254. Kruzel, M.L., P. Olszewska, B. Pazdrak, A.M. Krupinska, and J.K. Actor, *New insights into the systemic effects of oral lactoferrin: transcriptome profiling.* Biochem Cell Biol, 2021. **99**(1): p. 47-53.

255. Choi, B.K., J.K. Actor, S. Rios, M. d'Anjou, T.A. Stadheim, S. Warburton, E. Giaccone, M. Cukan, H. Li, A. Kull, N. Sharkey, P. Gollnick, M. Kocieba, J. Artym, M. Zimecki,

M.L. Kruzel, and S. Wildt, *Recombinant human lactoferrin expressed in glycoengineered Pichia pastoris: effect of terminal N-acetylneuraminic acid on in vitro secondary humoral immune response.* Glycoconj J, 2008. **25**(6): p. 581-93.

256. Batard, E., F. Jamme, S. Villette, C. Jacqueline, M.F. de la Cochetiere, J. Caillon, and M. Refregiers, *Diffusion of ofloxacin in the endocarditis vegetation assessed with synchrotron radiation UV fluorescence microspectroscopy.* PLoS One, 2011. **6**(4): p. e19440.

257. Hwang, S.A., K. Wilk, M.L. Kruzel, and J.K. Actor, *A novel recombinant human lactoferrin augments the BCG vaccine and protects alveolar integrity upon infection with Mycobacterium tuberculosis in mice.* Vaccine, 2009. **27**(23): p. 3026-34.

258. Hwang, S.A., C.D. Byerly, and J.K. Actor, *Mycobacterial trehalose 6,6'-dimycolate induced vascular occlusion is accompanied by subendothelial inflammation.* Tuberculosis (Edinb), 2019. **116S**: p. S118-S122.

259. Pisu, D., L. Huang, J.K. Grenier, and D.G. Russell, *Dual RNA-Seq of Mtb-Infected Macrophages In Vivo Reveals Ontologically Distinct Host-Pathogen Interactions.* Cell Rep, 2020. **30**(2): p. 335-350 e4.

260. Young, C., G. Walzl, and N. Du Plessis, *Therapeutic host-directed strategies to improve outcome in tuberculosis.* Mucosal Immunol, 2020. **13**(2): p. 190-204.

261. Thiriot, J.D., Y.B. Martinez-Martinez, J.J. Endsley, and A.G. Torres, *Hacking the host: exploitation of macrophage polarization by intracellular bacterial pathogens.* Pathog Dis, 2020. **78**(1).

262. Schmitz, N., M. Kurrer, M.F. Bachmann, and M. Kopf, *Interleukin-1 is responsible for acute lung immunopathology but increases survival of respiratory influenza virus infection.* J Virol, 2005. **79**(10): p. 6441-8.

263. Page, M.J., J. Bester, and E. Pretorius, *The inflammatory effects of TNF-alpha and complement component 3 on coagulation.* Sci Rep, 2018. **8**(1): p. 1812.

264. Hunter, R.L., J.K. Actor, S.A. Hwang, A. Khan, M.E. Urbanowski, D. Kaushal, and C. Jagannath, *Pathogenesis and Animal Models of Post-Primary (Bronchogenic) Tuberculosis, A Review.* Pathogens, 2018. **7**(1).

265. Drago-Serrano, M.E., R. Campos-Rodriguez, J.C. Carrero, and M. de la Garza, *Lactoferrin: Balancing Ups and Downs of Inflammation Due to Microbial Infections.* Int J Mol Sci, 2017. **18**(3).

266. Sienkiewicz, M., A. Jaskiewicz, A. Tarasiuk, and J. Fichna, *Lactoferrin: an overview of its main functions, immunomodulatory and antimicrobial role, and clinical significance.* Crit Rev Food Sci Nutr, 2021: p. 1-18.

267. Doursout, M.F., H. Horton, L. Hoang, Y. Liang, S.A. Hwang, S. Boyd, J.K. Actor, and M.L. Kruzel, *Lactoferrin moderates LPS-induced hypotensive response and gut injury in rats.* Int Immunopharmacol, 2013. **15**(2): p. 227-31.

268. Manzoni, P., M. Rinaldi, S. Cattani, L. Pugni, M.G. Romeo, H. Messner, I. Stolfi, L. Decembrino, N. Laforgia, F. Vagnarelli, L. Memo, L. Bordignon, O.S. Saia, M. Maule, E. Gallo, M. Mostert, C. Magnani, M. Quercia, L. Bollani, R. Pedicino, L. Renzullo, P. Betta, F. Mosca, F. Ferrari, R. Magaldi, M. Stronati, D. Farina, S. Italian Task Force for the, and I.S.o.N. Prevention of Neonatal Fungal Infections, *Bovine lactoferrin*

supplementation for prevention of late-onset sepsis in very low-birth-weight neonates: a randomized trial. JAMA, 2009. **302**(13): p. 1421-8.

269. Turin, C.G., A. Zea-Vera, A. Pezo, K. Cruz, J. Zegarra, S. Bellomo, L. Cam, R. Llanos, A. Castaneda, L. Tucto, T.J. Ochoa, and N.R. Group, *Lactoferrin for prevention of neonatal sepsis.* Biometals, 2014. **27**(5): p. 1007-16.

270. Yount, N.Y., M.T. Andres, J.F. Fierro, and M.R. Yeaman, *The gamma-core motif correlates with antimicrobial activity in cysteine-containing kaliocin-1 originating from transferrins.* Biochim Biophys Acta, 2007. **1768**(11): p. 2862-72.

271. Moore, S.A., B.F. Anderson, C.R. Groom, M. Haridas, and E.N. Baker, *Three-dimensional structure of diferric bovine lactoferrin at 2.8 A resolution.* J Mol Biol, 1997. **274**(2): p. 222-36.

272. Baker, H.M., C.J. Baker, C.A. Smith, and E.N. Baker, *Metal substitution in transferrins: specific binding of cerium(IV) revealed by the crystal structure of cerium-substituted human lactoferrin.* J Biol Inorg Chem, 2000. **5**(6): p. 692-8.

273. Kruzel, M.L., J.K. Actor, M. Zimecki, J. Wise, P. Ploszaj, S. Mirza, M. Kruzel, S.A. Hwang, X. Ba, and I. Boldogh, *Novel recombinant human lactoferrin: differential activation of oxidative stress related gene expression.* J Biotechnol, 2013. **168**(4): p. 666-75.

274. Rascon-Cruz, Q., E.A. Espinoza-Sanchez, T.S. Siqueiros-Cendon, S.I. Nakamura-Bencomo, S. Arevalo-Gallegos, and B.F. Iglesias-Figueroa, *Lactoferrin: A Glycoprotein Involved in Immunomodulation, Anticancer, and Antimicrobial Processes.* Molecules, 2021. **26**(1).

275. de la Rosa, G., D. Yang, P. Tewary, A. Varadhachary, and J.J. Oppenheim, *Lactoferrin acts as an alarmin to promote the recruitment and activation of APCs and antigen-specific immune responses.* J Immunol, 2008. **180**(10): p. 6868-76.

276. Hwang, S.A. and J.K. Actor, *Lactoferrin modulation of BCG-infected dendritic cell functions.* Int Immunol, 2009. **21**(10): p. 1185-97.

277. Hwang, S.A., M.L. Kruzel, and J.K. Actor, *Effects of CHO-expressed recombinant lactoferrins on mouse dendritic cell presentation and function.* Innate Immun, 2015. **21**(5): p. 553-61.

278. Spadaro, M., M. Montone, M. Arigoni, D. Cantarella, G. Forni, F. Pericle, S. Pascolo, R.A. Calogero, and F. Cavallo, *Recombinant human lactoferrin induces human and mouse dendritic cell maturation via Toll-like receptors 2 and 4.* FASEB J, 2014. **28**(1): p. 416-29.

279. Hwang, S.A., M.L. Kruzel, and J.K. Actor, *Influence of bovine lactoferrin on expression of presentation molecules on BCG-infected bone marrow derived macrophages.* Biochimie, 2009. **91**(1): p. 76-85.

280. Zimecki, M., J. Mazurier, M. Machnicki, Z. Wieczorek, J. Montreuil, and G. Spik, *Immunostimulatory activity of lactotransferrin and maturation of CD4- CD8- murine thymocytes.* Immunol Lett, 1991. **30**(1): p. 119-23.

281. Dhennin-Duthille, I., M. Masson, E. Damiens, C. Fillebeen, G. Spik, and J. Mazurier, *Lactoferrin upregulates the expression of CD4 antigen through the stimulation of the mitogen-activated protein kinase in the human lymphoblastic T Jurkat cell line.* J Cell Biochem, 2000. **79**(4): p. 583-93.

282. Frydecka, I., M. Zimecki, D. Bocko, A. Kosmaczewska, R. Teodorowska, L. Ciszak, M. Kruzel, J. Wlodarska-Polinsk, K. Kuliczkowski, and J. Kornafel, *Lactoferrin-induced up-regulation of zeta (zeta) chain expression in peripheral blood T lymphocytes from cervical cancer patients.* Anticancer Res, 2002. **22**(3): p. 1897-901.

283. Zimecki, M., R. Miedzybrodzki, J. Mazurier, and G. Spik, *Regulatory effects of lactoferrin and lipopolysaccharide on LFA-1 expression on human peripheral blood mononuclear cells.* Arch Immunol Ther Exp (Warsz), 1999. **47**(4): p. 257-64.

284. Takakura, N., H. Wakabayashi, K. Yamauchi, and M. Takase, *Influences of orally administered lactoferrin on IFN-gamma and IL-10 production by intestinal intraepithelial lymphocytes and mesenteric lymph-node cells.* Biochem Cell Biol, 2006. **84**(3): p. 363-8.

285. Kuhara, T., K. Yamauchi, Y. Tamura, and H. Okamura, *Oral administration of lactoferrin increases NK cell activity in mice via increased production of IL-18 and type I IFN in the small intestine.* J Interferon Cytokine Res, 2006. **26**(7): p. 489-99.

286. Hwang, S.A., K.M. Wilk, Y.A. Bangale, M.L. Kruzel, and J.K. Actor, *Lactoferrin modulation of IL-12 and IL-10 response from activated murine leukocytes.* Med Microbiol Immunol, 2007. **196**(3): p. 171-80.

287. Hunter, R.L., N. Venkataprasad, and M.R. Olsen, *The role of trehalose dimycolate (cord factor) on morphology of virulent M. tuberculosis in vitro.* Tuberculosis (Edinb), 2006. **86**(5): p. 349-56.

288. Baveye, S., E. Elass, D.G. Fernig, C. Blanquart, J. Mazurier, and D. Legrand, *Human lactoferrin interacts with soluble CD14 and inhibits expression of endothelial*

adhesion molecules, E-selectin and ICAM-1, induced by the CD14-lipopolysaccharide complex. Infect Immun, 2000. **68**(12): p. 6519-25.

289. Yeom, M., J. Park, B. Lee, S.Y. Choi, K.S. Kim, H. Lee, and D.H. Hahm, *Lactoferrin inhibits the inflammatory and angiogenic activation of bovine aortic endothelial cells.* Inflamm Res, 2011. **60**(5): p. 475-82.

290. Mantovani, A., A. Sica, S. Sozzani, P. Allavena, A. Vecchi, and M. Locati, *The chemokine system in diverse forms of macrophage activation and polarization.* Trends Immunol, 2004. **25**(12): p. 677-86.

291. Wang, N., H. Liang, and K. Zen, *Molecular mechanisms that influence the macrophage m1-m2 polarization balance.* Front Immunol, 2014. **5**: p. 614.

292. Kruzel, M.L., P. Olszewska, B. Pazdrak, A.M. Krupinska, and J.K. Actor, *New Insights into the Systemic Effects of Oral Lactoferrin: Transcriptome Profiling.* Biochem Cell Biol, 2020.

VITA

Thao Khanh Thanh Nguyen is originally from Viet Nam, Ho Chi Minh city, where she finished her education in high school before traveling to the United States to attend college. After transferring to the University of St. Thomas in Houston, Texas, she pursued her undergraduate education in Biology with an internship at the Texas Children Hospital and Baylor College of Medicine in Dr. Thuy Phung's laboratory. She received the degree of Bachelor of Arts in May, 2016. For the next three years, she worked as a research assistant in the Department of Pathology and Laboratory Medicines at the UTHealth McGovern Medical School. In August of 2019, she entered The University of Texas MD Anderson Cancer Center UTHealth Graduate School of Biomedical Sciences to pursue her Master of Science degree.